

Dissertation
submitted to the
Combined Faculties for the Natural Sciences and for Mathematics
of the Ruperto-Carola University of Heidelberg, Germany
for the degree of

Doctor of Natural Sciences

presented by

Diplom-Biologe Ioannis Legouras
born in: Patra, Greece
Oral-examination:

Growth zone instability in T-shaped
Schizosaccharomyces pombe **cells**

Supervisor:

Dr. François Nédélec

Referees:

Dr. Damian Brunner

Dr. Jochen Wittbrodt

Contents

1	Introduction	5
1.1	Overview	5
1.2	The Cytoskeleton	6
1.3	An introduction to <i>Schizosaccharomyces pombe</i>	7
1.3.1	History and General information	7
1.3.2	Establishment of polarity in <i>S. pombe</i>	7
1.4	Microtubule-dependent growth in <i>S. pombe</i>	9
1.4.1	MT plus-end tips	10
1.4.2	Polarity machinery	13
1.4.3	Ectopic Growth Studies	26
1.5	Summary	28
1.6	Methods for shape change	29
1.7	Aim of Thesis	30
2	Results	31
2.1	Overview	31
2.1.1	Terminology	31
2.2	Wild Type cells (WT)	32
2.2.1	Polarity in the presence or absence of MTs	32
2.2.2	Polarity of T-shaped cells	34
2.2.3	Geometry - Growth - Nucleus	36
2.2.4	Geometry vs Growth	37
2.2.5	MTs vs Growth	40
2.2.6	Geometry vs MTs	41
2.2.7	Growth Maintenance - Growth Switch	44
2.2.8	Conclusions	45
2.3	<i>Tea1</i> Δ	46
2.3.1	Polarity of T-shaped cells	46
2.3.2	Geometry - Growth - Nucleus	47
2.3.3	Geometry vs Growth	49
2.3.4	MTs vs Growth	50
2.3.5	Geometry vs MTs	52
2.3.6	Growth Maintenance - Growth Switch	53

2.3.7	Conclusions	53
2.4	<i>Tea4</i> Δ	54
2.4.1	Polarity of T-shaped cells	54
2.4.2	Geometry - Growth - Nucleus	55
2.4.3	Geometry vs Growth	57
2.4.4	MTs vs Growth	58
2.4.5	Geometry vs MTs	60
2.4.6	Growth Maintenance - Growth Switch	60
2.4.7	Conclusions	60
2.5	<i>Mod5</i> Δ	62
2.5.1	Polarity of T-shaped cells	62
2.5.2	Geometry - Growth - Nucleus	63
2.5.3	Geometry vs Growth	66
2.5.4	MTs vs Growth	66
2.5.5	Geometry vs MTs	68
2.5.6	Growth Maintenance - Growth Switch	69
2.5.7	Conclusions	69
2.6	<i>Bud6</i> Δ	71
2.6.1	Polarity of T-shaped cells	71
2.6.2	Geometry - Growth - Nucleus	72
2.6.3	Geometry vs Growth	75
2.6.4	MTs vs Growth	75
2.6.5	Geometry vs MTs	78
2.6.6	Growth Maintenance - Growth Switch	79
2.6.7	Conclusions	80
3	Discussion	81
3.1	Summary	81
3.2	Nuclear localization	82
3.3	Growth dependencies	83
3.4	Growth switch	84
4	Methods	87
4.1	Overview	87
4.2	Cell Growing	87
4.3	Branching protocols	87
4.3.1	Heterogeneity of branching efficiency	87
4.4	Strain preparations	88
4.5	Microscopy	88
4.5.1	Sample preparation	88
4.5.2	Confocal Spinning Disk	88
4.5.3	Movie acquisition	88
4.6	Image processing	88
4.6.1	Cell Outlines	88

4.6.2	Cell Center - Cell Ends	89
4.6.3	Nucleus	89
4.6.4	Microtubules	89
4.7	Analysis	89
4.7.1	Box plots	89
4.7.2	Scatterplots	89
Bibliography		91
Acknowledgements		103
A List of strains		105
B Quantifications		107
C Summarizing graphs		109

Abstract

Morphogenesis is a complex process which in unicellular organisms involves mainly polarized cell growth and cell division. Microtubules (MTs) are a key player in spatial regulation of cytokinesis and polarization. The fission yeast *Schizosaccharomyces pombe* is a convenient model organism for morphogenesis studies because of its simple cylindrical shape and its polarized growth at the cell tips. MT plus ends contact and shrink from the cell tips and contribute to polarity regulation. There is a strong crosstalk between MTs, actin and cell shape.

Here we perturb the cell shape and we investigate the effects on MTs, nuclear position and polarization machinery. We use the MT-depolymerizing drug thiabendazole (TBZ) to depolymerize the interphase microtubules. MT depolymerization causes formation of arms around the middle of the cell perpendicular to the long axis of the cell. The organization of the MT cytoskeleton exhibits heterogeneity in these T-shaped cells and depends on the cell geometry. We found that growth zones that were formed in the absence of microtubules, have different properties compared to the old ends of the cell and they exhibit an inherent instability, as measured by their growth potential. This growth potential in the arm is proportional to the initial size and to the number of MTs that reach the arm cortex. These effects are Tea1p-Tea4p-Mod5p dependent but Bud6p independent.

These studies provide a demonstration of how MTs influence the growth potential at cell ends in fission yeast and begin to suggest a new model of growth zone instability. MT interactions with the cortex are important not only for establishment but also for maintenance of growth zones. These findings highlight a previously hidden role of MTs responsible for cell morphogenesis.

Zusammenfassung

Morphogenese ist ein komplexer Prozess. In einzelligen Organismen basiert er hauptsächlich auf polarisiertem Zellwachstum und Zellteilung. Mikrotubuli (MTs) sind Schlüsselfaktoren in der räumlichen Regulierung von Zytokinese und Polarisierung. Die Spaltheefe *Schizosaccharomyces pombe* ist ein guter Modellorganismus für die Studie der Morphogenese, aufgrund seiner einfachen zylindrischen Form und polarisiertem Zellwachstum an den Zellspitzen. MT Plus-Enden berühren die Zellspitzen, depolymerisieren dann und spielen somit eine wichtige Rolle in der Regulierung von Polarität. Ein enges Zusammenspiel zwischen MTs, Aktin und Zellform ist zu beobachten.

In dieser Arbeit führen wir Störungen in der Zellform herbei und untersuchen deren Auswirkungen auf MTs, die Polarisierungsmaschinerie und die Position des Zellkerns. Wir verwenden die Substanz Thiabendazole (TBZ) um Mikrotubuli in der Interphase zu depolymerisieren. Die Depolymerisierung von MTs führt zur Bildung von Ästen in der Zellmitte, die senkrecht zur Zellachse verlaufen. Die Organisation der MTs in diesen Zellen, die die Form eines Ts annehmen, ist heterogen und abhängig von der Zellgeometrie. Wir haben beobachtet, dass Wachstumszonen, die in der Abwesenheit von Mikrotubuli gebildet werden, andere Eigenschaften aufweisen als solche an den normalen Zellenden. Messungen des Wachstumspotentials zeigen eine inherente Instabilität. Das Wachstumspotential in den Armen ist proportional zu der Ausgangsgröße und der Zahl von MTs die den Cortex des Armes erreichen. Diese Effekte sind abhängig von Tea1p-Tea4p-Mod5p, aber unabhängig von Bud6p.

Die Studie zeigt den Einfluss von MTs auf das Wachstumspotential an Zellenden der Spaltheefe und deutet auf ein neues Modell für die Instabilität von Wachstumszonen hin. Die Interaktion zwischen MTs und Kortex spielt eine wichtige Rolle in der Anlage und dem Erhalt von Wachstumszonen. Unsere Ergebnisse weisen auf eine bisher unbekannt Rolle von MTs in der Zellmorphogenese hin.

Abbreviations and Terminology

MT Microtubule

iMTOC Interphase Microtubule organizing center

Lat A Latrunculin A

MBC Methyl-2-benzimidazole-carbamate

TBZ Thiabendazole

ts Temperature sensitive

EMM2 Edinburgh Minimal Media 2

+TIP plus end interacting protein

Chapter 1

Introduction

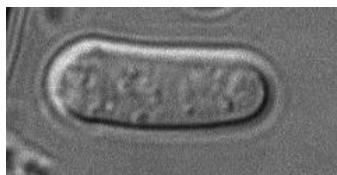


Figure 1.1: A DIC-picture of fission yeast.

1.1 Overview

Eukaryotic cells display a wide range of polarized morphologies. They devise various ways to establish morphogenesis, the core mechanisms of which are evolutionarily conserved (Nelson, 2003; Siegrist and Doe, 2007). External cues such as mating pheromones in budding and fission yeasts or sperm entry in *Caenorhabditis elegans* can direct cell polarity (Chant, 1999; Goldstein and Hird, 1996; Nielsen and Davey, 1995; Segall, 1993). The polarity of the single cell zygote also determines the organism's body plan in organisms such as *Drosophila melanogaster*, *Caenorhabditis elegans* and *Xenopus laevis* (Ruiz i Altaba and Melton, 1990; Bowerman and Shelton, 1999; Lall and Patel, 2001). Polarized shape is generally defined by organized dynamic interactions between the cytoskeletal filaments, with actin located at the sites of growth and microtubules directing the overall cell shape. Neuronal axons have stable, parallel and polarized arrays of microtubule bundles (Laferrriere et al., 1997) and dynamic fibroblasts have dynamic microtubules (Liao et al., 1995). Cell shape is also important in carcinogenesis, and there are indications that cancer cells can be made to form morphologically normal structures and are more resistant to apoptosis when grown in certain three-dimensional contexts that force specific shapes on them (Wang et al., 2002; Weaver et al., 2002).

From simple molecular assemblies to cells, organs, and organisms, the generation of form is a central issue in biology. At the molecular level, assemblies are governed by short-range interactions. At the cellular level, however, distinct mechanisms must exist

to ensure the maintenance of form throughout the cell cycle.

A common feature of eukaryotic cell polarity is the crosstalk between MTs and the actin cytoskeleton (Drubin and Nelson, 1996; Yarm et al., 2001; Small and Kaverina, 2003) in numerous cellular processes such as cell locomotion, cell polarity, spindle orientation and cytokinesis (Goode et al., 2000; Waterman-Storer and Salmon, 1999). For example, the plus ends of microtubules at the leading edge of migrating fibroblasts are required for the organization of F-actin assembly at the lamellipodia (Waterman-Storer et al., 1999). Neurons grow branches in inappropriate directions when microtubules are disrupted (Bray et al., 1978; Tanaka et al., 1995; Tanaka and Sabry, 1995). In cytokinesis, the association between microtubules and the mitotic spindle is important for the specification of the site of contractile ring assembly (Maddox and Oegema, 2003). In the next section, the main components of the cytoskeleton are outlined, namely actin, intermediate filaments and microtubules.

1.2 The Cytoskeleton

Most animal cells have three types of cytoskeletal filaments that are responsible for the cell's spatial organization and mechanical properties. Each type of filament has distinct mechanical properties, dynamics and biological roles, but all three share basic fundamental principles.

Actin filaments (microfilaments) measure approximately 7 nm in diameter and are the thinnest cytoskeletal filaments. They are composed of actin, which is the most abundant intracellular eukaryotic protein. They form cytoplasmatic networks as well as networks at the cell cortex, the region just below the plasma membrane. Actin filaments are involved in various processes such as cytokinesis, cell motility and muscle contraction (Alberts et al., 2002).

Intermediate filaments (IMs) get their name from their diameter, being intermediate between actin and microtubules. They are 10 nm in diameter and they are found in most animals, but are absent in plants and fungi. They are formed through lateral association of monomers, and there are many different types of IMs in different cell types: epithelial cells contain keratin, muscle cells contain desmin, and neural cells contain neurofilaments. They are known to be less dynamic in nature than actin and microtubules (Alberts et al., 2002).

Microtubules are long hollow cylinders with a diameter of 25 nm. They are found in all eukaryotic cells and they often interact with actin in various processes including motility, morphogenesis and vesicle transport (Alberts et al., 2002). They are composed of 9-13 protofilaments that associate laterally and are composed of tubulin dimers. Their most striking characteristic is their dynamics.

Actin filaments and MTs show a different dynamic behavior. Actin filaments grow at the plus end and simultaneously shrink at the minus end, a process that is called treadmilling. At steady state, the amount of subunits added at one end is balanced by the loss of subunits at the other end, so that the total length of the filament will remain constant. MTs usually don't undergo treadmilling, but instead exhibit dynamic insta-

bility, during which individual MTs alternate stochastically between periods of growth and shrinkage (Mitchison and Kirschner, 1984).

1.3 An introduction to *Schizosaccharomyces pombe*

Schizosaccharomyces pombe (*S. pombe* or fission yeast), has emerged as a major model for morphogenesis studies. In the following chapters the organism is introduced, some background information on its biology is outlined and its importance and usefulness in morphogenesis studies is discussed.

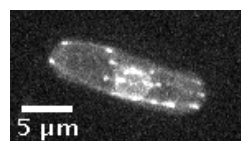
1.3.1 History and General information

Most *S. pombe* laboratory strains can be traced back to an isolation of a homothallic strain by A. Osterwalder in 1928 in Southern France. Its name originated from the Swahili word for beer. Different aspects of this yeast were investigated independently and for different reasons in the 1950's by Murdoch Mitchison in Edinburgh (mechanisms and kinetics of growth) and Urs Leupold in Zürich (genetics). Paul Nurse in the 1970's successfully merged genetic and cell cycle tools and led to the acceptance of *S. pombe* as a major model system.

Fission yeast propagates as free-living, non-motile cells that can differentiate between resting stages and sexual reproduction. Under affluent conditions it alternates between growth and division (in line with eukaryotic cells) and its nuclear envelope remains intact throughout mitosis as in many other fungi. The spindle polar body (SPB) is important for the organization of interphase microtubules and mitotic spindle.

There is a tight coordination between the nuclear division cycle and morphogenetic cycle of polarized tip growth and cytokinesis. Young fission yeast cells in the cells cycle grow only from the old end by tip extension, and they shift to bipolar growth later. There is a small pause in tip growth during septum formation right after mitosis. All these alterations are accompanied by dramatic relocation of actin and microtubule cytoskeletons as well as cell wall synthesizing components.

1.3.2 Establishment of polarity in *S. pombe*



(a)

Figure 1.2: Interphasic microtubule cytoskeleton in fission yeast. Maximum projection of 14 slices of a strain expressing Mal3p-GFP to visualize the MTs and Cut11p-GFP to visualize the nucleus.

S. pombe is a useful model organism for studying morphogenesis (Mata and Nurse, 1998; Nurse, 1994; Verde, 1998). Both microtubules and actin are important for the regulation of polarized cell growth, in contrast to *S. cerevisiae* where only actin is important. Fission yeast cells are cylindrical $\sim 4\ \mu\text{m}$ in diameter and $\sim 7\text{-}14\ \mu\text{m}$ in length. Fission yeast divides at the center of the cell by binary fission. The position of the division site is defined at the onset of mitosis by signals emanating from the nucleus and results in the assembly of an actomyosin-based contractile ring at the cell cortex (Chang and Nurse, 1996). After division, each of the daughter cells grows initially from the old end of the cell, and at some point close to the beginning of G2 phase of the cell cycle it initiates growth from the new end as well in a transition termed “new end take-off” (NETO). Minimal cell size and completion of S phase are two requirements for this transition (Mitchison and Nurse, 1985).

Both microtubules and actin are important regulators for polarization and cell growth in *S. pombe*. A newly divided fission yeast cell has one end that is at least one cell cycle older than the other end. Therefore each cell inherits a cell end that existed in the previous cell cycle (the old end) and one end that was created during cytokinesis (the new end). The changes in the growth patterns are mirrored by changes in the distribution of polymerized actin (Marks et al., 1986). F-actin is organized as actin patches at sites of cell growth, and actin cables, which traverse the long axis of the cell and function as tracks for the transport of secretory vesicles to growing cell tips. These actin cables are composed of bundles of short linear actin filaments (Kamasaki et al., 2005). Myosin S1 decoration revealed that within an actin cable most of the individual filaments are oriented in a parallel manner with their barbed (fast growing) ends facing the growing cell tips during interphase and facing the site of cell division during cytokinesis (Kamasaki et al., 2005). Actin cables are not essential for cell viability in fission yeast but contribute to polarized cell growth and serve as tracks for the delivery of myosin V-driven vesicles to the sites of cell growth (Feierbach and Chang, 2001; Motegi et al., 2001) and for the Arp2/3-dependent movement of actin patches toward the cell interior (Pelham and Chang, 2001). Patches of F-actin are initially found at the old end of the cell, after NETO they reorganize from a monopolar distribution to a bipolar distribution and are found at both growing ends, and during cytokinesis the actomyosin ring forms at the future position of the septum (Marks et al., 1986). Cables of F-actin follow a similar course throughout the cell cycle, extending along the axis of the interphase cell (Pelham and Chang, 2001), and being involved in the formation of the contractile ring at mitosis (Kamasaki et al., 2005). Transient depolymerization of actin by Latrunculin A treatment can trigger NETO, suggesting that reorganization of actin contributes to the initiation of polarized growth at the new end (Rupes et al., 1999).

The interphase microtubule cytoskeleton is organized in 3-4 bundles of antiparallel microtubules with minus ends bundled in an antiparallel fashion at the cell center and with dynamic plus ends emanating from the center and interacting distally with the cell tips (Tran et al., 2001; Drummond and Cross, 2000; Hagan, 1998). The stable overlap zone at their minus ends is termed the interphase microtubule-organizing center (iMTOC). The iMTOC is attached to the nuclear envelope in the cell center. These

minus ends show no spatial preference for specific sites at the nuclear membrane, but are instead scattered in the perinuclear region and along existing MTs (Hoog et al., 2007). The MTs bundle with each other and with the nucleus with ~ 25 nm long crossbridges (Hoog et al., 2007). The microtubules grow towards the cell ends, contact the cortex for about 100 seconds and then depolymerize towards the center of the cell (Brunner and Nurse, 2000). The large majority of catastrophe events occurs upon contact at the cell tip (Drummond and Cross, 2000). Electron microscopy studies have revealed the MTs close to the cell tips to have flared ends, a characteristic associated with depolymerizing plus ends (Hoog et al., 2007). The nucleus is positioned by the microtubules through a pushing mechanism that is dynein-independent (figure 1.3) (Tran et al., 2001; Drummond and Cross, 2000; Hagan, 1998; Yamamoto et al., 1999; Foethke et al., 2009).

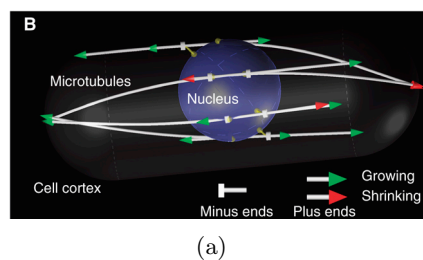


Figure 1.3: Model of interphasic microtubule cytoskeleton in fission yeast. Interphase Mts are organized in antiparallel bundles that have their minus-ends attached to the nucleus and their plus-ends extending towards the cell tips. Adapted from Foethke et al. (2009).

Although the actin cytoskeleton seems to be needed for the deposition of the growth material (Marks et al., 1986; Kobori et al., 1989; Steinberg and McIntosh, 1998), the cytoplasmic MT network has been shown to have a role in defining the site of growth (Mata and Nurse, 1998). Depolymerization of MTs either through drugs or through utilization of temperature sensitive tubulin mutants, results in the formation of T-shaped cells (Toda et al., 1983; Umesono et al., 1983; Sawin and Nurse, 1998). Polarized cell growth is also achieved in part by the localized delivery of membranes and proteins involved in cell-wall remodeling to the cell tip by means of myosin V-based transport on actin cables (Chang and Peter, 2003).

1.4 Microtubule-dependent growth in *S. pombe*

Fission yeast cells possess a distinct set of interphase microtubules with a defined spatial organization, which is important for the correct positioning of the growth zones, the nucleus, and the division site (Hagan, 1998; Mata and Nurse, 1997; Sawin and Nurse, 1998; Tran et al., 2000). The interphasic MTs in fission yeast serve as tracks for the bidirectional, long-range delivery of vesicles and molecules and for the proper positioning of cellular organelles. In vivo, the intrinsic dynamics of microtubules are controlled by

a considerable number of microtubule-associated proteins (MAPs) that can influence growth and shrinkage rates or the frequency of catastrophe and rescue (Cassimeris and Spittle, 2001).

The process of morphogenesis in fission yeast involves a plethora of proteins. In the following sections many of these proteins are looked at in detail, in particular the plus-end microtubule binding proteins (+ TIPs), which play an important role in the regulation of MT stability and cell polarity in interphase.

1.4.1 MT plus-end tips

A subset of microtubule-associated proteins (MAPs - CLIP-170, EB1 and Tea2p), which accumulates at the growing microtubule plus ends, is central to the spatial control of microtubule dynamics (Schuyler and Pellman, 2001; Schroer, 2001; Mata and Nurse, 1997; Sawin and Nurse, 1998). The molecular mechanisms of plus-end association by + TIPs though, are not well understood. Recently, a minimal plus-end tracking *in vitro* system, consisting of three fission yeast proteins, Mal3p, Tea2p and Tea1p has been described (Bieling et al., 2007). It has been shown that Mal3p has an enhanced affinity for growing MT end structures as opposed to the MT lattice. Mal3p also mediates the loading of the kinesin Tea2p, and its cargo, the CLIP-170 homolog Tip1p onto the MT lattice (Bieling et al., 2007). This work suggested that *in vivo* as well, these three proteins might constitute a minimal plus-end tracking system and for that reason we will explore their *in vivo* role in detail.

Mal3p

EB1 is a factor that was identified as a binding partner to the tumor suppressor protein adenomatous polyposis coli (APC) (Su et al., 1995). In mitosis, EB1 proteins are involved in spindle formation and in chromosome capture (Rogers et al., 2002; Tirnauer et al., 2002a), and in *Drosophila melanogaster* and budding yeast the EB1 homologs control the astral microtubules and thus play a role in spindle orientation (Rogers et al., 2002; Tirnauer et al., 1999). EB1 proteins also affect the dynamics of interphase microtubules. Human EB1, when added to *Xenopus laevis* egg extracts, promotes microtubule rescue and decreases catastrophe rates (Tirnauer et al., 2002b). *In vitro*, purified human EB1 can also promote microtubule growth (Nakamura et al., 2001) and it can partially rescue the phenotype of the Mal3p deletion in fission yeast (Beinhauer et al., 1997; Browning et al., 2003), suggesting that the functions of EB1 protein family members are highly conserved.

EB1 proteins have a calponin homology domain at the N-terminal that binds to MTs and the structure of this domain has recently been solved by crystallography (Hayashi and Ikura, 2003). The C-terminal region of EB1 contains a predicted coiled coil that is likely responsible for oligomerization and a conserved domain that mediates interaction with a number of other proteins. EB1 also plays a role in attachment of MT ends to kinetochores (Tirnauer et al., 2002a) and in targeting to the minus ends of MTs at the centrosome.

Mal3p localizes to the MT lattice, it accumulates at MT tips and there is also a large cytoplasmic pool of it (Busch and Brunner, 2004; Sandblad et al., 2006). Fluorescently labeled Mal3p is observed along the length of the MTs (Browning et al., 2003; Busch et al., 2004). Its localization is Tea2p independent (Busch et al., 2004). The localization of Mal3p to interphase microtubules is independent of Tip1p but Tip1p is needed to restrict the dissociation of microtubule tip associated Mal3p particles to the cell-end regions (Busch and Brunner, 2004).

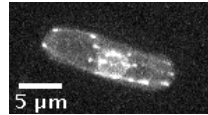


Figure 1.4: Localization of Mal3p in interphase.

Maximum projection of images of cells expressing Mal3p-GFP.

Mal3p is implicated in regulation of MT-plus-end dynamics and may function in part to load other MT-associated proteins onto MTs (Beinhauer et al., 1997). In *mal3Δ* cells there is a slight increase in the MT rescue events (Busch and Brunner, 2004). In the absence of Mal3p, catastrophe events are no longer spatially restricted, suggesting that Mal3p promotes MT growth (Busch and Brunner, 2004). MTs in *mal3Δ* mutants are short, as a result of premature catastrophe events, but display normal growth and shrinkage rates (Beinhauer et al., 1997). Mal3p associates with MTs less stably than Tip1p and Tea2p (Busch et al., 2004). These MT defects are very similar to those seen in *tip1Δ* mutants, which have no Bud6p-localization defects, suggesting that the *mal3Δ* defects are not solely due to abnormal MT behavior (Beinhauer et al., 1997).

Tip1p

CLIP-170 is a MT plus-end tracking protein that links microtubules and specialized membrane domains such as endosomes and desmosomal plaques (Rickard and Kreis, 1996). It is a conserved protein that binds to the microtubule plus end and it regulates microtubule stability by reducing the frequency of catastrophes (Carvalho et al., 2003; Busch et al., 2004). CLIP-170 can also link the MTs to specialized membrane structures (Brunner and Nurse, 2000). CLIP-170 family members also contain an N-terminal MT binding domain and a C-terminal coiled coil that is involved in protein-protein interactions (Brunner and Nurse, 2000).

In fission yeast, the CLIP-170 Tip1p stabilizes the microtubules when they contact the cell cortex at the sides of cells (Brunner and Nurse, 2000). This allows the microtubules to continue growing below the cortex, automatically orienting them parallel to the long cell axis of the cell and allowing them to efficiently target the cell ends (Brunner and Nurse, 2000). In addition, Tip1p also functions to attach Tea1p to the microtubule plus end (Feierbach et al., 2004). Tip1 mutants exhibit MTs with a shortened dwell time

at the cortex (Brunner and Nurse, 2000) and reduced Tea2p that can still associate with MTs (Busch et al., 2004). In *mal3Δ* cells, Tip1p only appears to be able to associate with microtubules at the iMTOCs, but not along the microtubules or at their tips.

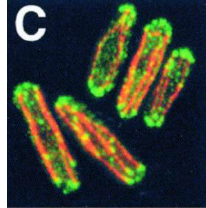


Figure 1.5: Localization of Tip1p in interphase.

Overlay of anti-Tip1p (green) and anti-tubulin (red) antibody staining (adapted from Brunner and Nurse (2000)).

In *tip1Δ* cells (similar to the *mal3Δ* cells), interphase microtubules are shortened because catastrophes can occur prematurely at the cell cortex in central regions of the cell (Beinhauer et al., 1997; Browning et al., 2003). The central region in the coiled coil domain of Tip1p is required for the Tea1p interaction (Feierbach et al., 2004). It has been shown that Tip1p (but not For3p or Bud6p) colocalizes with Tea1p on the microtubule plus end (Brunner and Nurse, 2000). Tip1p is required for proper localization of Tea1p to the microtubule plus ends and cell tips, and *tip1Δ* mutants exhibit similar morphological defects as *tea1Δ* cells (Brunner and Nurse, 2000). In *tip1Δ* mutants Tea1p dots are in multiple dots or dashes all along the microtubule and the regions of microtubule overlap with many of them being non-motile (Feierbach et al., 2004). Many Tea1p dots move in either a minus end- or plus end-directed manner and are present on all sides of microtubules (Feierbach et al., 2004).

Recently a new role of Tip1p was found in mitosis. Loss of Tip1p affects metaphase plate formation, leads to the activation of the spindle assembly checkpoint and causes appearance of lagging chromosomes, suggesting that *S. pombe* Tip1p is required for correct chromosome poleward movement independently of Mal3p (Goldstone et al., 2010).

Tea2p

Tea2p was first identified in a screen for morphology mutants (Verde et al., 1995) and was later discovered to be identical to the kinesin gene Klp4p that was identified by a search for kinesin family members in *S. pombe* (Browning et al., 2000).

Tea2p has a conserved kinesin motor domain with an N-terminal extension of 120 amino acids and a C-terminal region that includes two predicted coiled coil regions (Browning et al., 2000). It is similar to BimC and some other kinesin superfamily members in that it has an N-terminal type motor domain near its N terminus but also has an additional domain (N-terminal extension (Nte)) before the motor domain (Browning and Hackney, 2005). The rest of the molecule contains two predicted coiled coil regions and a final C-terminal non-coiled coil region (Browning and Hackney, 2005).

Tea2p has been shown to be required for normal behavior of the cell's growing tip (Verde et al., 1995). It is localized in large clusters at the cell tips in a MT-dependent manner (Fig. 1.6) and is often found in punctate dots at ends of cytoplasmic microtubules, including microtubules that do not reach the cell tip (Browning et al., 2000, 2003; Busch et al., 2004). When the growing MT reaches the cell end, part of the dot of Tea2p is deposited and remains attached to the cell end on retraction of the MT by depolymerization (Browning et al., 2003). It appears to move factors such as Tea1p and CLIP-170 to the microtubule plus end (Browning et al., 2000, 2003).

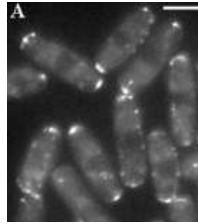


Figure 1.6: Localization of Tea2p in logarithmic phase cells

Tea2p-GFP viewed in live cells (adapted from Browning et al. (2000), scale-bar=5 μm).

Other proteins that interact with Tea2p include Mal3p, Tip1p, and Tea1p, of which Tip1p and Tea1p are deposited at the cell tips but not Mal3p (Browning et al., 2003; Brunner and Nurse, 2000; Behrens and Nurse, 2002; Busch and Brunner, 2004). It colocalizes and interacts with Tip1p through the coiled coil region of Tip1p (Busch et al., 2004). It also interacts with Mal3p, although Tea2p speckles move independently of Mal3p (Busch et al., 2004; Browning et al., 2003).

Tea2p deletion results in MTs array and cell shape defects, with many cells becoming T-shaped (Verde et al., 1995). Its deletion also reduces the MT localization of Tip1p (Busch et al., 2004). The shape abnormalities are more dramatic in long cells, either diploids or mutants that are longer than haploid wild-type cells, and in cells progressing from a phase of nongrowth to a phase of growth, suggesting that the importance of microtubules for normal cell growth varies with cell length and growth stage (Browning et al., 2000).

1.4.2 Polarity machinery

Once the plus-tip tracking system is in place, it guides the polarity machinery to direct morphogenesis. The polarity machinery is downstream of the + tip tracking system. Many proteins are known to be involved in polarity establishment, and their role is looked at in detail in the following sections.

Tea1p

Tea1p is a key player linking MTs and the actin cytoskeleton (Hayles and Nurse, 2001). Tea1p mutants were initially identified in genetic screens as mutants with curved or

T-shaped cells (Mata and Nurse, 1997; Snell and Nurse, 1994; Verde et al., 1995).

Tea1p consists of 1147 amino acids. The c-terminal regions of Tea1p are predicted to be alpha-helical coiled coil. The N-terminal part contains six kelch repeats which are likely involved in protein-protein interactions (Adams et al., 2000; Prag and Adams, 2003; Li et al., 2004).

Tea1p dots are transported to both cell tips from the middle of the cell on the growing plus end of MTs (Behrens and Nurse, 2002; Snaith and Sawin, 2003; Feierbach et al., 2004), dependent on the kip-like kinesin Tea2p (Browning et al., 2000; Brunner and Nurse, 2000; Busch et al., 2004), and the CLIP-170 like protein Tip1p, but not dependent on F-actin (Mata and Nurse, 1997). At the cell tips they are unloaded from microtubules by direct deposition and retained at the cortex (Fig. 1.7) (Feierbach et al., 2004). This retention is defective in mutants lacking either the 200 C-terminal amino acids of Tea1p or the membrane protein Mod5p (from MORphology mutant Defective 5) (Behrens and Nurse, 2002; Martin and Chang, 2003; Snaith and Sawin, 2003), but Snaith et al. (2005) suggested that this anchoring defect does not correlate with the failure to bind Mod5p. Tea1p associated at the cortex contributes to the organization of actin filaments through interactions with proteins like Tea4p and Bud6p ensuring bipolar growth (Glynn et al., 2001; Verde, 2001; Snaith et al., 2005; Tatebe et al., 2005). Tea1p appears to reside in two types of protein complexes: a 12S Tea1p-Tip1p complex and large (75S and possibly a 45S) Tea1p-Bud6p-For3p complexes, which might be a result of molecular aspects of Tea1p in the multi-step process of polarity establishment (Feierbach et al., 2004).



Figure 1.7: Localization of Tea1p-GFP in vivo.

Living cells expressing the endogenous *tea1* gene tagged with GFP. Scalebar, 3 μm . Adapted from (Behrens and Nurse, 2002).

Under stress, *tea1* Δ cells will become T-shaped or bent (Verde et al., 1995; Mata and Nurse, 1997; Niccoli et al., 2003; Sawin and Snaith, 2004). The reason for this is the inability of MTs to specify positional information at the cell cortex (Sawin and Nurse, 1998; Feierbach et al., 2004; Sawin and Snaith, 2004). In addition, *tea1* Δ cells grow in a mostly monopolar fashion (Mata and Nurse, 1997; Glynn et al., 2001) and have defects in the cortical localization of polarity factors such as the actin binding protein Bud6p (Glynn et al., 2001; Jin and Amberg, 2001), the formin For3p (Feierbach and Chang, 2001; Feierbach et al., 2004), the SH3-domain protein Tea4p (Martin et al., 2005; Tatebe et al., 2005) and Tea3p (Arellano et al., 2002). In *tea1* Δ cells, Mod5p is

localized around the cell's entire cortex (Snaith and Sawin, 2003). In *tea1* Δ cells For3p is generally localized at only one of the cell tips, and in T-shaped *tea1* Δ cells, For3p is located in the arms and is absent from both cell ends (Feierbach et al., 2004). Consistent with this, For3p is shown to be located only at the actively growing end of *tea1* Δ cells (Feierbach et al., 2004).

In rod-shaped *tea1* Δ cells, actin patches are generally more concentrated at one cell tip (consistent with their monopolar growth pattern) and actin cables are robust (Feierbach et al., 2004; Mata and Nurse, 1997). Although the numbers of actin cables close to the growing cell tip are similar in *tea1* Δ and wild-type cells, the number of actin cables at the nongrowing cell tip in *tea1* Δ cells is reduced (Feierbach et al., 2004). These distributions of actin cables are consistent with a monopolar distribution of For3p in *tea1* Δ mutants and a bipolar distribution in wild-type cells. In T-shaped *tea1* Δ cells, actin cables appear to emanate primarily from the abnormal arms, which contain For3p (Feierbach et al., 2004).

Tea1p also has a role in inhibiting cell branching upon recovery from starvation (Sawin and Snaith, 2004). The protein Mod5p is important for Tea1p anchoring at the cell ends (Snaith and Sawin, 2003). In *mod5* Δ Tea1p transport is normal, but it cannot accumulate at the cell ends (Snaith and Sawin, 2003). Mod5p, which is unusually rich in serine, proline and threonine residues, is localized to membranes at the cell tips via its C-terminal prenylation sequence.

Tea1p co-immunoprecipitates with Mod5p, independently of Tea3p (Snaith et al., 2005). Tea1p, Tea3p and Mod5p can interact pair-wisely (figure 1.8). The central region of Mod5p has been shown to be important for Tea1p and Tea3p binding. Deletion of the C-terminus of Tea1p (*tea1* Δ 200p), leads to a truncated protein that can still bind to Mod5p. Nevertheless, GFP-Mod5p localization is spread all around the membrane in *tea1* Δ 200p cells, suggesting that stable binding of Tea1p at the cortex is also required for restricting Mod5p at the cell tips Snaith et al. (2005).

In return-to-growth experiments, where cells start re-growing after having stopped at the stationary phase, the penetrance of polarity mutant phenotypes can be increased. In such experiments, wild-type cells grow from the pre-existing ends, *tea1* Δ mutants form arms and *mod5* Δ mutants re-establish polarity normally unless the microtubules are disturbed with MBC (Browning et al., 2000; Snaith et al., 2005; Snaith and Sawin, 2003). *mod5* Δ *tea3* Δ double mutants form arms at significantly higher numbers than the single mutants, suggesting that they have a distinct contribution to growth and Tea1p function. In addition, since *tea1* Δ 200 cells form arms in both the presence and the absence of MBC but can still bind to Mod5p, it is suggested that the C-terminal region of Tea1p is likely to interact not only with Tea3p but other proteins as well (Snaith et al., 2005). Also, the fact that the majority (>50%) of *mod5* Δ cells grow in a fashion reminiscent of wild-type cells, supports the view that Mod5p and Tea3p have overlapping but distinct functions and that some bipolar growth potential is maintained despite the absence of Mod5p at the cell tips (Snaith et al., 2005). This bipolar growth potential may arise as a result of Tea3p being required for proper cortical anchoring of Tea1p, especially at non-growing ends (Snaith et al., 2005).

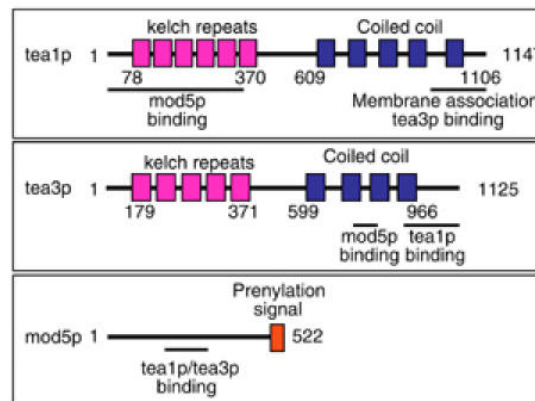


Figure 1.8: Interactions between Tea1p-Tea3p-Mod5p.

Schematic diagram summarizing interactions between Tea1p, Tea3p and Mod5p (adapted from Snaith et al. (2005)).

Therefore the targeting of Tea1p to the cell end is a two-step process which consists of microtubule-dependent transport and microtubule-independent anchoring at the cortex. In the absence of microtubules Tea1p might still diffuse to the cortex and eventually associate there, but this is dependent on the presence of Mod5p (Snaith and Sawin, 2003). This is supported by the frequency of T-shaped cells in the *tea1Δ* and *mod5Δ* cells in the presence and absence of MBC (figure 1.9). Wild type cells branch with extremely low efficiency, *mod5Δ* cells branch only in the presence of MBC, while *tea1Δ* cells branch in both the presence and the absence of MBC, suggesting that the reason the *mod5Δ* cells that are treated with TBZ phenocopy the *tea1Δ* cells is the further loss of Tea1p from the tips of the cell because of microtubule depolymerization.

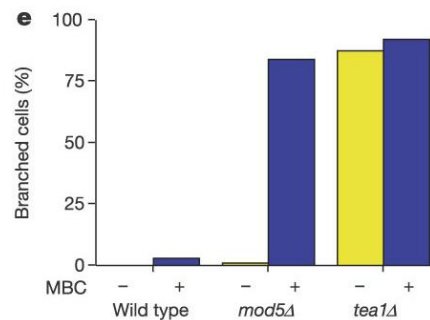


Figure 1.9: Percentage of cells forming branches in in WT, *mod5Δ* and *tea1Δ*.

Cells 3h after release to growth in the presence and absence of MBC (adapted from Snaith and Sawin (2003)).

Mod5p

Mod5p is a non-essential gene that was discovered from an insertional mutagenesis screen designed to identify genes regulating cell polarity in fission yeast (Snaith and Sawin, 2003). Early research predicted that Mod5p was membrane associated since the last four amino acids of the Mod5p are a consensus signal for C-terminal prenylation (CaaX, where C is cysteine, a is an aliphatic amino acid and X is any amino acid) (Snaith and Sawin, 2003). This motif is functionally significant since both deletions and mutations lead to disruption of the normal localization of Modp5.

The intracellular distribution of Mod5p has been investigated by immunostaining and amino-terminally tagged GFP-Mod5p and has been found to be at the cell tips (figure 1.10) (Snaith and Sawin, 2003).

Although Tea1p remains associated with microtubule ends in *mod5Δ* cells, it no longer accumulates to high levels at cell tips (Snaith and Sawin, 2003). Microtubule organization is also generally similar between wild-type and *mod5Δ* cells, although a small percentage of *mod5Δ* cells contain a microtubule curling around the cell tip (Snaith and Sawin, 2003). The role of Mod5p in the cortical localization of Tea1p has been investigated by disrupting microtubules during return-to-growth experiments (Snaith and Sawin, 2003). This procedure increases the penetrance of polarity mutant phenotypes during the first cell cycle after dilution into fresh medium (Browning et al., 2000). Through these experiments it has been concluded that a major defect associated with the loss of Mod5p is a failure to retain Tea1p at cell tips, and that this is likely to be independent of the microtubule-based targeting of Tea1p (Snaith and Sawin, 2003).

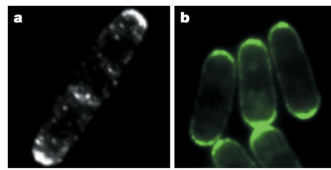


Figure 1.10: Localization of Mod5p in interphase.

a, Anti-Mod5p immunofluorescence in wild-type cells. b, Localization of GFP-Mod5p in wild-type cells (adapted from Snaith and Sawin (2003)).

Looking at Tea1p-GFP particles with live-cell microscopy, (Snaith and Sawin, 2003) found that these particles move at similar speeds in WT and *mod5Δ*. There are, though, several differences:

- 1) Upon reaching the cell cortex in *mod5Δ*, the particles either disassembled or moved away from the cortex
- 2) *Mod5Δ* cells contain more than double the Tea1p-GFP particles per cell than the WT cells
- 3) In *mod5Δ* cells the Tea1p-GFP particles are 2-3 fold brighter.

These results indicate that the targeting of Tea1p to cell tips might be a two-step process in which microtubule-dependent delivery is followed by a microtubule-independent, but Mod5p-dependent, cortical anchoring mechanism. It has been speculated that, in the

absence of microtubules, diffusion of Tea1p might allow its eventual cortical association, provided that Mod5p is present. This interpretation is supported by the frequency of abnormal, T-shaped cells observed in polarity re-establishment experiments (Fig. 1.9). In *tea1Δ* cells, a high frequency of cell branching was seen both in the absence and in the presence of MBC, whereas *mod5Δ* cells phenocopy *tea1Δ* cells only in the absence of MTs.

In *tea1Δ* cells, GFP-Mod5p is no longer at the cell tips but spreads out across the entire plasma membrane (Snaith and Sawin, 2003). In *tip1Δ* cells, in which short microtubules lead to defects in Tea1p targeting to cell tips (Brunner and Nurse, 2000), cortical GFP-Mod5p is similarly mislocalized (Snaith and Sawin, 2003). In *tea2Δ* mutants, which have a similar microtubule defect, GFP-Mod5p localization is nearly normal (Snaith and Sawin, 2003). *tea3Δ* cells show a slight spreading of GFP-Mod5p away from cell tips (Snaith and Sawin, 2003). *bud6Δ* cells have normal GFP-Mod5p localization (Snaith and Sawin, 2003).

Collectively these results suggest a positive-feedback loop in which cortically localized Mod5p at cell tips promotes the anchoring of microtubule-delivered Tea1p.

Tea3p

Tea3p was revealed through homology searches for proteins with significant morphology to Tea1p. Tea1p and Tea3p share 21% identity and 45% similarity and have similar domain structures (Arellano et al., 2002). They both have the protein-protein interaction Kelch repeats in their amino-termini and coiled-coil structures in their carboxy-termini (Adams et al., 2000; Prag and Adams, 2003; Li et al., 2004; Arellano et al., 2002).

tea3Δ cells are viable and have a NETO defect since 70% of them grow in a monopolar fashion (Arellano et al., 2002). *tea3Δ* cells resume growth from their old ends after cell division; daughter cells that inherited a previously growing end were able to use this as a site for growth (figure 1.12, (Arellano et al., 2002; Niccoli et al., 2003)). Tea3p is required to promote efficient switching from unipolar to bipolar growth.

Tea3p does not significantly associate with microtubules or Tea1p in the cytoplasm in wild-type cells (Snaith et al., 2005). It has been reported to bind to Tea1p in the yeast two-hybrid system (Arellano et al., 2002), as well as biochemically through immunoprecipitation (Snaith et al., 2005). Mod5p and Tea3p interaction has been confirmed in GST pulldown experiments and co-immunoprecipitation assays (Snaith et al., 2005).

Mutants unable to reinitiate growth efficiently at their previously growing end, generally reinitiate growth from the new end generated at cytokinesis (figure 1.13). Cells which do not inherit a previously growing end and the mutants that exhibit the most defective growth patterns, show a preference for reinitiating growth at the new end, as they activate growth at the last place where actin was located, which is the former site of septation (Niccoli et al., 2003).

Tea3p and Mod5p form a stable cortical complex. This becomes clear from both the strong chemical interaction between Tea3p and Mod5p (both in absence and in presence of Tea1p) and delocalized Tea3p in the *tea1Δ* mutants which is still associated with the cortex in a manner reminiscent of Mod5p localization in *tea1Δ* mutants (Snaith et al.,

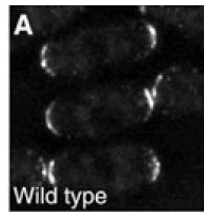


Figure 1.11: Localization of Tea3p in interphase

Tea3p-GFP localization in interphase fission yeast cells (adapted from Snaith et al. (2005)).

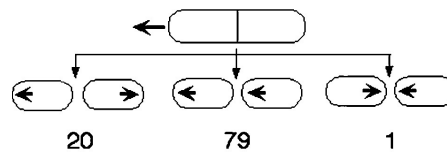


Figure 1.12: Growth patterns in WT, *tea1*Δ and *pom1*Δ cells

*tea3*Δ cells were placed on an agar pad and filmed for 16 hr. The growth patterns of pairs of daughter cells after cell division were monitored. The three patterns of growth observed are shown, and scores are expressed as percentages of total cells scored (adapted from Arellano et al. (2002)).

wt	* ←→	* ←←	* →←	* →→
	96	3	1	0
<i>tea3</i> Δ	20	79	1	0
<i>tea1</i> Δ	8	78	14	0
<i>pom1</i> Δ	10	60	30	0
<i>tea3</i> Δ <i>tea1</i> Δ	12	59	29	0
<i>tea3</i> Δ <i>pom1</i> Δ	17	22	47	14
<i>pom1</i> Δ <i>tea1</i> Δ	10	28	59	3

Figure 1.13: Growth patterns in *tea1*Δ, *tea3*Δ, *pom1*Δ cells and double mutants.

Pairs of daughter cells were monitored after cell division and four possible growth patterns were observed. The cell end marked with an asterisk (*) had been growing in the previous cell cycle. In wild-type cells both ends had been growing in the previous cell cycle. Scores are expressed as percentages of total cells scored. n=100 (Niccoli et al., 2003)

2005; Arellano et al., 2002). Furthermore *tea1*Δ*200p*, which is found at microtubule tips but is unable to stably anchor at the cell tip (Behrens and Nurse, 2002), can indeed interact with Mod5p, suggesting that the phenotype of *tea1*Δ*200* mutants which cannot bind Mod5p is a result of possible Tea1p interactions with other polarity factors through its C-terminus.

These results together suggest a positive feedback loop mechanism that guarantees spatially selective anchoring of Tea1p at the cells tips. There is localization interdependence between microtubule transported Tea1p and the cortically associated Mod5p. Mod5p anchors Tea1p at the cell tips and the cortically associated Tea1p acts as well to

prevent the spreading of Mod5p across the plasma membrane, ensuring further anchoring of Tea1p at the cell ends (Snaith and Sawin, 2003).

Tea4p

Tea4p is an SH3 domain-containing protein that was identified as a Tea1p-interacting protein (Martin et al., 2005). The C-terminal half of Tea1p is necessary and sufficient to bind Tea4p, while the C-terminal third of Tea4p mediates the interaction with Tea1p. Both of these regions contain regions of predicted coiled-coils (Martin et al., 2005).

Tea4p localizes to cell ends and to the plus ends of growing MTs, with Tea4p dots, appearing to be deposited at the cell cortex when a growing MT reaches the cell end, similar to Tea1p (Martin et al., 2005). Tea4p localization is strictly dependent on Tea1p, with Tea4p dots diffuse in the cytoplasm of *tea1* Δ cells. Tea1 Δ 200, a protein with a truncation of the Tea4p-interacting region that is deficient in cell polarity regulation but still binds to microtubules, is deficient in Tea4p localization (Behrens and Nurse, 2002; Martin et al., 2005). The cell tip localization of Tea4p depends on the same factors necessary for Tea1p localization: in *tip1* Δ and *tea2* Δ , Tea4p dots are still associated with MTs, with only low amounts detected at cell tips; in *mod5* Δ cells, Tea4p dots are present at the end of MTs, but they fail to be anchored efficiently at the cell tips. Like Tea1p, Tea4p localization is independent of Tea3p and For3p (Arellano et al., 2002; Feierbach et al., 2004). In addition the association of Tea1p with Tip1p is Tea4p independent, while the association of Tea1p with Tea4p is Tip1p dependent (Martin et al., 2005).

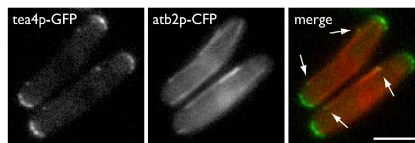


Figure 1.14: Localization of Tea4p in interphase.

Image of live cells expressing endogenous Tea4p-GFP (left; green) and CFP-Atb2p (α -tubulin) to label MTs (middle, red). Tea4p-GFP localizes to MT plus ends (arrows) and to cell tips (adapted from Martin et al. (2005), scalebar=5 μ m).

tea4 Δ cells are viable, grow at wild type rates and display defects in morphology similar to those in *tea1* Δ cells (Martin et al., 2005). They are also curved or T-shaped and grow in a monopolar fashion throughout interphase as they fail to initiate bipolar growth (Martin et al., 2005).

Tea4p is responsible for the targeting of For3p to the new end at NETO (Martin et al., 2005). In *tea4* Δ cells, For3p localizes to only the growing cell end in these monopolar cells, and it is not maintained at the nongrowing ends after cell division, showing that Tea4p is required for For3p localization at the cell tip, specifically during initiation of bipolar growth (Martin et al., 2005).

Surprisingly, Tea1p and other polarity factors associated with Tea1p, such as Mod5p,

Tip1p, Tea2p, and Tea3p are concentrated at the nongrowing cell tip in *tea4* Δ cells (Martin et al., 2005). The asymmetry of Tea1p localization is neither due to defective transport on MTs, since Tea1p dots move normally on MT plus ends toward both cell ends, nor due to abnormal For3p distribution or asymmetric actin cable organization, since Tea1p is still largely asymmetric in *tea4* Δ *for3* Δ double mutants (Martin et al., 2005). However, at the growing end, Tea1p dots are not maintained at the cortex after MT shrinkage (Martin et al., 2005).

Overexpression of Tea4p perturbs the localization of Tea1p, Tip1p, Mod5p and For3p and uncouples the localization of Tea1p and For3p (Martin et al., 2005). Overexpression of Tea4p also fills the cells with disorganized actin cables (For3p dependent) and reduced actin patches (Martin et al., 2005). An exogenous Tea1p-For3p fusion promotes NETO and restores bipolar growth in *tea4* Δ cells, showing endogenous For3p, actin cables and actin patches at both cell tips, suggesting that a major function of Tea4p may be to physically link Tea1p with For3p (Martin et al., 2005). However, in *tea4* Δ cells, For3p movements at the one growing cell tip were not significantly different from wild-type (Martin and Chang, 2006). Thus, although Tea4p is needed for establishment of For3p at a new end, at preexisting sites of growth at the old end it does not contribute significantly to formin activity (Martin and Chang, 2006).

In summary, *tea4* Δ mutants have a phenotype in which sets of polarity factors are distinct from each other; actin and formin concentrate at the growing cell tip, and Tea1p and its associated factors concentrate at the nongrowing cell tip. Thus, one function of Tea4p is to directly or indirectly bring these distinct sets of polarity factors together at cell tips for bipolar growth. As Tea1p and Tea4p are present at the new end prior to For3p, Tea4p may recruit and maintain For3p at the new end for the establishment of cell polarity.

Bud6p

Bud6p was identified on the basis of its homology to *Saccharomyces cerevisiae* Bud6/aip3 (Sc Bud6) (Jin and Amberg, 2000).

During interphase, Bud6p is localized in a crescent of dynamic dots at the cortex of both cell tips, similar to other cell tip markers such as Tea1p (Mata and Nurse, 1997; Glynn et al., 2001). During mitosis, Bud6p is localized in a broad cortical band around the nucleus and in a discrete single medial ring (Glynn et al., 2001). In addition, it is localized at both growing and non-growing ends throughout the cell cycle (Glynn et al., 2001). Lat A treatment causes first rapid loss of motility of Bud6p dots at the cell ends, and later complete delocalization of Bud6p (Glynn et al., 2001). Disruption of the microtubule cytoskeleton, on the other hand, by MBC (methyl-benzidazole-carbamate) has no apparent effects on Bud6p localization or motility (Glynn et al., 2001).

bud6 Δ mutants are viable, grow at wild-type rates and exhibit normal rod cell shapes and cell division patterns (Glynn et al., 2001). They grow in a monopolar fashion throughout interphase from the old end only, with over 50% of cells showing no new growth after NETO (Glynn et al., 2001). *bud6* Δ was also examined for cell polarity defects as a double mutant with the septation initiation factor Cdc11p. Cdc11p was

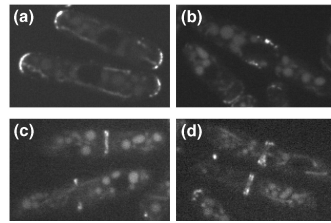


Figure 1.15: Localization of Bud6p in interphase and mitosis

Localization of Bud6p-GFP to cell tips and the cytokinesis ring. Bud6-GFP cells were imaged for GFP fluorescence confocal microscopy. In interphase cells, Bud6p-GFP is localized to cortical dots at both cell tips (a). In mitotic cells, Bud6p-GFP is localized to medial ring-like structures (b,c,d). Confocal microscopy revealed three distinct medial patterns: a medial cortical punctate band (b), a single ring (c), and double rings (d) (adapted from Glynn et al. (2001)).

identified in screens for mutants defective in cytokinesis and cell cycle progression (Nurse et al., 1976; Balasubramanian et al., 1998; Fournier et al., 2001). At the restrictive temperature, *cdc11-123* temperature sensitive cells cannot septate and accumulate as rod shaped cells with multiple nuclei (Nurse et al., 1976; Glynn et al., 2001). Almost all *cdc11-123 bud6Δ* cells become T-shaped after 4h at 36°C (Glynn et al., 2001).

When checked for possible cytoskeletal defects, *bud6Δ* cells had mostly normal actin cytoskeletons with actin patches and cables organized in a polarized distribution and with normal medial actin ring assembly and localization (Glynn et al., 2001). The microtubule organization was also normal, with interphase microtubule arrays, plus-end regulation and catastrophe and dwell times all showing no apparent difference from those in wild type cells (Glynn et al., 2001). This lack of cytoskeletal defects suggests a role of Bud6p in the regulation of cell polarity and not on cytoskeletal organization (Glynn et al., 2001).

When the patterns of growth after cell division are followed, *bud6Δ* and *tea1Δ* cells show distinct differences (figure 1.16). In *bud6Δ* mutants both daughter cells after cell division initiate growth at the old ends, while in most *tea1Δ* mutants, one daughter cell grows at the old end and the other at the new end. *Bud6Δ tea1Δ* double mutants behave similarly to *tea1Δ* cells, suggesting that instead of a structural role, Bud6p most likely has a regulatory role (Glynn et al., 2001).

Bud6Δ mutants exhibit normal concentration of actin patches at the growing end, but faint actin cables. Individual actin cables in *bud6Δ* mutants are ~50% less bright than those in wild-type cells, consistent with the fact that For3p is partially delocalized in a *bud6Δ* mutant and that budding yeast Bud6p stimulates formin activity in vitro (Moseley et al., 2004).

To summarize, Bud6p is required for the efficient establishment of polarity at the previous cell division site, it is actin associated (actin dependent localization and motility) and it functions downstream of Tea1p (Glynn et al., 2001).

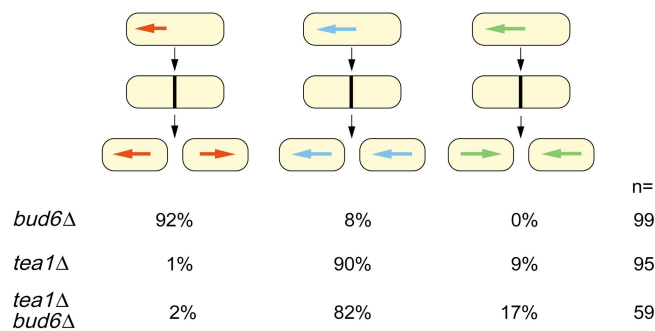


Figure 1.16: Growth pattern of *bud6Δ*, *tea1Δ* and *bud6Δ tea1Δ* double mutants.

Percentage of cells with each indicated growth pattern. Cells of the indicated genotypes were grown and imaged by time lapse light microscopy on agarose pads at room temperature for a period of 3-5 hr. Pairs of daughter cells were imaged from the time of septation or cell-cell separation. The direction of initial growth after cell division relative to the septum site was scored (adapted from Glynn et al. (2001)).

For3p

Formins are a conserved protein family of actin nucleators that have functions in the assembly of diverse actin structures and roles in cytoskeletal organization, cytokinesis and cell polarity (Wasserman, 1998; Heil-Chapdelaine et al., 1999; Pruyne and Bretscher, 2000; Wallar and Alberts, 2003). They directly nucleate actin filament assembly *in vitro* and regulate and promote actin filament elongation while bound to the growing barbed end of actin filaments through their formin homology (FH) 2 domain (Evangelista et al., 2002; Zigmond et al., 2003; Pruyne et al., 2002). The adjacent FH1 domain binds profilin, a ubiquitous actin monomer-associated protein that promotes actin nucleotide exchange and increases the rate of formin-mediated barbed end elongation (Romero et al., 2004; Kovar et al., 2003, 2006). They are also responsible for the formation of diverse actin structures such as contractile rings, actin cables, filopodia and adherens junctions (Evangelista et al., 2002; Gasman et al., 2003; Kobiela et al., 2004). Many formins bind to small GTPases such as Rho and Cdc42 proteins, which regulate autoinhibitory intramolecular interactions in the formin (Li and Higgs, 2005; Alberts, 2001). The actin nucleation activity of formins is regulated by the actin monomer binding proteins profilin and Bud6p, which bind to the proline-rich FH1 domain and the C-terminus of formins, respectively (Feierbach et al., 2004; Kovar et al., 2003; Pruyne et al., 2002; Sagot et al., 2002). The less conserved N-terminal FH3 domain targets formins to specific locations *in vivo* (Kato et al., 2001; Petersen et al., 1998).

In fission yeast 3 formins have been identified, each responsible for the formation of a distinct actin structure. The first, Cdc12p, is an essential gene required for the assembly of the medial actin-myosin ring in cytokinesis (Chang et al., 1997). The second, Fus1p, is required for cell fusion during mating and the polarization of actin (Petersen et al., 1995).

Here we will concentrate on For3p which was identified on the basis of its sequence similarity to the other formins and contains formin homology domains FH1, FH2 and FH3 and rho binding sites (Feierbach and Chang, 2001). For3p is implicated in cell polarity and the formation of actin cables (Feierbach and Chang, 2001; Nakano et al., 2002). It shows a crescent-shaped localization pattern at the cortex of growing cell tips and to the cytokinetic ring during mitosis (Feierbach and Chang, 2001; Pruyne et al., 2004; Ozaki-Kuroda et al., 2001). It interacts with Bud6p, which is necessary for efficient actin cable formation *in vivo* (Feierbach et al., 2004).

For3p is required specifically for assembly of actin cables in interphase cells (Feierbach and Chang, 2001; Nakano et al., 2002). *for3Δ* cells display a variety of different cell shapes: swollen, round, lemon shaped, banana shaped or normal rod shaped (Feierbach and Chang, 2001). *for3Δ* cells produce non-equivalent daughter cells when dividing, with one daughter cell growing in a monopolar fashion from the old end (no NETO or delayed NETO), and the other growing from both ends (premature NETO), irrespective of the pattern of growth of the parent cell (Feierbach and Chang, 2001). This inequality of daughter cells is apparent in growth pattern, cell shape and cell cycle periods (Feierbach and Chang, 2001). Cells with a birth scar from a previous division grow mostly in a bipolar manner, while the sister cells grow mostly from one end only, showing that the history of cells divisions can influence the asymmetrical cell fate (figure 1.17) (Feierbach and Chang, 2001).

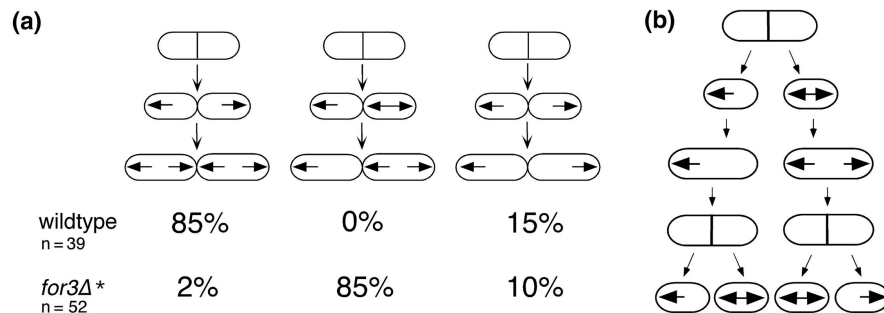


Figure 1.17: Growth patterns of WT and *for3Δ* cells.

For3p is required for symmetric division and regulation of polarized cell growth. Growth pattern lineages of wild-type and *for3Δ* cells were obtained by time-lapse DIC microscopy. (a) Growth patterns of wild-type and *for3Δ* cells over a cell cycle. Arrows represent the directions of growth in pairs of daughter cells. (b) A *for3Δ* mother cell divides medially to produce a monopolar daughter cell and a bipolar daughter cell (adapted from Feierbach and Chang (2001)).

for3Δ mutants completely lack actin cables and as a result their actin patches are disorganized. In addition, they have more microtubule bundles than wild type cells, while the growth and shrinkage rate of microtubules are normal (Feierbach and Chang, 2001). Some of the more swollen cells, however, show more disorganized microtubules that exhibit catastrophes both at the cell ends and at the cell sides.

For3p has been reported to reside as highly dynamic small cortical dots at both

cell ends of interphase wild-type cells (Feierbach and Chang, 2001; Nakano et al., 2002; Martin and Chang, 2006), but it has also been suggested that For3p is present only at the growing end of monopolar pre-NETO cells (Martin et al., 2005). For3p dots remains at cell tips for only a few seconds before either disappearing or detaching from the cortex and moving inward (Martin and Chang, 2006). Martin et al. (2005) suggested that, although some residual For3p is left at the new end immediately after cell division, it then leaves the new end, before being retargeted to the new end at NETO. Through treatment with Lat A and MBC it was found that For3p localization is dependent on actin and not on microtubules (Feierbach and Chang, 2001; Martin and Chang, 2006). Since the delivery and binding of For3p to cortical docking sites appears to be largely independent of actin, the decrease in turnover in LatA-treated cells may reflect a reduced rate of For3p departure from the cell tip (Martin and Chang, 2006). In wild type cells, For3p is established at the ends by localizing to the cell division tip and septum (Feierbach et al., 2004). In rod-shaped *tea1* Δ cells in one of the daughter cells, For3p was established at the new end (where previously the septum was), but not the old end (the end that did not grow in the previous cell cycle); in the other daughter cell, For3p was initially present at both the old and new ends immediately after cell division, but then was not maintained at the new end. This pattern is reminiscent of the Bud6p localization in *tea1* Δ mutants (Glynn et al., 2001). Bud6p and Tea1p appear to be required for the proper localization of For3p at the cell ends but not at the cell division site (Feierbach et al., 2004).

A low dose of LatA (1 μ M), which leads to loss of actin cables but not actin patches in almost all cells, results in accumulation of For3p at the cell cortex and abolishes For3p movements completely in most cells, showing that For3p movements require actin cables (Martin and Chang, 2006). In addition, For3p dots do not colocalize with actin patches, therefore For3p moves away from the cell tips on actin cables (Martin and Chang, 2006). The actin interaction domain of For3p is required for association with actin cables, but not for cortical docking (Martin and Chang, 2006). For3p needs to bind to the barbed end of the actin filament to leave the cell tip and travel down the actin cable (Martin and Chang, 2006).

Rho3p also binds the N-terminal region of For3p, but the role of this interaction is unclear (Nakano et al., 2002). In *rho3* Δ cells, For3p behavior is not significantly different from wild-type, suggesting that rho3p is not essential for For3p activation (Martin and Chang, 2006). Profilin and Bud6p contribute to the rate of formin-driven actin polymerization in vivo (Martin and Chang, 2006). In addition For3p may associate only transiently with its activator Bud6p at the cortex (Martin and Chang, 2006). For3p is regulated by the GTPase *cdc42* (Martin et al., 2007).

In *for3* Δ mutants Tea1p localization is normal at the cell tips, whereas Bud6p had normal localization in some *for3* Δ cells but was reduced from one or both ends in some others (Feierbach et al., 2004).

For3 Δ *tea1* Δ cells grow slower and have more aberrant morphology than either single mutant, as most of the cells are ovoid in shape (Moseley et al., 2004). These double mutants do not form T-shaped cells seen in *tea1* Δ cells, suggesting that For3p is required

for cell growth from the sides of cells, as is Bud6p (Moseley et al., 2004; Jin and Amberg, 2001). In addition, some of these *for3Δtea1Δ* cells exhibit long cells with multiple septa, a different morphology that was not apparent in either single mutant. This phenotype is indicative of a cell-cell separation defect and suggests a defect in initiating cell growth at the new ends (Moseley et al., 2004). *For3Δbud6Δ* double mutants were similar to *for3Δ* single mutants, whereas *bud6Δtea1Δ* mutants exhibited no synthetic effects and resembled *tea1Δ* mutants (Glynn et al., 2001). Strikingly, the *for3Δbud6Δtea1Δ* triple-mutant cells are extremely slow growing and formed round or oval cell shapes (Feierbach et al., 2004). The severe polarization defect in the triple mutant indicates that these proteins do not simply regulate the transitions from monopolar to bipolar growth as previously thought, but work together to organize general polarized growth. These synthetic genetic interactions demonstrate that these genes do not operate in a linear pathway, but may function in parallel pathways (Feierbach et al., 2004). Furthermore Tea1p, Bud6p and For3p have been shown to physically associate (Feierbach et al., 2004). These three genes localize as multiple dots at the cell tips during interphase even at non-growing cell tips and they reside at the cell division site during cell division. In just-divided cells Tea1p localization precedes For3p and Bud6p at the old cell tips. At the cell tips a subset of For3p dots colocalize with Tea1p dots while all the For3p dots colocalize with Bud6p dots (Feierbach et al., 2004).

1.4.3 Ectopic Growth Studies

Much of the research targeted at the elucidation of the polarity machinery, involved mutations in proteins that result in abnormal shapes. There has been recent work testing hypotheses from the opposite direction: examining the effects of external shape manipulation on the polarity machinery. In this section we discuss about these recent findings.

Methods

Soft-lithography and microfluidics technologies were used to create light-microscopy-enabled, polydimethylsiloxane (PDMS) elastomer-based chambers containing micrometer-scale channels of controlled shapes and appropriate dimensions for fission yeast (Terenna et al., 2008). The cells can be forced to grow normally into these channels while conforming to specific shapes, e.g., rod-shaped wild-type cells can be made to grow in a curved manner, and bent or round mutant cells can be made to grow in a straight manner (Terenna et al., 2008).

In an alternative method fission yeast cells were placed on a microfabricated PDMS array of cylindrical wells (Minc et al., 2009). Cells were then physically pushed into the wells, buckled into the chamber and adopted a bent morphology (Minc et al., 2009).

Upon bending, cells remain viable, continue to grow from their tips without any major effect on the growth rate, and go on to divide (Minc et al., 2009). Bending the cell does not create any notable stress response, such as the presence of large vacuoles and only the cell wall on the outer curvature is stretched (Minc et al., 2009).

Effects on cells

When straight fission yeast cells are forced to grow bent, there are immediate effects on the microtubule cytoskeleton in response to their new shape (Terenna et al., 2008; Minc et al., 2009). Most MTs no longer reach the cell tips, but are aligned on an axis tangential to the cell curvature and contacted the cortex primarily along the outer curvature (Minc et al., 2009). MTs exhibit normal rates of growth and shrinkage, as well as cortical dwell times, suggesting that the general mechanisms of MT regulation are not perturbed (Minc et al., 2009). The sites of MT catastrophe, though, are altered and in bent cells, most catastrophe events occur on the sides of the cells along the outer curvature (Minc et al., 2009). In most cases, the nucleus is centered, and MT catastrophes occur symmetrically on the outer curvature of the cell to both sides of the nucleus (Minc et al., 2009).

Prior to catastrophe MTs may attach to the cortex and accumulate compressive and also lateral strain as they progressively grow more bent being confined by the curved cell shape (Minc et al., 2009). “Hot spots” are present on the cortex as any MTs appeared to target to and shrink from a small number of specific sites persisting for many minutes (Minc et al., 2009). Cells in bent channels show diffuse localization of actin markers that also accumulate at the MT contact points and initiate polarized cell growth to develop a new cell tip, while the old cell tip that no longer receives microtubule contact continues polarized cell growth (Terenna et al., 2008).

Bud6p accumulates in the regions where MTs contact the cortex. Importantly, Bud6p ectopic recruitment is blocked by MBC, but not by Lat A (Minc et al., 2009). Dots of Bud6p appear within the first minute of cell bending and accumulate later (Minc et al., 2009). MTs are thus needed to recruit Bud6p and establish the ectopic site of Bud6p localization, but once established, the site can continuously recruit Bud6p from the cytoplasm (Minc et al., 2009). These direct observations provide strong evidence that MT-plus-end contact induces the local recruitment of Bud6p (Minc et al., 2009). Apart from that, the formin For3p is also redistributed to these cortical sites (Minc et al., 2009).

In bent cells, Tea1p is deposited to these ectopic sites (Minc et al., 2009). Surprisingly, Bud6p is still recruited in mutants of the Tea1p-Tea4p pathway: *tea1* Δ , *tea4* Δ , *tip1* Δ , *mod5* Δ , *pom1* Δ , *tea2* Δ , and *tea3* Δ (Minc et al., 2009). The recruitment of For3p is also Tea1p independent (Minc et al., 2009). Recruitment of Bud6p occurs normally in Tip1p mutants (Bratman and Chang, 2007; Grallert et al., 2006; Minc et al., 2009). Notably, the targeting of Bud6p to the sides is strongly reduced in *mal3* Δ , *moe1* Δ , and *mor3* Δ , although the cells can still localize Bud6p properly at cell tips (Minc et al., 2009). Moe1p is a protein has been shown to interact directly with Mal3p (Chen et al., 2000). *moe1* Δ mutants have abundant interphase MT bundles of normal length and dynamics (Chen et al., 2000). Moe1p could regulate formin For3p through its interactions with Scd1p, a Cdc42p GEF (Martin et al., 2007; Chen et al., 1999). For3p coimmunoprecipitates with Moe1p in yeast extracts (Minc et al., 2009). The recruitment of For3p is also inhibited in *mal3* Δ and *moe1* Δ mutants and it is actin independent (Minc et al., 2009).

moe1 Δ defects in Bud6p recruitment are downstream of MTs and probably also of

Mal3p (Feierbach et al., 2004). It is interesting to note that in normal cells, Bud6p localization is independent of For3p (Feierbach et al., 2004), whereas in bent cells, it is strictly dependent.

Conclusions

Taken together, these results provide the outlines of a new pathway, functionally distinct from the Tea1p-based pathway, in which MT plus ends, in conjunction with Mal3p, Moe1p, and For3p, act to recruit Bud6p to these cortical sites (Feierbach et al., 2004). In particular, Moe1p and Mal3p single mutants exhibited no NETO defects (Feierbach et al., 2004). Further, characterization of *mal3Δtea1Δ* and *moe1Δmal3Δ* double mutants does not reveal synthetic effects on cell shape or NETO, suggesting that this new Mal3p-Moe1p pathway may play a role more specifically in regulating polarity factors on the sides of cells. (Feierbach et al., 2004).

The presence of Tea1p, is responsible for repressing branching in these bent cells as is found by the branching of *tea1Δcdc25* cells (Minc et al., 2009). The sites of cell branching in the Tea1p mutants are situated at predicted sites of MT contact and are anticipated by accumulation of Bud6p at these sites (Minc et al., 2009). It is likely that this ectopic growth is driven by the collection of polarity factors at these sites, as arm formation in Tea1p mutants is formin dependent (Feierbach et al., 2004). The positions of these growth sites are dependent on MTs. *moe1Δtea1Δ* double-mutant cells, which have intact MTs, form arms, indicating that the placement of these ectopic growth sites at the sites of MT contact is dependent on MTs and Moe1p (Minc et al., 2009).

In fission yeast, the orientation of the MTs along the long axis of the cell is thought to be due to the rod cell shape and its cortical interactions (Brunner and Nurse, 2000). Terenna et al. (2008) and Minc et al. (2009) argue in favor of the existence a feedback loop between the cytoskeleton and cell shape reasoning that even a minor shape-induced focusing of microtubules would enhance subsequent focusing of +TIP and polarisome complexes in a feedback loop.

1.5 Summary

The current model for morphogenesis in fission yeast suggests a feedback loop between the cytoskeleton and cell shape with two key steps:

- Focusing of microtubules by cell shape induces focusing of polarisome deposition at cell tips.
- Retention of a focused polarisome is necessary for maintaining straight cell growth at cell tips.

The MT plus ends deliver a group of proteins known as the +TIP complex to the cell tips. This group is comprised of the kelch-repeat protein Tea1p, the kinesin-7 protein Tea2p, the CLIP-170 Tip1p and the EB1 protein Mal3p. At the cell tips Tea1p is docked to the membrane-bound receptor Mod5p. Tea1p subsequently recruits the polarisome

protein complex. The polarisome is comprised of the key polarity protein Bud6p and the formin protein For3p. For3p is responsible for the nucleation of actin filaments that serve as tracks directing the growth machinery toward cell tips (Martin and Chang, 2005; Sawin and Snaith, 2004). Mutations affecting microtubule number or dynamics cause cells to grow in a bent or T-shaped fashion (Mata and Nurse, 1997; Sawin et al., 2004; Toda et al., 1983; Umesono et al., 1983).

Overall the working model is that the actin cytoskeleton is responsible for maintaining cell polarity and cell growth and that the microtubule cytoskeleton is responsible for directing the axis of cell growth (Martin and Chang, 2005; Sawin and Snaith, 2004; Castagnetti et al., 2007). The latest results also suggest that there are at least three competing layers of polarity regulation:

- A MT-Tea1p-dependent pathway promoting tip growth.
- A MT-Moe1p-Mal3p-dependent pathway promoting polarization on the cell sides in bent cells.
- A nucleus pathway promoting branching near the nucleus when the other two pathways are absent (Castagnetti et al., 2007).

All three pathways ultimately act to recruit Bud6p and other polarity factors to discrete sites on the cortex (Minc et al., 2009).

In bent cells, Tea1p is deposited to these ectopic sites (Minc et al., 2009). Surprisingly, Bud6p is still recruited in mutants of the Tea1p-Tea4p pathway: *tea1Δ*, *tea4Δ*, *tip1Δ*, *mod5Δ*, *pom1Δ*, *tea2Δ*, and *tea3Δ* (Minc et al., 2009). The recruitment of For3p is also Tea1p independent (Minc et al., 2009).

1.6 Methods for shape change

Several mechanisms for morphogenesis outlined in the previous sections seem to be acting in parallel. These findings were made possible by perturbing the cell shape. Newly divided fission yeast cells already have a rod shape and defined cell tips, and the microtubule-membrane-actin pathway exists in a closed loop, making it difficult to determine causal relationships. In addition, fission yeast have a rigid cell wall that is remodeled by the cytoskeleton and affects shape. How this cell-wall-defined shape influences the underlying cytoskeleton is unknown.

Mutations - Mechanical perturbations

Abnormal shape can be created in fission yeast by deletions or mutations in polarity factors. This approach reveals parts of the function of the gene deleted but has the disadvantage that only a mutated genetic background can be observed, and the WT cell behavior cannot be easily extrapolated.

External (mechanical) perturbations, on the contrary, can be imposed on the WT cell and give the possibility to create different cell shapes. It is as to now unclear however how exactly the cell responds to external forces, and if some stress pathways are activated.

Microtubule depolymerization

We tried to combine advantages of both approaches by using MT depolymerizing drugs to affect the cell shape. This enables us to create T-shaped cells with a WT genetic background (as far as polarity factors are concerned) and without applying external forces. We are confident that this approach provides a valuable addition to our existing understanding of the system.

1.7 Aim of Thesis

Here, we examine the functional interplay between cell shape and the internal organization of the cell. We perturb the shape of living yeast cells in order to investigate causality between the cytoskeleton, cell polarity, and cell shape. We acquired ~1000 movies of T-shaped cells and measured geometry, MTs and cell growth. We tested the current working model, and our findings indicate that microtubules can initiate new sites of polarized cell growth in a Tea1p-Tea4p-Mod5p dependent manner. Furthermore we discovered inherent growth instability of the growth zones that were established in the absence of MTs at an ectopic site. These growth zones can cease growing and subsequently another (previously non-growing) site starts growing. This occurs only in the presence of MTs with a functional Tea1p pathway. This work reveals how simple measurements of cell parameters in large scale analyses can uncover hidden properties of biological systems.

Chapter 2

Results

2.1 Overview

First, we perturbed the cell shape with MT depolymerizing drugs in WT cells and created T-shaped cells. We assessed the growth patterns and the MT effects on growth in these cells. We found that MTs are important both for the initiation and maintenance of growth zones in G2 phase. Therefore, we decided to analyze the mutants in the Tea1p-Tea4p pathway, a well established determinant of cell polarity and Mod5p, the Tea1p anchor at the cell cortex. These results were significantly different compared to the results from the WT cells. The absence of Tea1p and Tea4p has a dramatic effect on cell behavior. We therefore tested the other proposed marker of MT-dependent polarity establishment, Bud6p. This work reveals some novel aspects of growth and MT behavior in T-shaped fission yeast cells. These aspects of growth in fission yeast cells become apparent through shape perturbation without applying external mechanical stress.

2.1.1 Terminology

In the subsequent chapters the term body is used to denote the old axis of the cell before branching and the term arm is used for the new part of the cell that is perpendicular to the old axis of the cell. In the analysis we also distinguish between the two body ends, i.e. left end and right end and also between the short or long part of the body, as measured by their dimensions at the start of the experiment. The ends were called left or right depending on where they are when we align the cells so that the body axis is horizontal and the arm axis is facing upwards. In order to create T-shaped cells we used an approach similar to Sawin and Nurse (1998), with some adaptations (figure 2.2).

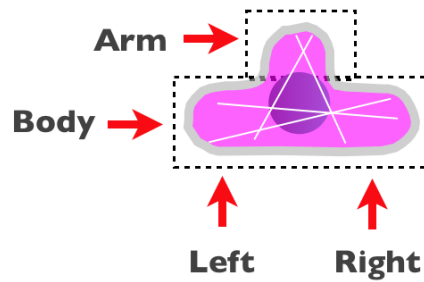


Figure 2.1: Terminology of the different parts of T-shaped cells.

2.2 Wild Type cells (WT)

2.2.1 Polarity in the presence or absence of MTs

Aim

The first issue we had to address was the behavior of the cell in the presence or absence of MTs. To perturb the shape and produce T-shaped cells, we used 3-hour treatment with the MT-depolymerizing drug TBZ and subsequent wash with minimal medium (EMM2). In a parallel experiment we washed TBZ to another MT-depolymerizing drug (MBC) to isolate the effects of MT repolymerization on the cell behavior. In that way, the polarity of the 3 ends of the T-shaped cells in the presence and absence of MT could be investigated.

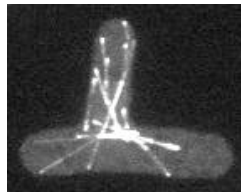


Figure 2.2: Microtubule organization in a T-shaped cell.

Maximum projection of a confocal stack of images of GFP-mal3 labeled MTs in an interphase T-shaped cell.

The branching protocol as described in the methods section was used (washing with EMM2-allowing MT repolymerization), but also in a parallel experiment the cells were treated with EMM2 containing $25 \mu\text{g}/\text{mL}$ MBC to keep the microtubules depolymerized. The strain used was FN0096.

Results

When MTs are kept depolymerized (through MBC treatment, figure 2.3, blue bars), cells keep growing only from the arm. When MTs are allowed to repolymerize (EMM2, figure 2.3, red bars), then $\sim 30\%$ of the cells stop growing from the arm and grow only from the body. Since no T-shaped cells can be found in a normal cell population, we know that all these cells were created by the protocol we used. Therefore arm growth, that was initiated in the absence of MTs is maintained if MTs are kept depolymerized.

Furthermore, a small percentage of cells ($\sim 10\%$) exhibited an interesting behavior. Upon MT repolymerization, arms continued growing for a period of 10-30 min and then they ceased growing (figure 2.3, 'Switch' bar). At the same time, growth was initiated in previously non-growing parts of the body (figure 2.4).

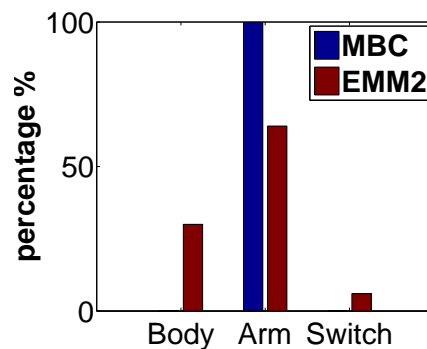


Figure 2.3: Heterogeneity of growth fates in the presence of MTs.

Percentage of cells growing only from the body parts (Body bars), only from the arm (Arm bar) or growing first from the arm and then from the body (Switch bars). Cells containing the *cdc10-129* temperature-sensitive (*ts*) mutation were synchronized at the G1-S transition through incubation at 36°C for 4 hours. Subsequently, cells were returned to 25°C to resume cell cycle progression and TBZ was added. After 3h of TBZ treatment, cells were washed with normal minimal media (red bars) or media containing containing $25\ \mu\text{g}/\text{mL}$ MBC to keep the MTs depolymerized. (n=161 cells).

Conclusion

We set out to investigate the possible contribution of MTs to cell polarity. We assessed the maintenance of growth zones in G2. The experiment showed that the growth zone that was formed in the absence of MTs (i.e. the arm) will continue growing. When MTs are allowed to repolymerize, they can reposition growth from the arm to the body of the cell. The repositioning can occur immediately after MT polymerization, or can occur later. This was an unexpected finding as it shows that MTs can influence both the maintenance and the establishment of growth zones in post-NETO T-shaped fission yeast cells.

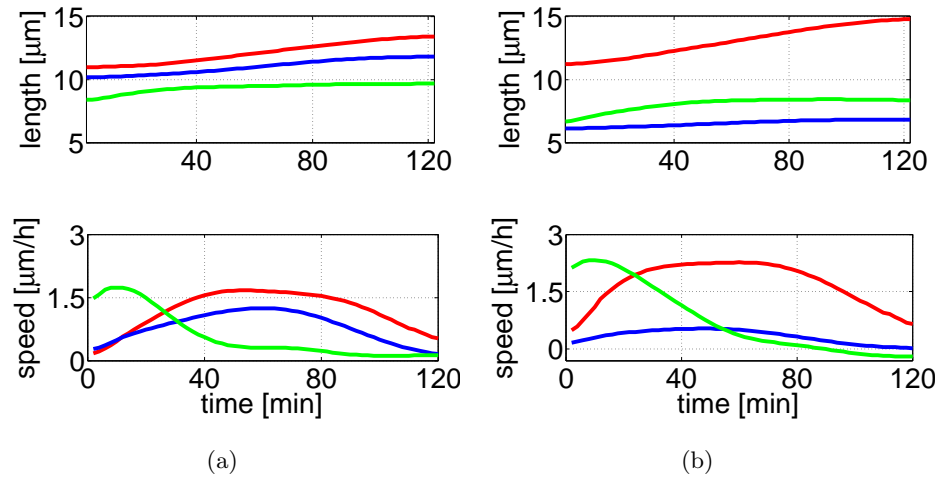


Figure 2.4: Growth plots WT T-shaped cells switching growth.

Length plots of 2 different switching cells (top panel), and growth speed plots of the same cells (bottom panel). Red=left end, blue=right end, green=arm.

In all subsequent chapters, the imaging and the analysis corresponds to the time-point of TBZ wash, that is the time of MT depolymerization.

2.2.2 Polarity of T-shaped cells

Aim

In order to assess in detail the growth patterns of cells, we imaged T-shaped cells to measure which ends are growing. In their natural (non-perturbed) state and during G2 phase of the cell cycle, WT cells are bipolar. It is interesting to see how these cells will behave at the three-end state and to categorize the cells according to which end grew during the course of the experiments. To this end, only length changes exceeding $0.5 \mu\text{m}$ were considered for further analysis.

Results

As expected, the majority of cells grew in a bipolar fashion (52.5%), consistent with their behavior at the WT-shape state (figure 3.2(a), bi. bar). Interestingly, 26.2% of cells grew monopolarly, despite being in the G2 phase of the cell cycle (figure 3.2(a), mono. bar). 50% of those monopolar cells were identified as being G2 cells since a spindle was observed forming in the course of the experiment. For the other 50% of monopolar cells, the possibility that they are unsynchronized cannot be excluded. There were also 20.6% of WT cells that exhibited growth from all 3 ends (figure 3.2(a), tri. bar). Furthermore, we noticed that T-shaped cells that have an arm with length $\sim \leq 2 \mu\text{m}$ fail to continue growing after MT repolymerization. These cells were excluded from the analysis.

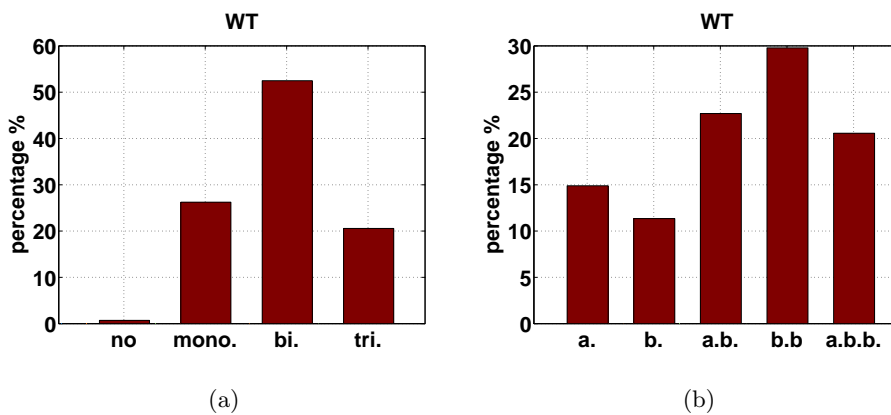


Figure 2.5: Polarity of WT T-shaped cells.

(a) Percentages of cells growing from from 0, 1, 2 or all 3 ends. For each cell in the population the total growth in the course of the experiment of each end was measured (no=no growth, mono.=monopolar growth, bi.=bipolar growth, tri.=tripolar growth). (b) Sub-categorization of monopolar, bipolar and tripolar cells according to which part of the cell was growing (a.=growth only from arm, b. growth only from 1 body end, a.b. growth from arm and 1 body end, b.b. growth from 2 body ends, a.b.b. growth from all 3 cell ends). n=282 cells.

In order to gain more insight into the process, we decided to analyze each individual end independently and understand in detail which are the ends that are growing. We found that both the monopolar and the bipolar population of WT cells can be subdivided in further categories depending on which exactly end is growing. It is interesting to note that $\sim 40\%$ of cells ceased growing from the arm (figure 2.5(b), b. b.b. bars). Furthermore $\sim 20\%$ of cells grew from all 3 ends. More careful examination revealed that in the majority of those cells growth was not sustained in all three ends throughout the experiment, but on the contrary, cells displayed switch of growth from the arm to the old end (figure 2.4).

Conclusions

The polarity differences constitute interesting observations, that at least in the case of tripolar cells and 50% of monopolar cells, cannot be explained with pre-existing knowledge. The bipolar subset of WT cells is subdivided between [arm, one body end] growth and [two body ends] growth, so bipolar WT cells can either grow or not from the arm. These observations raise further questions. Since no T-shaped cells can be found in the normal-non perturbed state of WT cells, all the T-shaped cells analyzed here were the result of the drug treatment. And since all T-shaped cells keep growing from the arm in the presence of TBZ (figure 2.3), the changes observed can only be a result of MT repolymerization.

These conclusions point out to the direction of MTs as important regulators of po-

larity in T-shaped cells. Before assessing the role of MTs in polarity, we need to measure parameters of growth and MT organization in T-shaped cells.

2.2.3 Geometry - Growth - Nucleus

Aim

The differences in the growth of the three ends triggered us to analyze the amount of growth and the growth speed of the ends. The growth speeds of T-shaped *S. pombe* cells have never been fully quantified.

Results

We accurately measured the total size of the cells. We used the central point of the cells at the base of the arm and as total size we defined the sum of lengths from that center point to the 3 ends of the cell. The size of the T-shaped cells is larger than the size (7-14 μm) of cells in a normal exponential WT population (figure 2.6(a)). The reason for that is that the cell cycle has been blocked and the cells have become longer already prior to branching. In addition we quantified the total growth for the different parts of the cell, as well as the mean and the maximum speed of growth (figure 2.6).

We quantified the locations of the nucleus and we noticed that the nucleus localizes to the area at the base of the arm (figure 2.7). In the cases where the arms are growing, the nuclei are moving towards the arm end (black marks, figures 2.7(b), 2.7(c)). The nuclei stay in the bodies of the cells in 100% of the cases in the non-growing arms (black marks, figures 2.7(d), 2.7(e), 2.7(f)). We also compared the nuclear positions with body asymmetry. Body asymmetry is the ratio of the longer to the shorter body end. Nuclei localize preferentially towards the longer body part of asymmetric bodies (figure 2.7).

Conclusion

We have accurately quantified the initial geometry, total growth, mean speed and the maximum speed of growth for each end. In addition we quantified the nuclear coordinates and followed the nuclear movements in the course of the experiment. We found that a nucleus that is moving in the arm of the cell is always an indicator for arm growth. This movement, though, is not necessary for growth, since there are cells that have their nucleus staying in the body but their arms are growing. From the nuclear movements in the arm we cannot conclude whether the nuclear movement is a cause or an effect of arm growth. When we examine the nuclear location in the different cases of body asymmetry though, we find that the nucleus is preferentially positioned towards the longer part of the body. This suggests that the nuclear position is an effect of cell geometry and not the opposite.

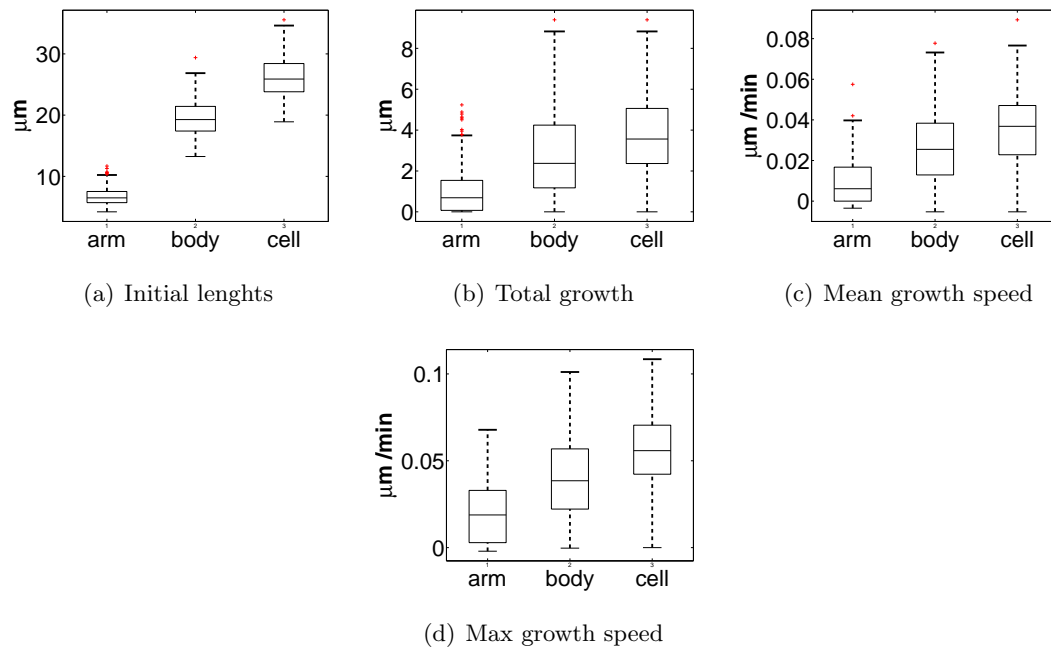


Figure 2.6: Boxplots of geometry, growth, mean and maximum speed of WT T-shaped cells.

On each box, the central mark is the median, the edges of the box are the 25th and 75th percentiles, the whiskers extend to the most extreme data points not considered outliers, and outliers are plotted individually. (a) Initial dimensions of the cell parts in μm at $t=0\text{h}$ (the time of TBZ washout). (b) Total growth of each part in the course of the experiment. (c) Mean growing speed of each part in $\mu\text{m}/\text{min}$. The mean speed was calculated by dividing the total growth of each end by the amount of time spent. (d) Maximum growing speed of each cell part in $\mu\text{m}/\text{min}$. $n=284$ cells.

2.2.4 Geometry vs Growth

Aim

It was mentioned earlier that T-shaped cells that have an arm with length $\sim \leq 2\mu\text{m}$ fail to continue growing after MT repolymerization and were excluded from the analysis. The cessation of growth of these short nascent branches led us to investigate the potential correlation of the initial length of the arm with the future growth of that arm.

Results

The initial length of the arm (arm length at MT repolymerization) displays a highly significant correlation with the total growth of the arm ($R=0.54$, $p\text{-value}=10^{-23}$). A highly significant correlation can also be found between initial length and mean speed of

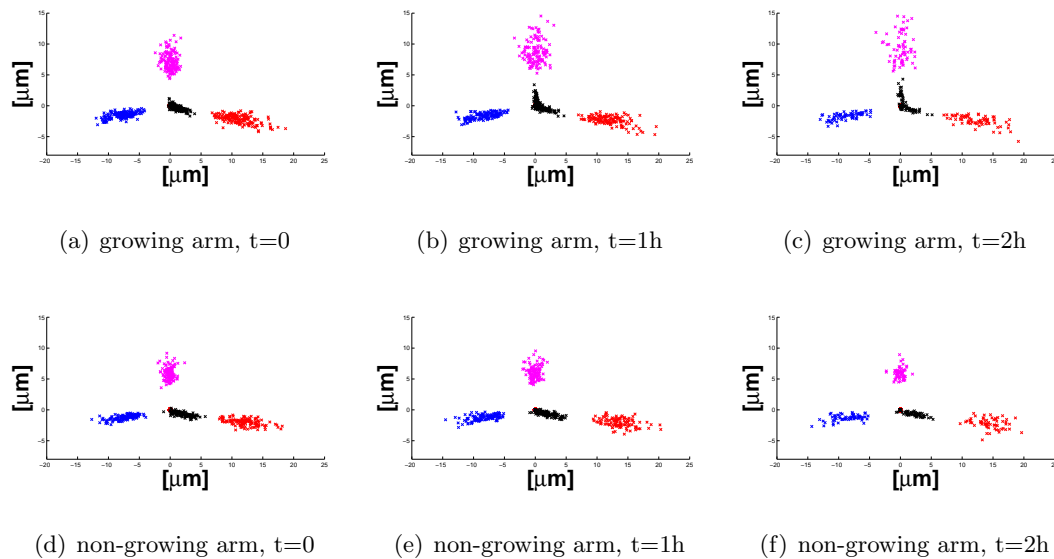


Figure 2.7: Nuclei and cell ends in growing and non-growing arms of WT T-shaped cells.

Cells were aligned at their center (see Methods) and subsequently the cells ends and the nucleus were plotted. a-c = growing arms, d-f = non-growing arms. Red=longer body end, blue=shorter body end, magenta=arm, black=nucleus, n=282 cells.

growth ($R=0.47$, $p\text{-value}=10^{-17}$, figure 2.8(b)), as well as initial length and maximum speed of growth ($R=0.59$, $p\text{-value}=10^{-28}$, figure 2.8(c)). Comparing initial length of the body, and total growth or growth speed of the body, the results are strikingly different. The correlation coefficient is low ($R=0.2\text{-}0.27$, figure 2.8 (d-f)). Similarly, there is no correlation if we look at the cell as a whole ($R=0\text{-}0.2$, figure 2.8 (g-i)). There is also negative correlation between the initial length of the arm and the growth and in the body (figure 2.9).

Conclusion

These results suggest that by looking at the initial size of the arm, we can predict to a large extent whether this arm will grow and also how much it will grow. This is not the case in the body of the cell, or if the cell is treated as a whole. Up to this point it is not clear why this correlation exists but there are some possibilities. Longer arms might have established a more mature growth zone, that can be more easily maintained after MT repolymerization. This maintenance could be MT, or nucleus dependent. In the experiments with short arms that stop growing upon MT repolymerization, the nucleus is very close to the arm ($\sim 2\text{-}3\ \mu\text{m}$). Therefore, although the the nucleus is important for

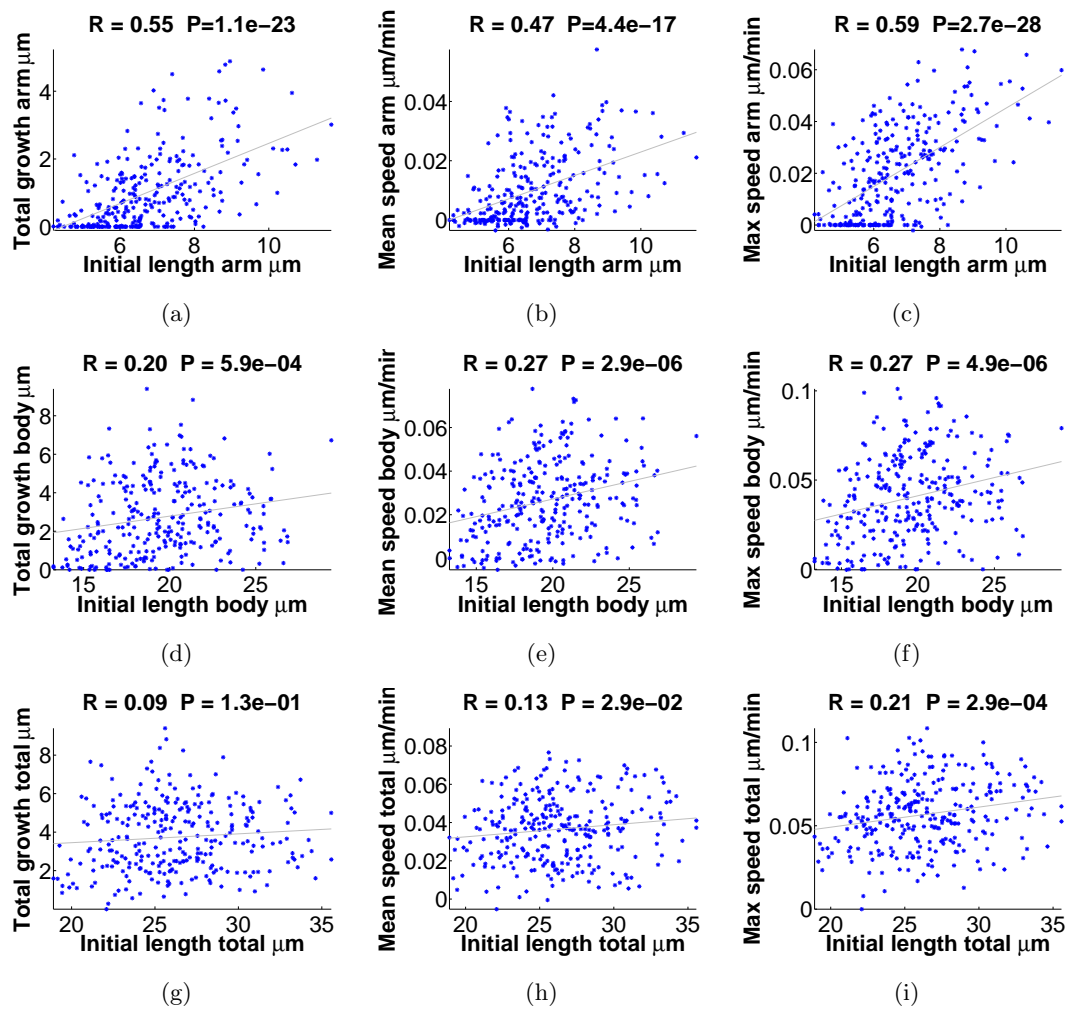


Figure 2.8: Initial length vs. growth in WT T-shaped cells.

Initial length vs. growth, mean speed and maximum speed in arms (a-c), bodies (d-f) and whole cells (g-i). Gray line = least-square line. $n=285$ cells.

establishing the growth zone at its proximity in the absence of MTs (Castagnetti et al. (2007)), it is not a positive determinant of growth zone maintenance in the presence of MTs. For that reason, we decided to assess the possible positive effect of MTs on growth.

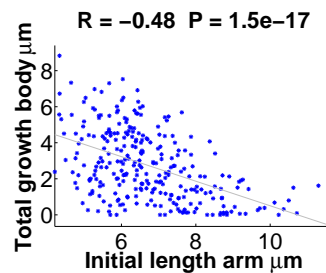


Figure 2.9: Arm-Body comparison in WT T-shaped cells.

Initial length of arm vs. total growth in body. $n=285$ cells.

2.2.5 MTs vs Growth

Aim

MTs are a key regulator of cell polarity. They transport polarity markers at the ends of the cell and are important for polarity establishment. For that reason we wanted to quantify MT organization inside the cell. We concentrated only on the tips of the cells where we quantified the distribution of MT plus ends by imaging cells with a GFP-tagged version of the plus-end MT marker Mal3p (EB1 homolog). We took into account all MT plus ends that were at a distance of less than $1.6 \mu\text{m}$ to the cell end. Afterwards, we investigated the possible relationship between MTs plus ends and cell growth. The MTs are known to be implicated in the establishment of growth zones (Castagnetti et al., 2007; Minc et al., 2009; Terenna et al., 2008), but to our knowledge the MT effect on growth speed of the cells has never been investigated.

Results

The mean number of MTs/minute in arm is 0.34 ± 0.29 MTs/min and in body $= 1.10 \pm 0.47$ MTs/min, mean \pm std (figure 2.10). On average, fewer MTs grow in the arm compared to each end of the body. Furthermore, there is negative correlation between cell size and MTs at the ends of the cell. Longer cells have fewer MTs, consistent with the length-dependent catastrophe model (figure 2.10(b)).

The mean number of MTs/min in the arm is correlated with the total growth of the arm ($R=0.58$, $p\text{-value}=10^{-27}$). A highly significant correlation is also seen between MTs/min in the arm and mean speed of growth ($R=0.51$, $p\text{-value}=10^{-21}$, figure 2.11(b)), as well as MTs/min in the arm and maximum speed of growth ($R=0.53$, $p\text{-value}=10^{-22}$, figure 2.11(c)). In the body, however, there is no correlation between MTs and growth, as measured by total growth, mean growth speed or maximum growth speed (figure 2.11, d-f). Similarly no correlation is found in the cell as a whole (figure 2.11, g-i).

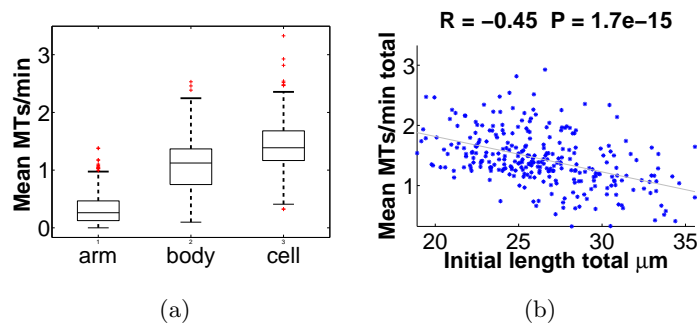


Figure 2.10: Microtubules in WT T-shaped cells in a region close to the tip.

(a) boxplot of mean MTs/min in the body. (b) scatterplot of total MTs (all MTs in all three ends) and initial total length (addition of the lengths of all cell parts). The gray line is the least-square line. $n=285$ cells.

Conclusion

We have accurately quantified the numbers of MTs plus ends that are in the proximity of the cell ends. From this analysis we conclude that MTs target preferentially the ends of the cell body. In addition we observe a significant negative correlation between total MTs and growth in the cell as a whole. These numbers can be used for more in-depth analysis and comparison between MTs and growth in the different parts of the cell. The average number of MT plus ends that reach the ends of the cell correlates with parameters that measure growth (Total growth, mean and maximum speed of growth per cell), only in the arm and not in the body of the cells. This is a novel finding that shows a fundamental difference in the nature of the growth zones in these parts of the cell. The nature of this difference is unclear but it might correspond to the different history of the growth zones: the arm was created while the MTs were absent and, as we mentioned earlier, in more than 50% of the cells it stops growing immediately upon MT repolymerization. It is already known that the history of growth of a specific end can affect this end's current growth in specific mutations. In *tea1 Δ* , if a growing end is inherited after cell division, it will continue growing, but if no growing end is inherited the new end will start growing (Glynn et al., 2001). In *for3 Δ* cells the situation is more complicated as cells divide and give rise to both monopolar and bipolar cells regardless of the pattern of growth of the parent cells (Feierbach and Chang, 2001). This finding might show an inherent instability of the growth zones that were formed in the absence of MT, or reveal a hidden role of MTs in the maintenance of growth zones.

2.2.6 Geometry vs MTs

Aim

Since MTs are correlated with growth and also geometry is correlated with growth, we wanted to assess the relationship between geometry and microtubules. We compared

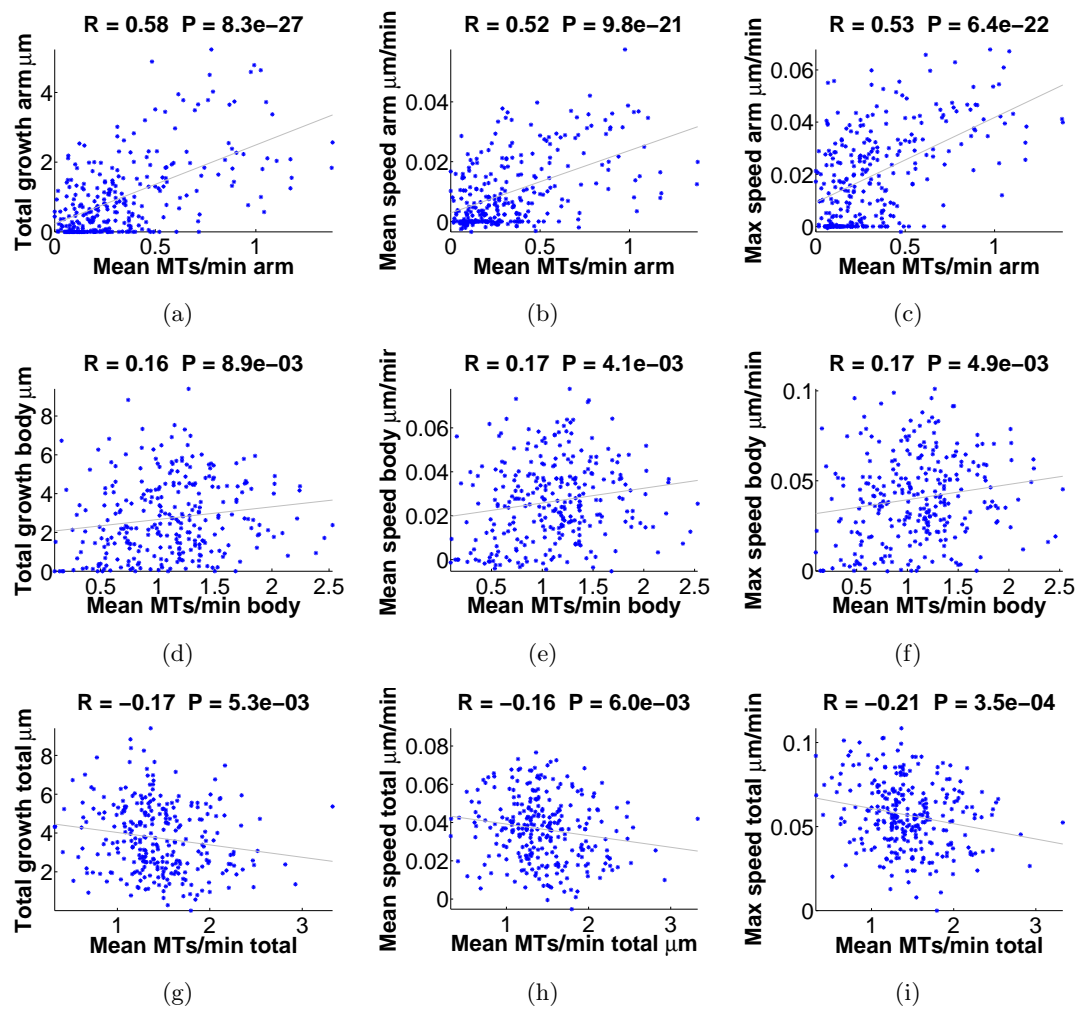


Figure 2.11: MTs vs. growth in WT T-shaped cells.

Mean MTs/min vs. growth, mean speed and maximum speed in arms (a-c), bodies (d-f) and whole cells (g-i). $n=285$ cells.

both the lengths of body ends and the body asymmetry with growth and MT organization. Body asymmetry is an inherent geometrical property of the T-shaped cells and we defined it as the ratio of the longer body end to the shorter body end.

Results

There is positive correlation between initial arm length and MTs in arm ($R=0.47$, figure 2.12(a)). This outcome is expected since both initial arm length and MTs correlate with growth (figures 2.8(a), 2.11(a)). Quite surprisingly though, the situation is reverse in the body (figure 2.12(b)): there is negative correlation between initial length and MTs.

This comes despite the fact that both initial length vs. growth and MTs vs. growth are uncorrelated in the body. Interestingly the negative correlation in the body is absent if we look at each body end individually. There is also negative correlation between body asymmetry and MTs in arm (figure 2.12(c)), but no correlation between body asymmetry and MTs in the body. Body asymmetry does not correlate with arm total growth, arm mean growth speed or arm max growth speed ($R \simeq 0.2$).

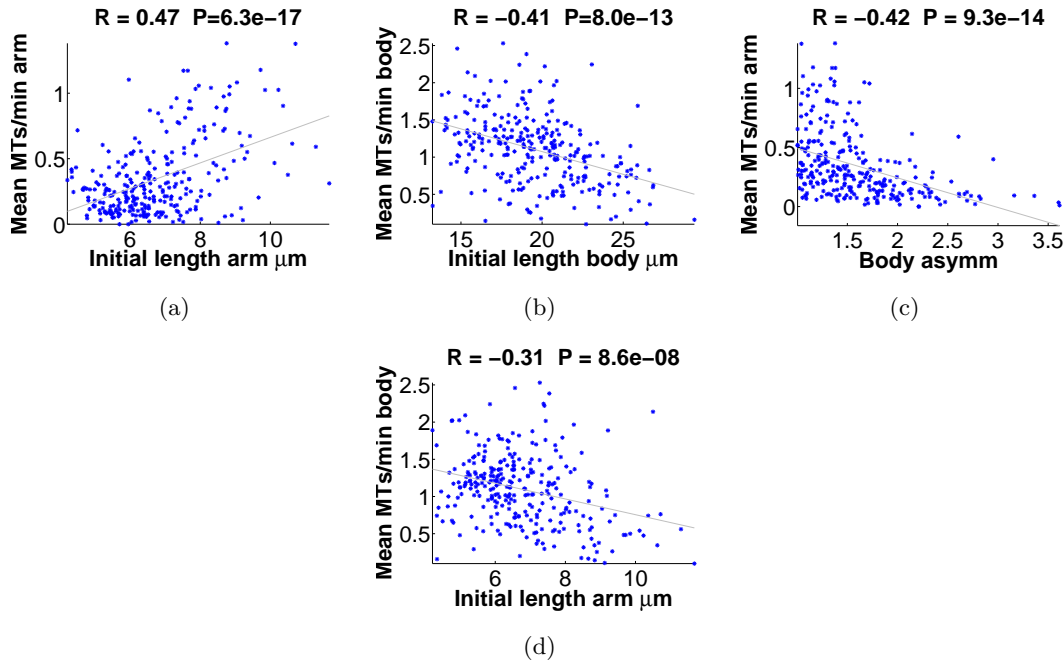


Figure 2.12: Geometry vs. MTs correlation in WT T-shaped cells.

Initial length vs. mean MTs/min in arms (a) and bodies (b), body asymmetry (ratio of long to short body end) vs. mean MTs/min in the arm (c), initial arm length vs. MTs in the body (d). $n=285$ cells.

Conclusion

These results point out to an interesting conclusion. The fact that length and MTs are negatively correlated in the body is quite expected, since longer cells have fewer MTs reaching the ends (figure 2.10(b)). Exactly for the same reason though, it is surprising that in arms the opposite holds true: the longer the arm, the more MTs it will have in the future, despite the general tendency of longer cells to have fewer MTs reaching their ends (figure 2.10(b)). In addition arms on more asymmetric bodies receive on average fewer MTs than those on symmetric bodies. We believe this is a result of different overall MT organization inside the asymmetric cells.

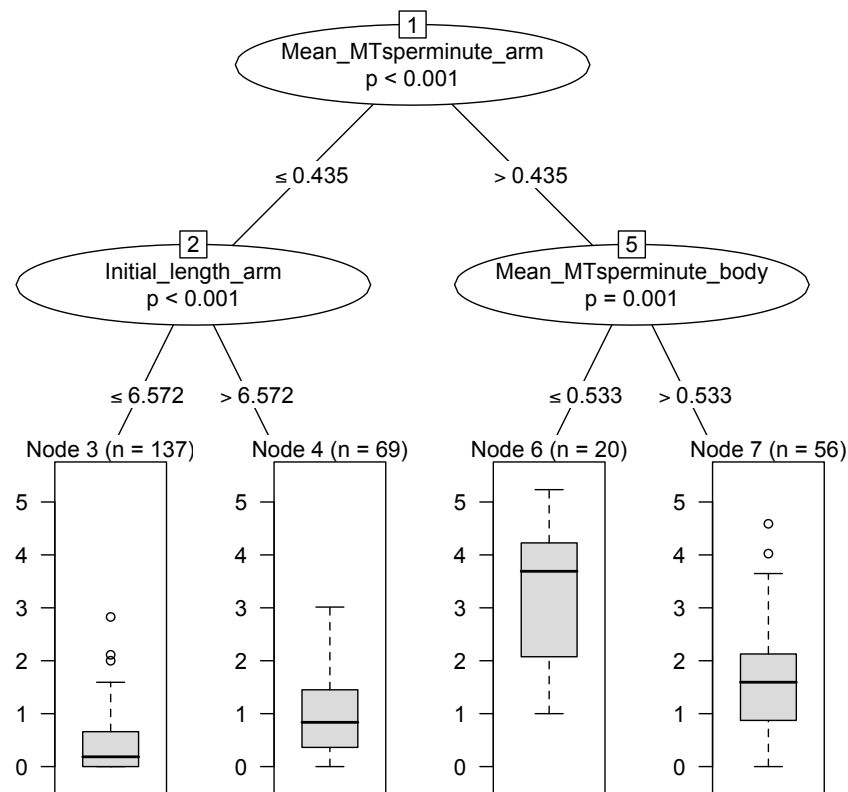


Figure 2.13: Conditional inference tree for arm total growth in WT T-shaped cells. Subdivision of the distribution of total growth for arm, according to (a) mean MTs/min in the arm and the body and (b) initial arm length.

2.2.7 Growth Maintenance - Growth Switch

As mentioned earlier, 146 out of 282 cells (51.8%), cease growing from the arm immediately upon MT repolymerization (figure 2.5, bars b., b.b.). This is a very interesting observation since it shows a drastic effect of MT repolymerization: 1) arms of the cell continue or cease growing, dependent on the number of MTs, and 2) the growth speed of arms is dependent on the number of MTs in the arm.

Furthermore, $\sim 10\%$ of cells continue growing from the arm for ~ 10 -30 min after MT repolymerization, but cease afterwards (figure 2.4). Simultaneously, one of the body ends that was not growing before starts growing. This behavior is exhibited only if MTs are present and therefore points out to the ability of MTs to establish a new growth zone in G2 phase of fission yeast cells.

2.2.8 Conclusions

We set out to investigate the growth properties of T-shaped WT cells. We successfully perturbed the shape of WT cells and produced T-shaped cells. We acquired numbers on cell geometry, cell growth, nuclear position and MT organization and found interesting pairwise dependencies (table 2.1). Most importantly we found that the repolymerization of MTs after branching is necessary for repositioning growth from the arm to the body of the cell, pointing out that MTs are important both for polarity establishment and polarity maintenance. This growth switch has not been described before and it is not in line with the current working polarity model in fission yeast. We can also use these analyses to predict possible behaviors of the different parts of the cell. Using the parameters that showed the strongest pairwise correlations we can construct a conditional inference tree predicting cell growth. Using the mean MTs/min in the arm, the initial length of the arm and the Mean MTs/min in the body we can subdivide the distribution of arm total growth in 4 subdistributions. Consistent to where our correlations point, the distribution with the highest mean is produced when we have many MTs in the arm and few in the body.

This analysis provides the framework to test some hypotheses on causality relationships, but it needs to be complemented with analyses of mutations in the Tea1p-Tea4p pathway that are the key determinants of cell polarity in *S. pombe*.

Comparison	arm	body	left	right
Initial length vs. growth	pos	no	pos	pos
MTs vs. growth	pos	pos	no	no
Initial length vs. MTs	pos	neg	no	no

Table 2.1: Pairwise correlations in WT T-shaped cells.

Summary of the main comparisons. pos=positive correlation, neg=negative correlation, no=no correlation.

2.3 *Tea1* Δ

We investigated mutants of protein Tea1p. Tea1p is a key player linking MTs and the actin cytoskeleton (Hayles and Nurse, 2001). Tea1p gets transported to both cell tips from the middle of the cell on the growing plus end of MTs (Behrens and Nurse, 2002; Snaith and Sawin, 2003; Feierbach et al., 2004). At the cell tips it is unloaded from microtubules by direct deposition and retained at the cortex (Feierbach et al., 2004). Tea1p associated at the cortex contributes to the organization of actin filaments ensuring bipolar growth (Glynn et al., 2001; Verde, 2001; Snaith et al., 2005; Tatebe et al., 2005). In T-shaped *tea1* Δ cells, actin cables appear to emanate primarily from the abnormal arms, which contain For3p (Feierbach et al., 2004).

2.3.1 Polarity of T-shaped cells

Aim

In order to assess in detail the patterns of growth of *tea1* Δ cells, we imaged T-shaped cells to measure which ends are growing. In their natural (non-perturbed) state and during G2 phase of the cell cycle, *tea1* Δ cells are monopolar and they show various abnormalities in cell shape. For imaging, we chose cells that were as similar as possible to the T-shaped of WT genetic background. That means we only took into consideration cells that had overall stable diameter, with the body of the cell on one axis, and the arm of the cell on an axis vertical to the axis of the body of the cell. It is interesting to see how these cells will behave at the three-end state and to categorize the cells according to which exactly ends grew during the course of our experiments. To this end, only length changes exceeding $0.5\ \mu\text{m}$ were considered for further analysis.

Results

As expected, the majority of cells grew in a monopolar fashion, consistent with their behavior at the unperturbed state (figure 2.14(a), bi. bar). Contrary to the WT T-shaped cells, which failed to continue growing from short arms ($\sim \leq 2\ \mu\text{m}$) after MT repolymerization, *tea1* Δ kept growing from the arm regardless of its size. In addition, almost all these monopolar cells were growing only from the arm. There were no monopolar cells that were growing from any of the body ends (figure 2.14(b)). The reasons for that remain elusive.

Conclusions

Tea1 Δ cells don't show diversity in the polarity of cells after MT depolymerization. This is consistent with their monopolar pattern of growth, but different from the effect of MT repolymerization on WT cells (figure 2.5). It is clear that Tea1p is required for the effect of MTs on the heterogeneity of growth from the three parts of the cell. It is unclear though, why these cells are growing only from the arm. The fact that they are monopolar in their non-perturbed state cannot explain the fact that only the arm

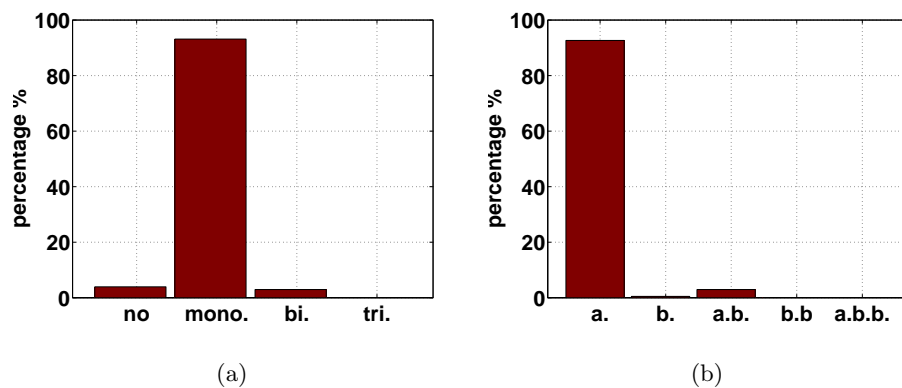


Figure 2.14: Polarity of *tea1* Δ T-shaped cells.

(a) Percentages of cells growing from from 1,2 or all 3 ends. For each cell in the population the total growth of each end was measured (no=no growth, mono.=monopolar growth, bi.=bipolar growth, tri.=tripolar growth). (b) Sub-categorization of monopolar, bipolar and tripolar cells according to which part of the cell was growing (a.=growth only from arm, b. growth only from 1 body end, a.b. growth from arm and 1 body end, b.b. growth from 2 body ends, a.b.b. growth from all 3 cell ends). n=205 cells.

will be growing. In order to shed more light into the differences between the strains, we will look in more detail into specific parameters of cell growth, cell geometry and MT behavior.

2.3.2 Geometry - Growth - Nucleus

Aim

The differences in the growth of the three ends triggered us to analyze the amount of growth and the growth speed of the ends. The growth speeds of T-shaped *tea1* Δ *S. pombe* cells have never been fully quantified.

Results

We accurately measured the total size of the cells. We used the central point of the cells at the base of the arm and as total size we defined the sum of lengths from that center point to the 3 ends of the cell. The size of the T-shaped cells is larger than the size (7-14 μ m) of cells in a normal exponential WT population (figure 2.15(a)). The reason for that is that the cell cycle has been blocked and the cells have become longer already prior to branching. In addition we quantified the total growth for the different parts of the cell, as well as the mean and the maximum speed of growth (figure 2.15).

We quantified the locations of the nucleus and we noticed that the nucleus localizes to the area at the base of the arm (figure 2.16). We did not divide the population in

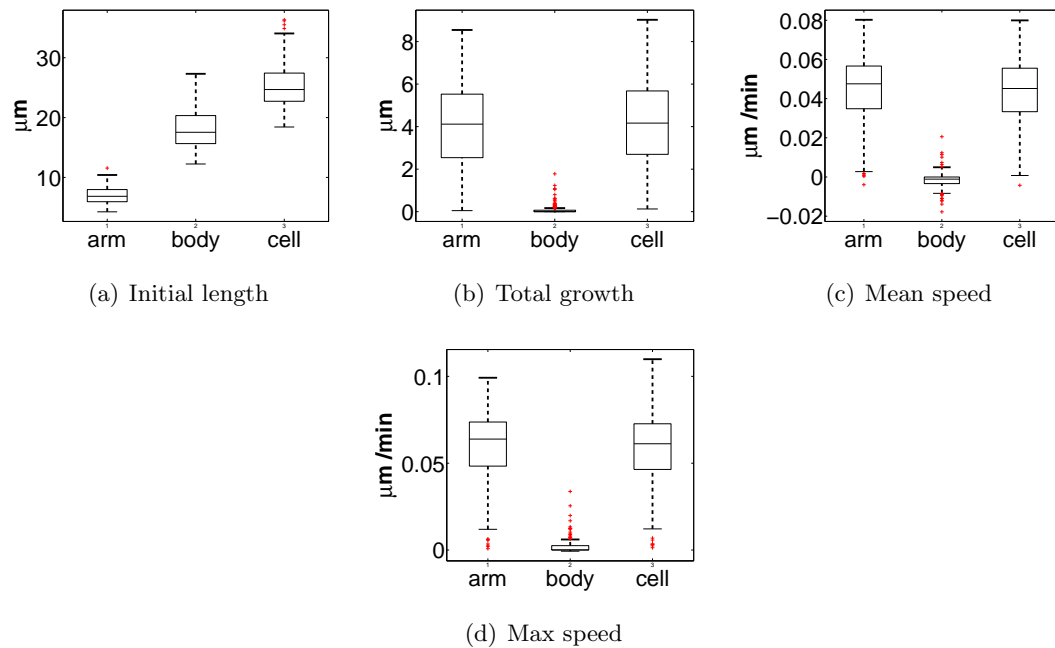


Figure 2.15: Boxplots of geometry, growth, mean and maximum speed of *tea1Δ* T-shaped cells.

(a) Initial dimensions of the cell parts in μm at $t=0\text{h}$. (b) Total growth of each part in the course of the experiment. (c) Mean growing speed of each part in $\mu\text{m}/\text{min}$. The mean speed was calculated by dividing the total growth of each end by the amount of time spent. (d) Maximum growing speed of each cell part in $\mu\text{m}/\text{min}$. $n=205$ cells.

growing and non-growing arms because in *tea1Δ* cells the majority of arms are growing. In most cells, the nuclei are moving towards the arm end (black marks, figure 2.16). We also compared the nucleus positions with body asymmetry. Body asymmetry is the ratio of the longer to the shorter body end. Nuclei localize preferentially towards the longer body part of asymmetric bodies (figure 2.16).

Conclusion

We have accurately quantified the initial geometry, total growth, mean speed and the maximum speed for each end of *tea1Δ* T-shaped cells. In addition we quantified the nuclear coordinates and followed the nuclear movements in the course of the experiment. We found that consistently with the WT cells, the nucleus is moving towards the growing arm. This movement though is not necessary for growth, since there are cells that have their nucleus staying in the body but their arms are growing. In addition, when we examine the nuclear location in the different cases of body asymmetry, we find that the nucleus is preferentially towards the longer part of the body. The fact that the nuclear

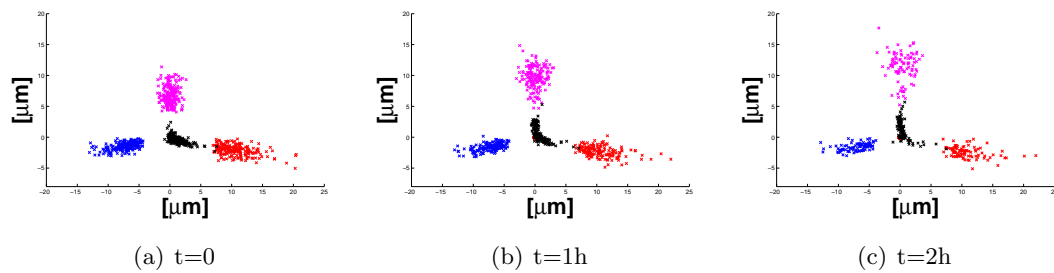


Figure 2.16: Nuclei and cell ends in *tea1* Δ T-shaped cells.

Cells were aligned at their center (see Methods) and subsequently the cell ends and the nucleus were plotted at time $t=0$ h (a), $t=1$ h (b) and $t=2$ h (c). Red=longer body end, blue=shorter body end, magenta=arm, black=nucleus, $n=205$ cells.

movements are similar in WT and *tea1* Δ suggests that they are a result of the cell geometry solely and they don't depend on the polarity mechanism. The inclusion of MT behavior in the analysis will shed more light on the causality of events, since MT organization and nuclear location are dependent on each other.

2.3.3 Geometry vs Growth

Aim

In WT cells, short arms ceased growing upon MT repolymerization, and initial arm length correlated with growth of that arm (figure 2.9). In *tea1* Δ this does not happen. Here we investigate potential correlation of the initial length of the arm with the future growth of that arm in *tea1* Δ T-shaped cells.

Results

In sharp contrast to the WT case, there is no correlation between initial dimensions of the arm and any aspects of growth in the arm (figure 2.17). On the contrary, there is a slight tendency for longer arms to grow less (figure 2.17).

Conclusions

Contrary to the WT cells, the initial size of the arm does not influence the arm growth speed or the arm total growth. Furthermore it is interesting to note that for *tea1* Δ cells, all the arms continued growing after TBZ wash irrespective of their initial length. This observation contrasts the WT cells where the very small arms ($\sim 2-3\mu\text{m}$) ceased growing upon MT repolymerization. In the next section we are assessing the possible effect of MTs on growth in *tea1* Δ T-shaped cells.

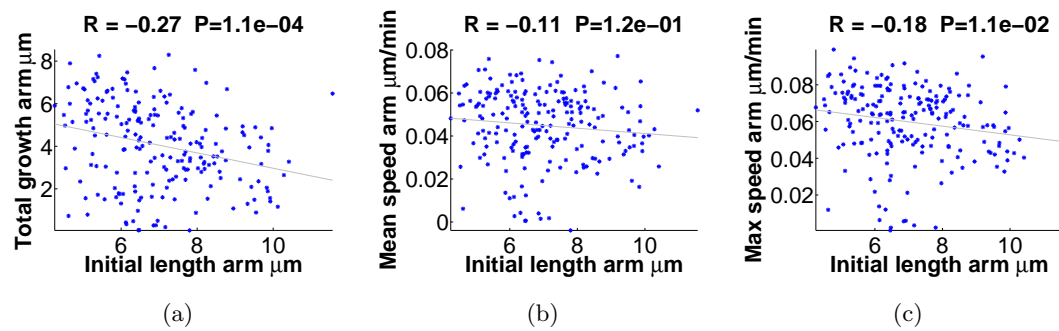


Figure 2.17: Initial length vs. growth in *tea1Δ* T-shaped cells.

Initial length vs. growth (a), mean speed (b) and maximum speed (c) in arms. $n=205$ cells.

2.3.4 MTs vs Growth

Aim

MTs, through the key polarity factor Tea1p, are regulators of cell polarity. For that reason we wanted to quantify MT organization in a *tea1Δ* background in T-shaped cells. We concentrated only on the tips of the cells where we quantified the distribution of MT plus ends by imaging cells with a GFP-tagged version of the plus-end MT marker Mal3p (EB1 homolog). We took into account all MT plus ends that were at a distance of less than $1.6 \mu\text{m}$ to the cell end. Afterwards, we investigated the possible relationship between MTs plus ends and cell growth. MTs have been known to be implicated in the establishment of growth zones (Castagnetti et al., 2007; Minc et al., 2009; Terenna et al., 2008), and here for the first time we showed that the number of MTs reaching the cell end is correlated with the growth speed in WT cells. Here we examine whether this holds true in *tea1Δ* T-shaped cells.

Results

The mean number of MTs/minute in arm is 0.41 ± 0.24 MTs/min and in body 0.8 ± 0.34 MTs/min, mean \pm std (figure 2.18(a)). On average the arm received the same number of MTs compared to each end of the body. Furthermore, there is slight negative correlation between cell size and MTs at the ends of the cell (figure 2.18(b)).

The mean number of MTs/min in the arm does not correlate with growth or growth speed in the arm (figure 2.19). This observation is different from the WT and it is expected. In the absence of *tea1p* MTs lose the ability to affect cell growth, since the master polarity regulator is missing.

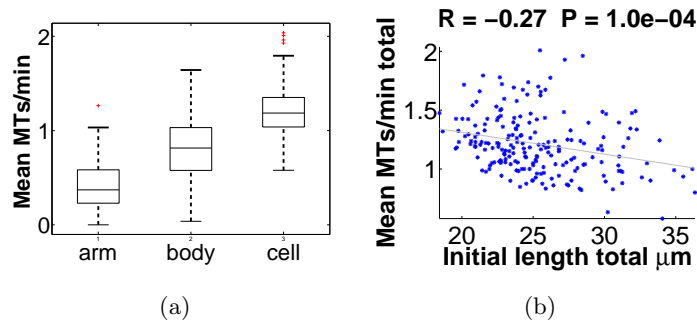


Figure 2.18: Microtubules in *tea1* Δ T-shaped cells in a region close to the tip.

(a) boxplot of mean MTs/min in the body. (b) scatterplot of total MTs (all MTs in all three ends) and initial total length (addition of the lengths of all cell parts). The gray line is the least-square line. $n=205$ cells.

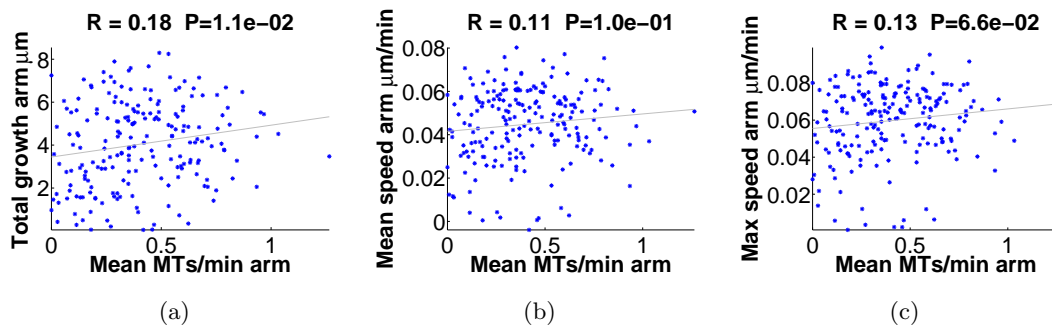


Figure 2.19: MTs vs. growth in *tea1* Δ T-shaped cells.

Mean MTs/min vs. growth (a), mean speed (b) and maximum speed (c) in arms. $n=205$ cells.

Conclusions

We have accurately quantified the numbers of MTs plus ends that are in the proximity of the cell ends. From this analysis we conclude that MTs target preferentially the ends of the cell body. In addition we observe a slight negative correlation between total MTs and growth in the cell as a whole. These numbers can be used for more in-depth analysis and comparison between MTs and growth in the different parts of the cell. The average number of MT plus ends that reach the ends of the cell does not correlate with parameters that measure growth (Total growth, mean and maximum speed of growth per cell), in *tea1* Δ T-shaped cells. This shows a fundamental difference in the nature of the arm in WT and *tea1* Δ . The inherent instability of growth zones that were formed in the absence of MT in WT cells is absent in *tea1* Δ cells. The nature of this difference is a result of the absence of the key polarity regulator Tea1p.

2.3.5 Geometry vs MTs

Aim

In this section we compare geometry with MTs. We compared both the lengths of body ends and the body asymmetry with growth and MT organization. Body asymmetry is an inherent geometrical property of the T-shaped cells and we defined it as the ratio of the longer body end to the shorter body end.

Results

There is positive correlation between initial arm length and MTs in arm ($R=0.45$, figure 2.20(a)). Quite surprisingly though, the reverse holds true in the body (figure 2.20(b)): there is no relationship between initial length and MTs. In addition we wondered whether we could see any competition between arm and body for potential growth or MTs. In figure 2.20(d) we can see how the initial length of the arm correlates inversely with MTs in the body. This is an organizational difference of the MT cytoskeleton inside the cell. There is also negative correlation between body asymmetry and MTs in arm (figure 2.20(c)).

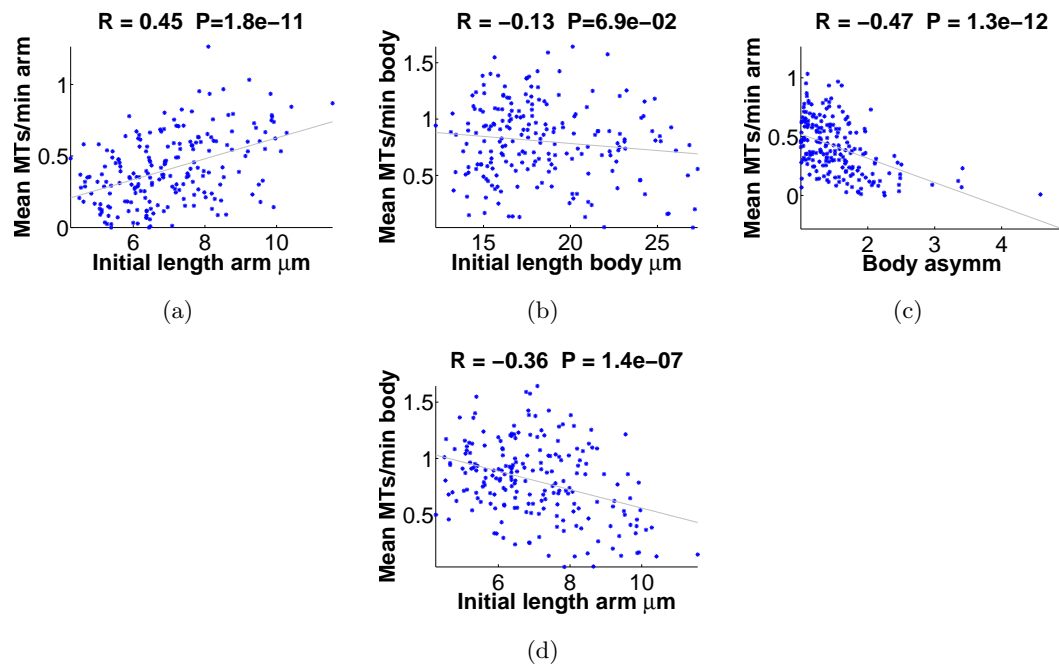


Figure 2.20: Geometry vs. MTs correlation in *tea1* Δ T-shaped cells.

Initial length vs. mean MTs/min in arms (a) and bodies (b) and body asymmetry (ratio of long to short body end) vs. mean MTs/min in the arm. (c) shows initial arm length vs. mean MTs/min in body, (d) shows initial arm length vs. MTs in the body. $n=205$ cells.

2.3.6 Growth Maintenance - Growth Switch

The *tea1* Δ cells don't exhibit any cessation of growth or switch of growth to any other end. The growth zones appear to be very stable and their maintenance is not affected by geometry or MTs.

2.3.7 Conclusions

These results point out to the direction that MTs in *tea1* Δ cells have a passive role and are organized in the cell depending on the geometry of the cell without having any obvious role in polarity. In short this comes because of the following reasons:

- 1) repolymerization of MTs does not have any noticeable effect on the previously characterized MT-dependent heterogeneity of growth fates of T-shaped cells.
- 2) MTs assume an organization that reflects the geometry of the T-shaped cells.
- 3) MTs don't correlate with any measure of growth in the *tea1* Δ T-shaped cells.

Comparison	arm	body	left	right
Initial length vs. growth	no	no	no	no
MTs vs. growth	no	no	no	no
Initial length vs. MTs	pos	no	no	no

Table 2.2: Pairwise correlations in *tea1* Δ T-shaped cells.

Summary of the main comparisons. pos=positive correlation, no=no correlation.

In the next chapter we analyze the other important polarity factor in the Tea1p polarity pathway, Tea4p.

2.4 *Tea4* Δ

We investigated mutants of protein Tea4p. Tea4p is a tea1p-interacting protein that localizes to cell ends and to the plus ends of growing MTs (Martin et al., 2005). *Tea4* Δ cells are viable, grow at wild type rates and display defects in morphology similar to the *tea1* Δ cells. They are also curved or T-shaped and they grow in a monopolar fashion throughout interphase as they fail to initiate bipolar growth (Martin et al., 2005).

2.4.1 Polarity of T-shaped cells

Aim

In order to assess in detail the patterns of growth of *tea4* Δ cells, we imaged T-shaped cells to measure which ends are growing. In their natural (non-perturbed) state and during G2 phase of the cell cycle, *tea4* Δ cells are monopolar and they show various abnormalities in cell shape, a phenotype very similar to the *tea1* Δ cells. For imaging, we chose cells that were as similar as possible to the T-shaped of WT genetic background. That means we only took into consideration cells that had overall stable diameter, with the body of the cell on one axis, and the arm of the cell on an axis vertical to the axis of the body of the cell.

Results

As expected, the majority of cells grew in a monopolar fashion, consistent with their behavior at the unperturbed state (figure 2.21(a), bi. bar). Contrary to the WT T-shaped cells, which failed to continue growing from short arms ($\sim \leq 2\mu\text{m}$) after MT repolymerization, *tea4* Δ kept growing from the arm regardless of its size. In addition, almost all these monopolar cells were growing only from the arm. There were very few monopolar cells that were growing from any of the body ends (figure 2.21(b)). There is also a small percentage of cells that exhibits some bipolarity.

Conclusions

Tea4 Δ cells (similarly to the *tea1* Δ cells), don't exhibit diversity in the polarity of cells after MT depolymerization. This is consistent with their monopolar pattern of growth, but different from the effect of MT repolymerization in WT cells (figure 2.5). Both Tea1p and Tea4p are required for this effect of MTs on the heterogeneity of growth from the three parts of the cell. After investigating each individual end independently we found that the *tea1* Δ cells, like *tea4* Δ grow only from the arm, a fact that cannot be explained just by the fact that they are monopolar. In order to shed more light into the differences between the strains, we will look in more detail into specific parameters of cell growth, cell geometry and MT behavior.

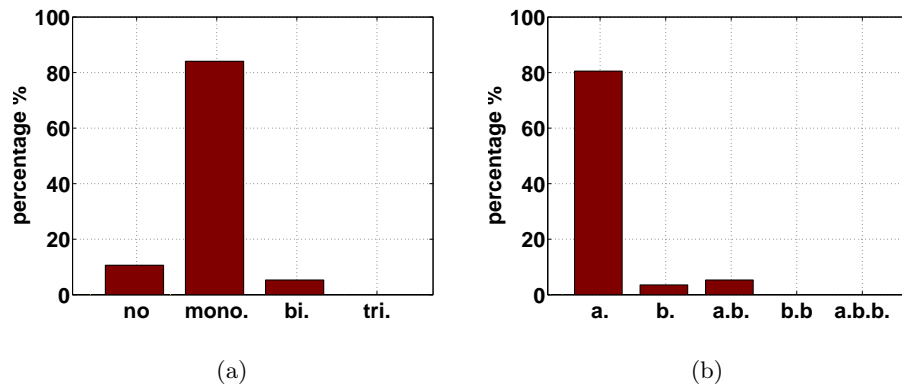


Figure 2.21: Polarity of *tea4* Δ T-shaped cells.

(a) Percentages of cells growing from from 1,2 or all 3 ends. For each cell in the population the total growth of each end was measured (no=no growth, mono.=monopolar growth, bi.=bipolar growth, tri.=tripolar growth). (b) Sub-categorization of monopolar, bipolar and tripolar cells according to which part of the cell was growing (a.=growth only from arm, b. growth only from 1 body end, a.b. growth from arm and 1 body end, b.b. growth from 2 body ends, a.b.b. growth from all 3 cell ends). n=114 cells.

2.4.2 Geometry - Growth - Nucleus

Aim

The differences in the growth of the three ends triggered us to analyze the amount of growth and the growth speed of the ends. The growth speeds of T-shaped *tea4*Δ *S. pombe* cells have never been fully quantified.

Results

We accurately measured the total size of the cells. We used the central point of the cells at the base of the arm and as total size we defined the sum of lengths from that center point to the three ends of the cell. The size of the T-shaped cells is larger than the size (7-14 μm) of cells in a normal exponential WT population (figure 2.22(a)). The reason for that is that the cell cycle has been blocked and the cells have become longer already prior to branching. In addition we quantified the total growth for the different parts of the cell, as well as the mean and the maximum speed of growth (figure 2.22).

Next, we quantified the locations of the nucleus and we noticed that the nucleus localizes to the area at the base of the arm (figure 2.23). In most cells, the nuclei are moving towards the arm end (black marks, figure 2.23). We also compared the nucleus positions with body asymmetry. We found that body asymmetry determines the nuclear position, since nuclei localize preferentially towards the longer body part (figure 2.23).

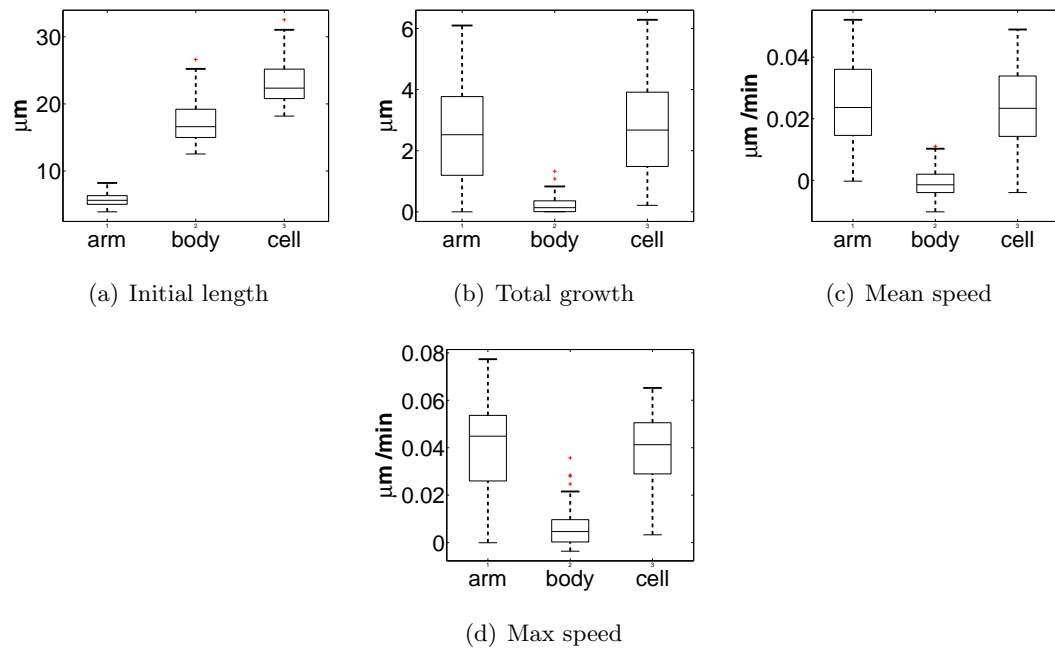


Figure 2.22: Boxplots of geometry, growth, mean and maximum speed of *tea4* Δ T-shaped cells.

(a) Initial dimensions of the cell parts in μm at $t=0\text{h}$. (b) Total growth of each part in the course of the experiment. (c) Mean growing speed of each part in $\mu\text{m}/\text{min}$. The mean speed was calculated by dividing the total growth of each end by the amount of time spent. (d) Maximum growing speed of each cell part in $\mu\text{m}/\text{min}$. $n=114$ cells.

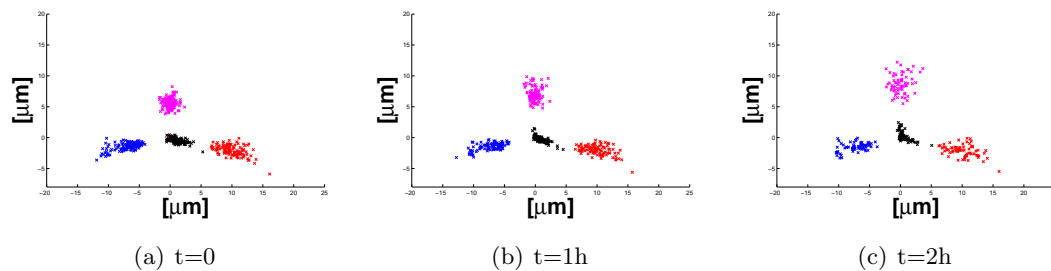


Figure 2.23: Nuclei and cell ends in *tea4* Δ T-shaped cells.

Cells were aligned at their center (see Methods) and subsequently the cell ends and the nucleus were plotted at time $t=0\text{h}$ (a), $t=1\text{h}$ (b) and $t=3\text{h}$ (c). Red=longer body end, blue=shorter body end, magenta=arm, black=nucleus, $n=205$ cells.

Conclusion

We have accurately quantified the initial geometry, total growth, mean speed and the maximum speed for each end of *tea4* Δ T-shaped cells. In addition we quantified the nuclear coordinates and followed the nuclear movements in the course of the experiment. We found that consistently with the WT and *tea1* Δ T-shaped cells, the nucleus is moving towards the growing arm. This movement though is not necessary for growth, since there are cells that have their nucleus staying in the body but their arms are growing. In addition, when we examine the nuclear location in the different cases of body asymmetry, we find that the nucleus is preferentially towards the longer part of the body. The fact that the nuclear movements are similar in WT, *tea1* Δ and *tea4* Δ cells, suggests that they are a result of the cell geometry solely and they don't depend on the polarity mechanism. The inclusion of MT behavior in the analysis will shed more light in the causality of events, since MT organization and nuclear location are dependent on each other.

2.4.3 Geometry vs Growth

Aim

In WT cells, short arms ceased growing upon MT repolymerization, and initial arm length correlated with growth of that arm (figure 2.9). In *tea1* Δ cells there was no relationship between geometry and growth in the arm (figure 2.17). Here we investigate potential correlation of the initial length of the arm with the future growth of that arm *tea4* Δ T-shaped cells.

Results

In sharp contrast to the WT cells (but similarly to the *tea1* Δ cells), there is no correlation between initial dimensions of the arm and any aspects of growth in the arm (figure 2.24).

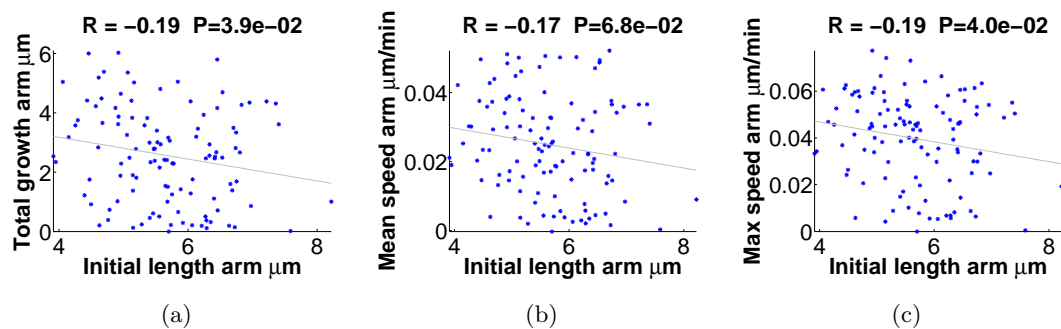


Figure 2.24: Initial length vs. growth in *tea4* Δ T-shaped cells.

Initial length vs. growth (a), mean speed (b) and maximum speed (c) in arms. $n=114$ cells.

Conclusions

These findings are very similar to the *tea1* Δ cells. Contrary to the WT cells, the initial size of the arm does not influence the arm growth speed or the arm total growth. Furthermore it is interesting to note that in *tea4* Δ cells, all the arms continued growing after TBZ wash irrespective of their initial length. This observation contrasts the WT cells, where the very small arms ($\sim 2\text{-}3\ \mu\text{m}$) ceased growing upon MT repolymerization. In the next section we are assessing the possible effect of MTs on growth in *tea4* Δ T-shaped cells.

2.4.4 MTs vs Growth

Aim

MTs are regulators of cell polarity. Here we measure properties of MTs in the *tea4* Δ T-shaped cells. We concentrated only on the tips of the cells where we quantified the distribution of MT plus ends by imaging cells with a GFP-tagged version of the plus-end MT marker Mal3p (EB1 homolog). We took into account all MT plus ends that were at a distance of less than $1.6\ \mu\text{m}$ to the cell end. In addition, we investigated the possible relationship between MTs plus ends and cell growth. The implication of MTs in the establishment of growth zones (Castagnetti et al., 2007; Minc et al., 2009; Terenna et al., 2008), led us to examine their behavior. For the first time we showed that the number of MTs reaching the cell end is correlated with the growth speed in WT cells. In *tea1* Δ this phenomenon is absent. Here we examine whether this holds true in *tea4* Δ T-shaped cells.

Results

The mean number of MTs/minute in arm is 0.37 ± 0.21 MTs/min and in body is 1.14 ± 0.33 MTs/min, mean \pm std (figure 2.25(a)). On average the arm received fewer MTs than each body end. Furthermore, there is a negative correlation between cell size and MTs at the ends of the cell, similar to WT cells and unlike *tea1* Δ cells (figures 2.10(b), 2.18(b), 2.25(b)).

The mean number of MTs/min in the arm does correlate with growth and growth speed in the arm (figure 2.26). This observation is quite surprising. It was expected that in the absence of Tea1p MTs lose their ability to affect cell growth, since the master polarity regulator is missing. Tea4p on the other hand, is a protein with very similar function to Tea1p, it functions in the same pathway, its deletions have very similar phenotype to the *tea4* Δ , but nevertheless a significant correlation can be found between growth and MTs in *tea4* Δ cells.

Conclusions

We have accurately quantified the numbers of MTs plus ends that are in the proximity of the cell ends. From this analysis we conclude that MTs target preferentially the ends of the cell body. These results are very similar to the results from *tea1* Δ , apart from the

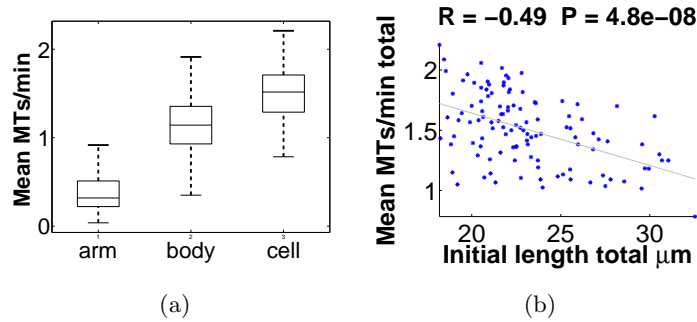


Figure 2.25: Microtubules in *tea4* Δ T-shaped cells in a region close to the tip.

(a) boxplot of mean MTs/min in the body. (b) scatterplot of total MTs (all MTs in all three ends) and initial total length (addition of the lengths of all cell parts). The gray line is the least-square line. $n=114$ cells.

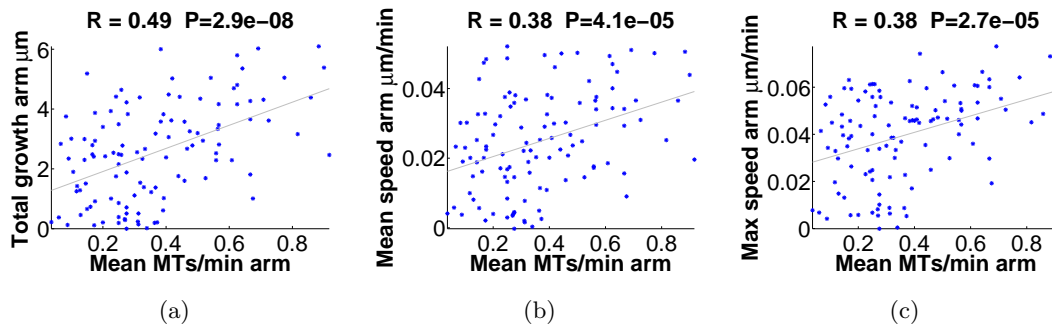


Figure 2.26: MTs vs. growth in *tea4* Δ T-shaped cells.

Mean MTs/min vs. growth (a), mean speed (b) and maximum speed (c) in arms. $n=114$ cells.

average number of MTs per minute in body, which is 0.81 in *tea1* Δ and 1.14 in *tea4* Δ , a difference that is statistically significant. This difference comes independently of the mean MTs in the arm, and therefore results in total higher number of MTs in *tea4* Δ . Furthermore there is negative correlation between cell size and total number of MTs in the *tea4* Δ (figure 2.25(b)). These numbers can be used for more in-depth analysis and comparison between MTs and growth in the different parts of the cell.

Here we have also found an aspect of the behavior of *tea4* Δ cells that is similar to the WT cells and unlike the *tea1* Δ cells. The average number of MT plus ends that reach the ends of the cell correlates with parameters that measure growth (Total growth, mean and maximum speed of growth per cell), only in the arm of *tea4* Δ cells. In the body of *tea4* Δ there is no such correlation. This shows a fundamental difference in the nature of the arm in *tea4* Δ and *tea1* Δ . The nature of this difference is unclear since both Tea1p and Tea4p are known to have very similar functions, and their deletions have very similar

phenotypes. This finding might reveal a difference in the function of Tea1p and Tea4p where *tea4Δ* cells can still partially use the Tea1p available to affect the growth of arms and provide a link between MTs and growth speed.

2.4.5 Geometry vs MTs

Aim

In this section we compare geometry with MTs. We compared both the lengths of body ends and the body asymmetry with growth and MT organization. Body asymmetry is an inherent geometrical property of the T-shaped cells and we defined it as the ratio of the longer body end to the shorter body end.

Results

There is no correlation between initial arm length and MTs in arm of *tea4Δ* T-shaped cells (figure 2.27(a)). Quite surprisingly though, the reverse holds true in the body (figure 2.27(b)): there is negative correlation between initial length and MTs. This finding is contrary to the situation in *tea1Δ* cells (figure 2.20(a)). In addition, higher body asymmetry leads to lower number of MTs in the arm (figure 2.27(c)). Apart from that, we wondered whether we could see any competition between arm and body for potential growth or MTs, but we found no correlation (figure 2.27(d)).

2.4.6 Growth Maintenance - Growth Switch

TeaΔ cells (similar to the *tea1Δ* cells) don't exhibit any cessation of growth or switch of growth to any other end. The growth zones appear to be very stable and their maintenance is not affected by geometry or MTs. It is only the speed of growth of the arms of *tea4Δ* T-shaped cells that seems to be affected by the presence of MTs.

2.4.7 Conclusions

These results point out to a novel direction. Although thought to be very similar to *tea1Δ* cells, MTs in *tea4Δ* cells can affect the growth speed of the arm. This role appears to be very limited because all the other aspects of our analysis of the *tea4Δ* cells reveals similar behaviors to the *tea1Δ* cells. The MTs in *tea4Δ* T-shaped cells have a mainly passive role and are organized in the cell depending on the geometry. They cannot refocus the growth zones to other parts of the cell, although they can exert a minor role in the growth of the arm that is already growing. In short:

- 1) repolymerization of MTs does not have any noticeable effect on the previously characterized MT-dependent heterogeneity of growth fates of T-shaped cells.
- 2) MTs assume an organization that reflects the geometry of the T-shaped cells.
- 3) MTs correlate with growth in the arms of *tea4Δ* T-shaped cells.

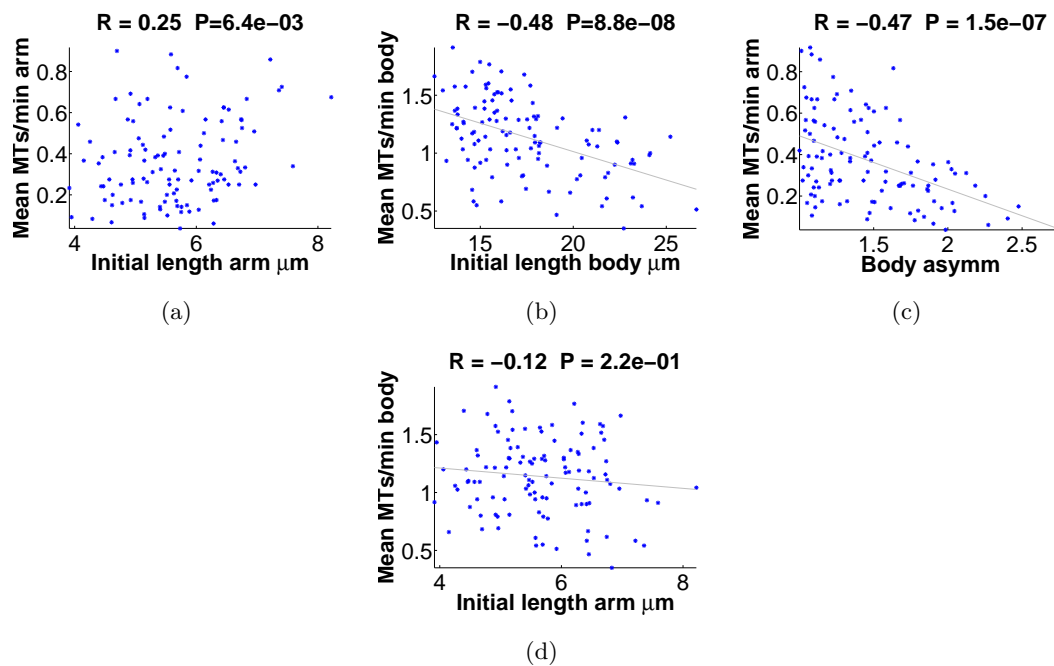


Figure 2.27: Geometry vs. MTs correlation in *tea4* Δ T-shaped cells.

Initial length vs. mean MTs/min in arms (a) and bodies (b) and body asymmetry (ratio of long to short body end) vs. mean MTs/min in the arm. (c) shows initial arm length vs. mean MTs/min in body. n=114 cells.

Comparison	arm	body	left	right
Initial length vs. growth	no	no	no	no
MTs vs. growth	pos	no	no	no
Initial length vs. MTs	no	neg	no	no

Table 2.3: Pairwise correlations in *tea4* Δ T-shaped cells.

Summary of the main comparisons. pos=positive, neg=negative and no=no correlation.

In the next chapter we analyze Mod5p, the cell end anchor of the polarity protein Tea1p.

2.5 *Mod5* Δ

The protein Mod5p has an elusive role in polarity determination. Despite being the anchor of Tea1p at the cells ends, its deletion phenotype is not severe: *mod5* Δ cells appear to be WT in appearance and it is only after MTs are depolymerized or cells recover from starvation that formation of T-shaped cells is observed. These properties make Mod5p an ideal candidate in our analysis, where we used the branching protocol outlined in the Methods section to form T-shaped *mod5* Δ cells.

2.5.1 Polarity of T-shaped cells

Aim

In order to assess in detail the patterns of growth of *mod5* Δ cells, we imaged T-shaped cells to measure which ends are growing. Mod5p is a member of the Tea1p pathway, but nevertheless its deletion has a mild phenotype. *Mod5* Δ resemble WT cells, they are bipolar and they don't show abnormalities of cell shape. Here we investigate the polarity of *mod5* Δ T-shaped cells. For imaging, we chose cells that were as similar as possible to the T-shaped of WT genetic background. That means we only took into consideration cells that had overall stable diameter, with the body of the cell on one axis, and the arm of the cell on an axis vertical to the axis of the body of the cell.

Results

In *mod5* Δ cells, $\sim 20\%$ of cells exhibit bipolar patterns of growth (figure 2.29). It is interesting to note that the majority of monopolar cells consists of cells growing only from the arm (figures 2.29(b), 2.28(a)). There is though a small percentage of cells that is growing only from one body end (4%). In addition a single cell was found (1 out of 216 cells) that was tripolar and exhibited switch of growth from the arm to the body (figure 2.28(b)). Also the bipolar set of cells consists exclusively of cells growing from the arm and one body end, and never from two body ends. Contrary to the WT T-shaped cells, which failed to continue growing from short arms ($\sim \leq 2 \mu\text{m}$) after MT repolymerization, *mod5* Δ kept growing from the arm regardless of its size.

Conclusions

Generally, *mod5* Δ cells (similarly to the *tea1* Δ and *tea4* Δ cells), don't show the great diversity in the polarity of cells after MT repolymerization. This is inconsistent with their bipolar pattern of growth, but different from the effect of MT repolymerization in WT cells (figure 2.5). Mod5p seems to be required for this effect of MTs on the heterogeneity of growth from the 3 parts of the cell. After investigating each individual end independently we found that most *mod5* Δ cells grow only from the arm, an observation that was seen in *tea1* Δ and *tea4* Δ cells. There was though a subset of cells (20%) displaying bipolar growth as well as a single cell exhibiting growth switch. In the next

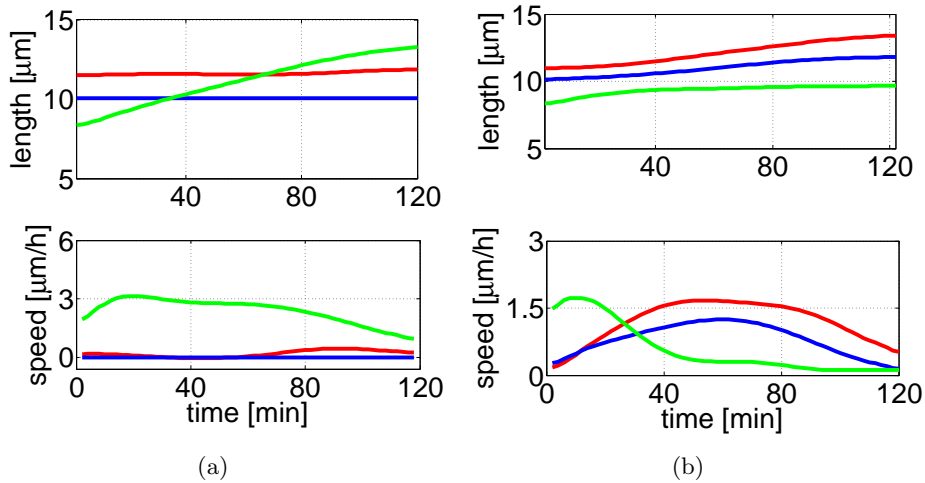


Figure 2.28: Growth plot of growing *mod5Δ* T-shaped cells.

Length plots of 2 different cells (top panel), and growth speed plots of the same cells (bottom panel). (a) monopolar cell growing only from the arm. (b) tripolar cell growing first from the arm and then switching to growth at 2 body ends. Red=left end, blue=right end, green=arm).

section we are looking in more detail into specific parameters of cell growth, cell geometry and MT behavior.

2.5.2 Geometry - Growth - Nucleus

Aim

The differences in the growth of the three ends triggered us to analyze the amount of growth and the growth speed of the ends. The growth speeds of T-shaped *mod5Δ S. pombe* cells have never been fully quantified.

Results

We accurately measured the total size of the cells. We used the central point of the cells at the base of the arm and as total size we defined the sum of lengths from that center point to the 3 ends of the cell. The size of the T-shaped cells is larger than the size (7-14 μm) of cells in a normal exponential WT population (figure 2.33(a)). The reason for that is that the cell cycle has been blocked and the cells have become longer already prior to branching. In addition we quantified the total growth for the different parts of the cell, as well as the mean and the maximum speed of growth (figure 2.30).

Next, we quantified the locations of the nucleus and we noticed that the nucleus localizes to the area at the base of the arm (figure 2.31). In most cells, the nuclei are moving towards the arm end (black marks, figure 2.31). We also compared the nucleus

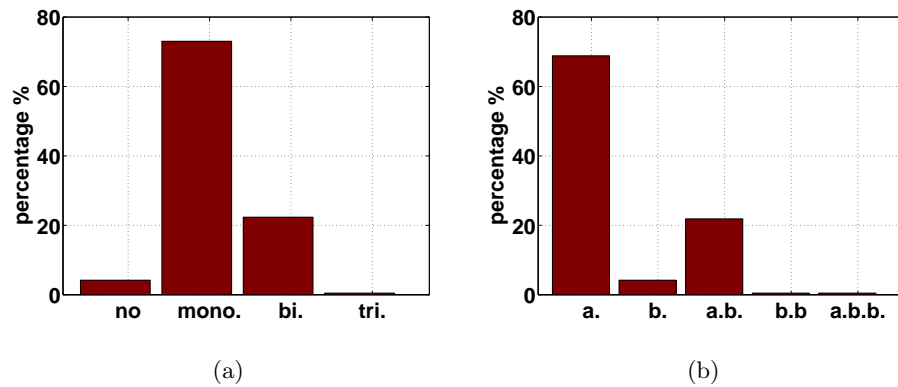


Figure 2.29: Polarity of *mod5* Δ T-shaped cells.

(a) Percentages of cells growing from from 1,2 or all 3 ends. For each cell in the population the total growth of each end was measured (no=no growth, mono.=monopolar growth, bi.=bipolar growth, tri.=tripolar growth). (b) Sub-categorization of monopolar, bipolar and tripolar cells according to which part of the cell was growing (a.=growth only from arm, b. growth only from 1 body end, a.b. growth from arm and 1 body end, b.b. growth from 2 body ends, a.b.b. growth from all 3 cell ends). n=216 cells.

positions with body asymmetry. We found that body asymmetry determines the nuclear position, since nuclei localize preferentially towards the longer body part (figure 2.31).

Conclusion

We have accurately quantified the initial geometry, total growth, mean speed and the maximum speed for each end of *mod5* Δ T-shaped cells. In addition we quantified the nuclear coordinates and followed the nuclear movements in the course of the experiment. We found that consistently with the WT, *tea1* Δ and *tea4* Δ T-shaped cells, the nucleus is moving towards the growing arm of *mod5* Δ T-shaped cells. This movement though is not necessary for growth, since there are cells that have their nucleus staying in the body but their arms are growing. In addition, when we examine the nuclear location in the different cases of body asymmetry, we find that the nucleus is preferentially towards the longer part of the body. The fact that the nuclear movements are similar in WT, *tea1* Δ , *tea4* Δ and *mod5* Δ cells, suggests that they are a result of the cell geometry solely and they don't depend and the polarity mechanism. The inclusion of MT behavior in the analysis will shed more light in the causality of events, since MT organization and nuclear location are dependent on each other.

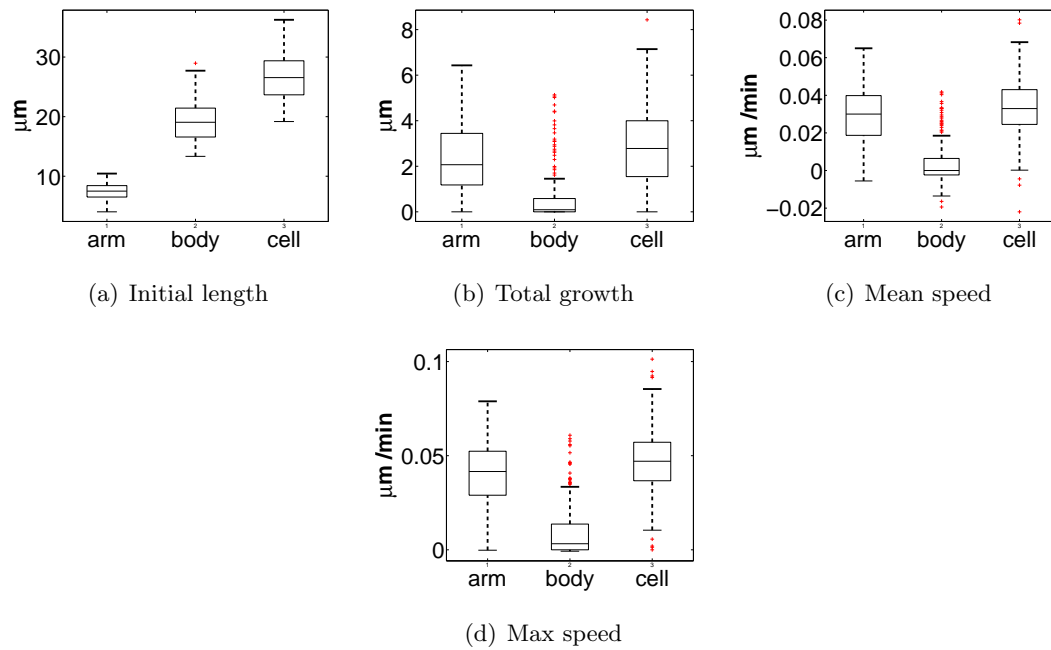


Figure 2.30: Boxplots of geometry, growth, mean and maximum speed of *mod5* Δ T-shaped cells.

(a) Initial dimensions of the cell parts in μm at $t=0\text{h}$. (b) Total growth of each part in the course of the experiment. (c) Mean growing speed of each part in $\mu\text{m}/\text{min}$. The mean speed was calculated by dividing the total growth of each end by the amount of time spent. (d) Maximum growing speed of each cell part in $\mu\text{m}/\text{min}$. $n=214$ cells.

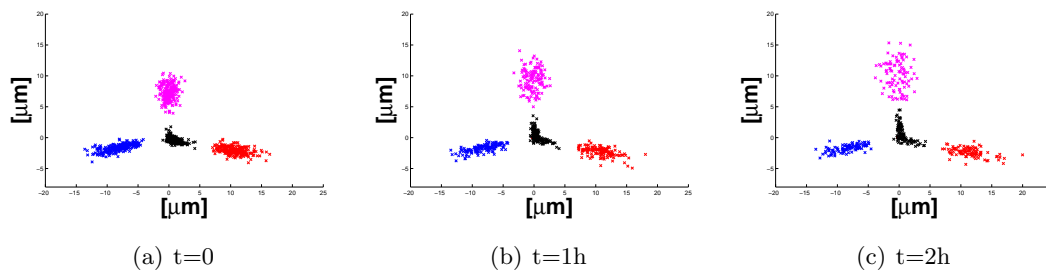


Figure 2.31: Nuclei and cell ends in *mod5* Δ T-shaped cells.

Cells were aligned at their center (see Methods) and subsequently the cells ends and the nucleus were plotted at time $t=0\text{h}$ (a), $t=1\text{h}$ (b) and $t=3\text{h}$ (c). Red=longer body end, blue=shorter body end, magenta=arm, black=nucleus, $n=214$ cells.

2.5.3 Geometry vs Growth

Aim

In WT cells short arms ceased growing upon MT repolymerization, and initial arm length correlated with growth of that arm (figure 2.9). In *tea1Δ* and *tea4Δ* cells there was no relationship between geometry and growth in the arm (figures 2.17, 2.24). Here we investigate potential correlation of the initial length of the arm with the future growth of that arm *mod5Δ* T-shaped cells.

Results

Mod5Δ cells don't show any correlation between initial arm length and growth like *tea1Δ* and *tea4Δ* cells and unlike WT cells (figure 2.32).

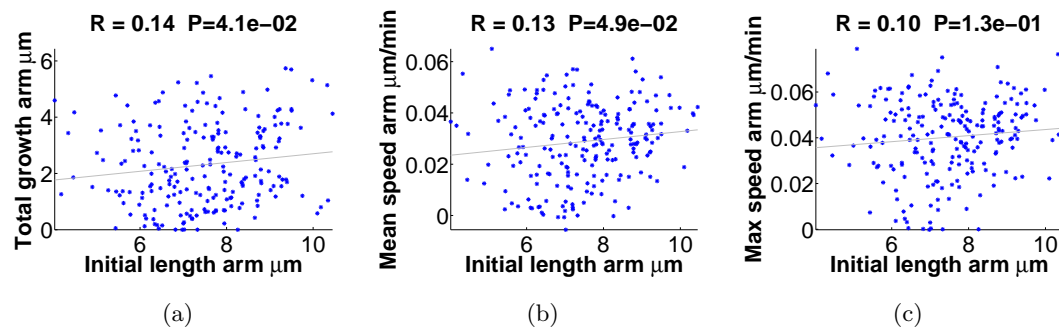


Figure 2.32: Initial length vs. growth in *mod5Δ* T-shaped cells.

Initial length vs. growth (a), mean speed (b) and maximum speed (c) in arms. n=214 cells.

Conclusions

These findings are very similar to the *tea1Δ* and *tea4Δ* cells. Contrary to the WT cells, the initial size of the arm does not influence the arm growth speed or the arm total growth. Nevertheless we could observe some cells (~10%) that had small arms (~2-3 μm) that ceased growing immediately after MT repolymerization.

2.5.4 MTs vs Growth

Aim

In this section we measure properties of MTs in the *mod5Δ* T-shaped cells. After finding in the previous sections that the role of MTs is mostly diminished in the *tea1Δ* and *tea4Δ* cells, it is interesting to examine the effects of MTs in *mod5Δ* cells. We concentrated only on the tips of the cells where we quantified the distribution of MT plus ends by imaging

cells with a GFP-tagged version of the plus-end MT marker Mal3p (EB1 homolog). We took into account all MT plus ends that were at a distance of less than $1.6\ \mu\text{m}$ to the cell end. We have already shown that the MTs that reach the cell end in the arm is correlated with the arm growth speed in WT cells and *tea4* Δ cells, but not in *tea1* Δ cells. Here we also examine the effects of MTs in *mod5* Δ cells.

Results

The mean number of MTs/minute in arm is 0.63 ± 0.36 MTs/min and in body is 1.35 ± 0.57 MTs/min, mean \pm std (figure 2.33(a)). On average the arm received the same MTs than each body end. Furthermore, there is strong negative correlation between cell size and MTs at the ends of the cell, similar to WT and *tea4* Δ cells, but unlike *tea1* Δ cells (figures 2.10(b), 2.18(b), 2.25(b), 2.33(b)). Furthermore there is a negative relationship between cell size and MTs contacts at the ends of the cell, similar to WT cells and *tea4* Δ and unlike *tea1* Δ cells (figure 2.10(b), 2.25(b), 2.33(b)).

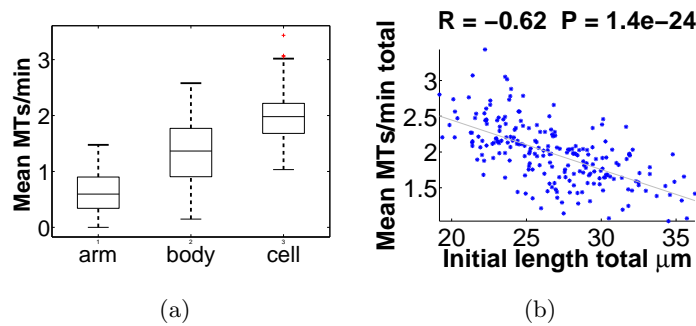


Figure 2.33: Microtubules in *mod5* Δ T-shaped cells in a region close to the tip.

(a) boxplot of mean MTs/min in the body. (b) scatterplot of total MTs (all MTs in all three ends) and initial total length (addition of the lengths of all cell parts). The gray line is the least-square line. $n=214$ cells.

The mean number of MTs/min in the arm exhibits very low positive correlation with growth and growth speed in the arm (figure 2.34). This observation is similar to the behavior of *tea1* Δ T-shaped cells.

The same comparison in the bodies of *mod5* Δ T-shaped cells shows no correlation as well (data not shown).

Conclusions

In *mod5* Δ cells we notice more MTs per minute in both the arms and the bodies of the cells if we compare them with *tea1* Δ , *tea4* Δ and WT cells. Some possible explanations for this difference could be that there is indeed higher number of MTs anyway in *mod5* Δ cells (for which we have no data), or that there is an abnormality in MT organization that interferes with our analysis. Indeed, it has been observed that in some *mod5* Δ

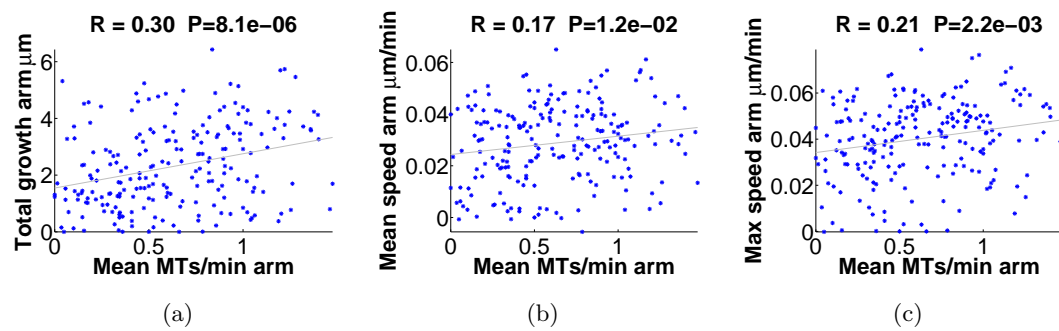


Figure 2.34: MTs vs. growth in *mod5Δ* T-shaped cells.

Mean MTs/min vs. growth (a), mean speed (b) and maximum speed (c) in arms.
n=214 cells.

cells some MTs can occasionally be seen curling around the cell ends (Snaith and Sawin, 2003). This percentage is only 6% though and cannot account for the differences we see in the mean number of MTS. Furthermore we failed to observe any curled MTs in the experiments we performed. In addition to these results we observe that longer *mod5Δ* T-shaped tend to have fewer MTs reaching the cell ends, a property that we found in *tea4Δ* and WT but not in *tea1Δ* cells (figure 2.33(b)).

In addition, the absence of Mod5p, similar to the absence of Tea1p, causes the MTs to be unable to influence the growth speed of arms. This finding is similar to *tea1Δ*. It is interesting to observe this similarity in the way MTs behave in *tea1Δ* and *mod5Δ* cells, despite the mild phenotype of *mod5Δ* cells. This shows a similarity in the nature of the growth zone in the arm of *tea1Δ* and *mod5Δ* T-shaped cells. It is interesting to observe this similarity, despite the mild phenotype of *mod5Δ* cells.

2.5.5 Geometry vs MTs

Aim

In this section we compare geometry with MTs. We compared both the lengths of body ends and the body asymmetry with growth and MT organization. Body asymmetry is an inherent geometrical property of the T-shaped cells and we defined it as the ratio of the longer body end to the shorter body end.

Results

There is strong positive correlation between initial arm length and MTs in arms of *mod5Δ* T-shaped cells (figure 2.35(a)). Quite surprisingly though, the reverse holds true in the body (figure 2.35(b)): there is strong negative correlation between initial length and MTs. This finding is similar to the situation in *tea1Δ* cells and WT cells, but different to *tea4Δ*. In addition, higher body asymmetry leads to lower number of

MTs in the arm (figure 2.35(a)). Apart from that, we wondered whether we could see any competition between arm and body for potential growth or MTs, but we found no significant correlation (figure 2.35(d)).

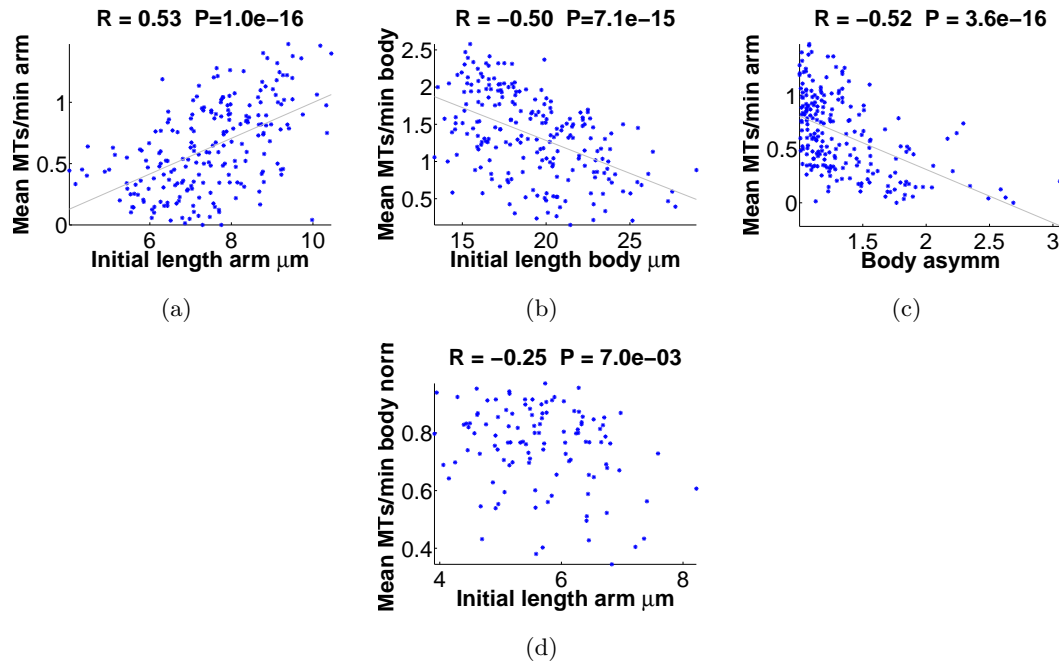


Figure 2.35: Geometry vs. MTs correlation in *mod5* Δ T-shaped cells.

Initial length vs. mean MTs/min in arms (a) and bodies (b) and body asymmetry (ratio of long to short body end) vs. mean MTs/min in the arm. (c) shows initial arm length vs. mean MTs/min in body. $n=214$ cells.

2.5.6 Growth Maintenance - Growth Switch

One out of 205 *mod5* Δ T-shaped cells that were analyzed exhibit growth switch from the arm to the old end (figure 2.28(b)). In addition $\sim 15\%$ of cells exhibit growth cessation of the small arms. The growth zones appear to be generally stable and their maintenance is only slightly affected by MTs.

2.5.7 Conclusions

The analysis of *mod5* mutants reveals interesting aspects of *mod5* function. Despite having a very mild phenotype, *mod5* Δ cells show many similar characteristics to those of *tea1* Δ and *tea4* Δ cells. On the other hand, the growth zone establishment capability of WT microtubules is seriously but not completely compromised in *mod5* Δ cells. These observations let us conclude that *mod5* Δ possess an intermediate phenotype between

that of *tea1Δ-tea4Δ* and that of WT cells; they cannot refocus the growth zones to other parts of the cell, although they can exert a minor role in the growth of the arm that is already growing. In short:

- 1) repolymerization of MTs has very limited effect on the heterogeneity of growth fates of T-shaped cells.
- 2) MTs assume an organization that reflects the geometry of the T-shaped cells.
- 3) MTs don't correlate with any measure of growth in the *mod5Δ* cells.

Comparison	arm	body	left	right
Initial length vs. growth	no	no	no	no
MTs vs. growth	no	no	no	no
Initial length vs. MTs	pos	neg	no	no

Table 2.4: Pairwise correlations in *mod5Δ* T-shaped cells.

Summary of the main comparisons. pos=positive, neg=negative and no=no correlation.

In the next chapter we analyze Bud6p, the protein that works downstream of Tea1p, functions in a different pathway that has been proposed to be independent of the Tea1p pathway (Minc et al., 2009), and is a recruiter of the formin For3p.

2.6 *Bud6* Δ

Bud6p is a protein that is required for the efficient establishment of polarity at the previous cell division site. It is actin associated and it functions downstream of Tea1p (Glynn et al., 2001). During interphase, bud6p is localized in a crescent of dynamic dots at the cortex of both cell tips, similar to other cell tip markers such as Tea1p (Mata and Nurse, 1997; Glynn et al., 2001). *Bud6* Δ mutants are viable, grow at wild-type rates and exhibit normal rod cell shapes and cell division patterns (Glynn et al., 2001). They grow in a monopolar fashion throughout interphase from the old end only with over 50% of cells showing no new growth after NETO (Glynn et al., 2001).

2.6.1 Polarity of T-shaped cells

Aim

Bud6 Δ mutants exhibit normal rod cell shapes and cell division patterns and 50% of cells fail to establish bipolarity (Glynn et al., 2001). Here we investigate the polarity of *bud6* Δ T-shaped cells.

Results

As expected, the majority of cells grew in a bipolar fashion (51.2%), consistent with their behavior at the WT-shape state (figure 2.36(a), bi. bar). Interestingly, 33.5% of cells grew monopolarly, consistent with a high percentage of monopolar cells in G2 (Glynn et al., 2001). There were also 12.9% of *bud6* Δ cells that exhibited growth from all 3 ends (figure 2.36(b)). In order to gain more insight into the process, we decided to measure each individual end independently and understand which are exactly the ends that are growing. We found that both the monopolar and the bipolar population of *bud6* Δ cells can be subdivided in further categories depending on which exactly end is growing. It is interesting to note that \sim 45% of cells ceased growing from the arm (figure 2.36(b), b. b.b. bars). Furthermore, we can look at the specific growth speeds of the cell ends at the individual cell level (2.37). We can observe switching growth from the arm to one body end (figure 2.37), or a bipolar cell (figure 2.37(b)).

Conclusions

Bud6 Δ T-shaped cells exhibit the same heterogeneity of growth as the WT T-shaped cells. These results point out to the direction of MTs as important regulators of polarity in T-shaped cells. Before assessing the role of MTs in polarity, we need to measure parameters of growth and MT organization in T-shaped cells.

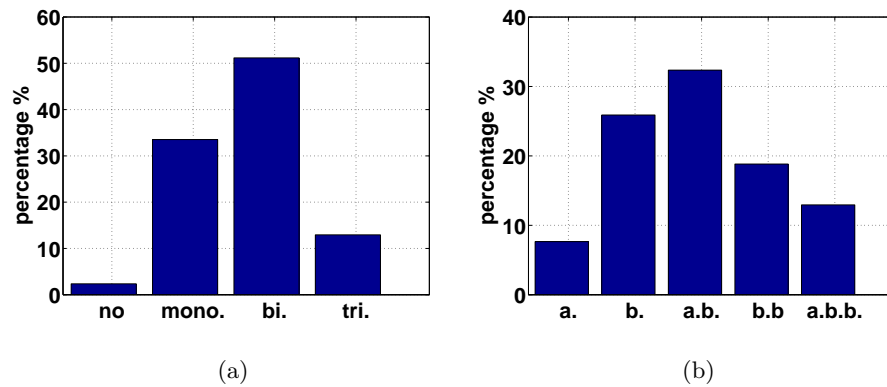


Figure 2.36: Polarity of *bud6Δ* T-shaped cells.

(a) Percentages of cells growing from from 1,2 or all 3 ends. For each cell in the population the total growth of each end was measured (no=no growth, mono.=monopolar growth, bi.=bipolar growth, tri.=tripolar growth). (b) Sub-categorization of monopolar, bipolar and tripolar cells according to which part of the cell was growing (a.=growth only from arm, b. growth only from 1 body end, a.b. growth from arm and 1 body end, b.b. growth from 2 body ends, a.b.b. growth from all 3 cell ends). n=170 cells.

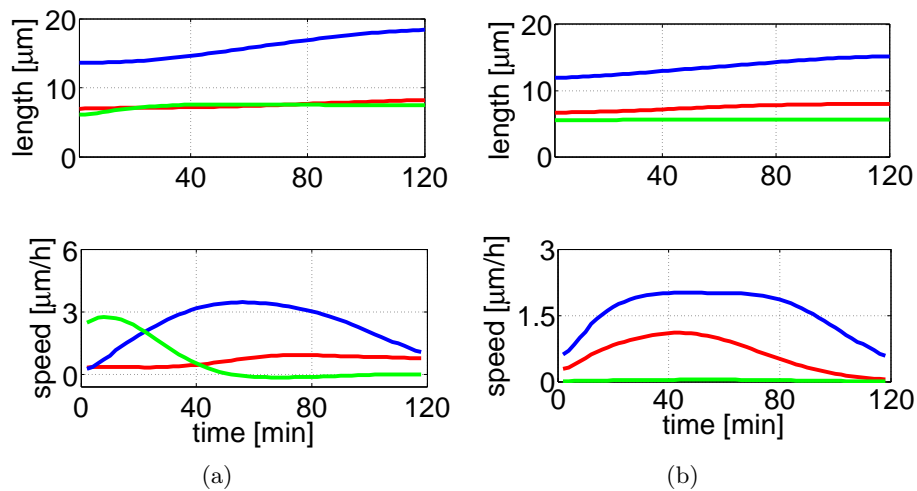


Figure 2.37: Growth plot of growing *bud6Δ* T-shaped cells.

Length plots of 2 different cells (top panel), and growth speed plots of the same cells (bottom panel). (a) cell growing first from the arm and then switching to growth from the body. (b) bipolar cell growing only from the body. Red=left end, blue=right end, green=arm).

2.6.2 Geometry - Growth - Nucleus

Aim

The differences in the growth of the three ends triggered us to analyze the amount of growth and the growth speed of the ends. The growth speeds of T-shaped *S. pombe* cells

have never been fully quantified.

Results

We accurately measured the total size of the cells. We used the central point of the cells at the base of the arm and as total size we defined the sum of lengths from that center point to the three ends of the cell. The T-shaped cells are bigger than the normal WT population (figure 2.38(a)). This happens because we have blocked the cell cycle and therefore the cells had already become longer prior to arm formation. In addition we quantified the total growth for the different parts of the cell, as well as the mean and the maximum speed of growth (figure 2.38).

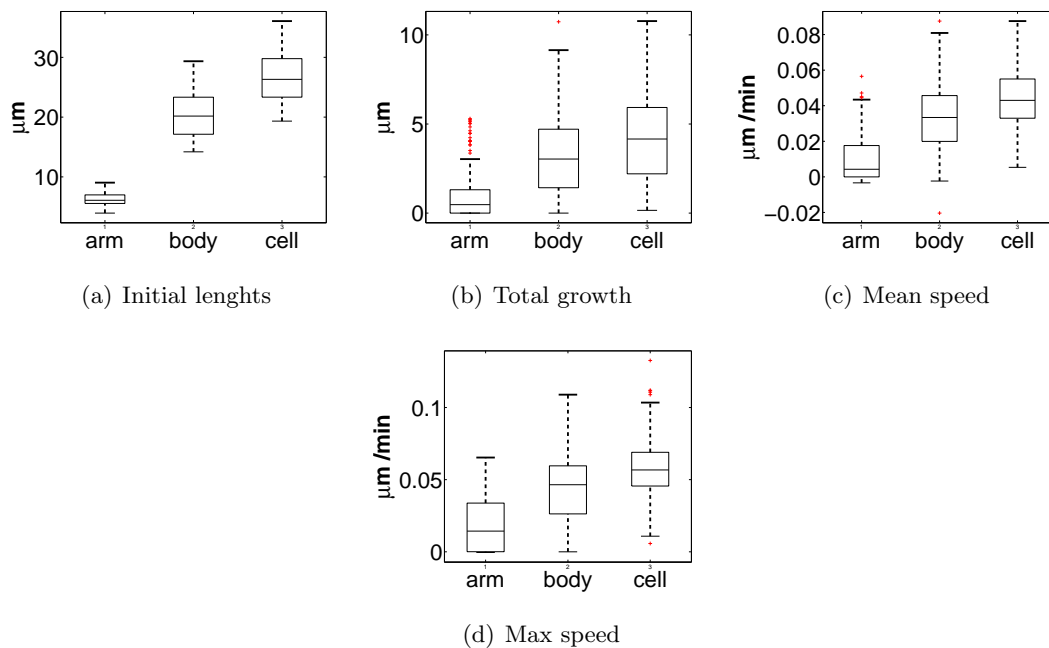


Figure 2.38: Boxplots of geometry, growth, mean and maximum speed of *bud6* Δ T-shaped cells.

(a) Initial dimensions of the cell parts in μm at $t=0\text{h}$. (b) Total growth of each part in the course of the experiment. (c) Mean growing speed of each part in $\mu\text{m}/\text{min}$. The mean speed was calculated by dividing the total growth of each end by the amount of time spent. (d) Maximum growing speed of each cell part in $\mu\text{m}/\text{min}$. $n=170$ cells.

We also quantified the locations of the nucleus and we noticed that the nucleus localizes to the area at the base of the arm (figure 2.39). In the cases where the arms are growing, the nuclei are moving towards the arm end (black marks, figures 2.39(b), 2.39(c)). The nuclei stay in the bodies of the cells in 100% of the cases in the non-growing arms (black marks, 2.39(d), 2.39(e), 2.39(f)). We also compared the nucleus positions

with body asymmetry. Body asymmetry is the ratio of the longer to the shorter body end. Nuclei localize preferentially towards the longer body part of asymmetric bodies (figure 2.39).

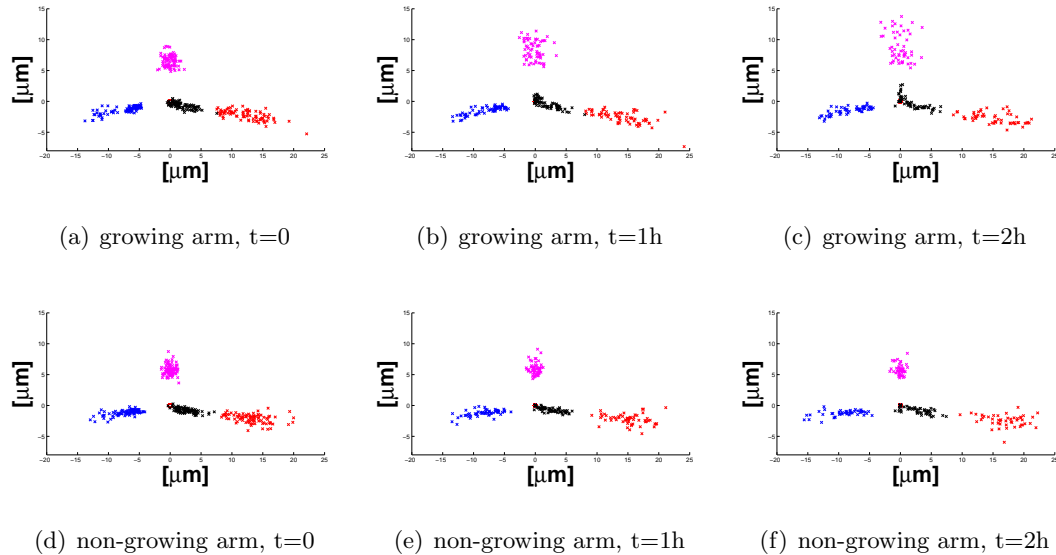


Figure 2.39: Nuclei and cell ends in growing and non-growing arms of *bud6* Δ T-shaped cells.

Cells were aligned at their center (see Methods) and subsequently the cells ends and the nucleus were plotted. a-c = growing arms, d-f = non-growing arms. Red=longer body end, blue=shorter body end, magenta=arm, black=nucleus, $n=170$ cells.

Conclusion

We have accurately quantified the initial geometry, total growth, mean speed and the maximum speed for each end. In addition we quantified the nuclear coordinates and followed the nuclear movements in the course of the experiment. We found that *bud6* Δ behave similar to all the other strains we have analyzed, as far as the nucleus is concerned: a nucleus that is moving in the arm of the cell is always an indicator for arm growth. This movement though is not necessary for growth, since there are cells that have their nucleus moving in the arm but their arms are not growing. When we examine the nuclear location in the different cases of body asymmetry, we find that the nucleus is preferentially towards the longer part of the body (again consistent with all the other strains we analyzed). This suggests that the nuclear position is an effect of cell geometry and not the opposite. In the next section we include the MT behavior in our analysis.

2.6.3 Geometry vs Growth

Aim

T-shaped cells that have an arm with length $\sim \leq 2 \mu\text{m}$ fail to continue growing after MT repolymerization and were excluded from the analysis. The cessation of growth of these short nascent branches led us to investigate the potential correlation of the initial length of the arm with the future growth of that arm.

Results

The initial length of the arm (arm length at MT repolymerization) displays a highly significant correlation with the total growth of the arm ($R=0.55$, $p\text{-value}=10^{-14}$, figure 2.40(a)). A highly significant correlation can also be found between initial length and mean speed of growth ($R=0.55$, $p\text{-value}=10^{-15}$, figure 2.40(b)), as well as initial length and maximum speed of growth ($R=0.55$, $p\text{-value}=10^{-15}$, figure 2.40(c)). We next compared the initial length of the body and the total growth or growth speed of the body. The correlation coefficient is low ($R=0.2\text{-}0.27$, figure 2.40 d-f). Similarly, there is slight positive correlation if we look at the cell as a whole ($R=0\text{-}0.2$, figure 2.40 g-i). There is also negative correlation between the initial length of the arm and the growth and in the body (figure 2.41).

Conclusion

These results suggest that by looking at the initial size of the arm, we can predict to a large extent whether this arm will grow and also how much it will grow. This positive relationship exists in the WT cells but not in the *tea1* Δ , *tea4* Δ and *mod5* Δ cells. One possibility is that longer arms might have established a more mature growth zone, that can be more easily retained after MT repolymerization. In the next section we evaluate the possible effects of MTs on growth.

2.6.4 MTs vs Growth

Aim

MTs are a key known regulator of cell polarity. They transport polarity markers at the ends of the cell and are important for polarity establishment. For that reason we quantified MT organization inside the cell. We concentrated only on the tips of the cells where we quantified the distribution of MT plus ends by imaging cells with a GFP-tagged version of the plus-end MT marker *male3p* (EB1 homolog). We took into account all MT plus ends that were at a distance of less than $1.6 \mu\text{m}$ to the cell end. In addition, we investigated the possible relationship between MTs plus ends and cell growth. The MTs are known to be implicated in the establishment of growth zones (Castagnetti et al., 2007; Minc et al., 2009; Terenna et al., 2008).

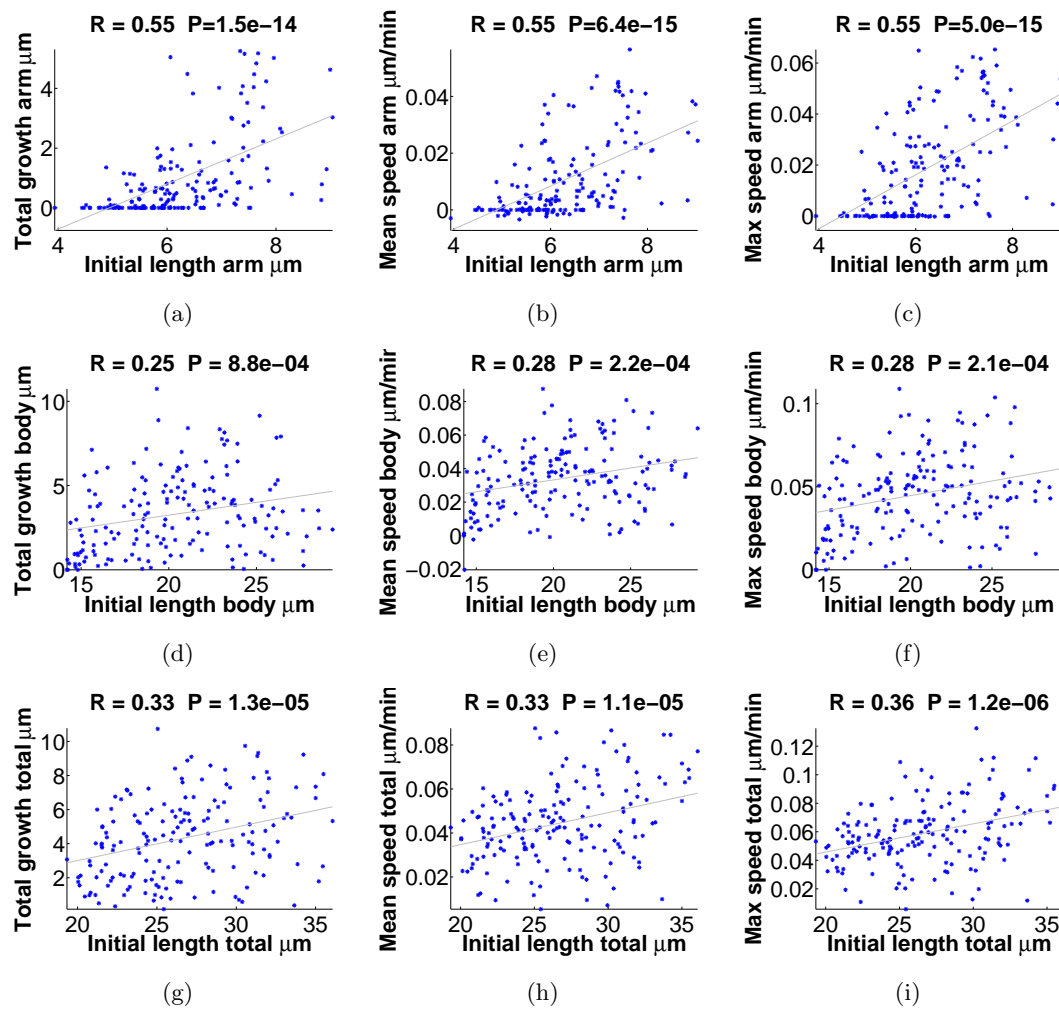


Figure 2.40: Initial length vs. growth in *bud6Δ* T-shaped cells.

Initial length vs. growth, mean speed and maximum speed in arms (a-c), bodies (d-f) and whole cells (g-i). $n=170$ cells.

Results

The mean number of MTs/minute in arm is 0.25 ± 0.24 MTs/min and in body 1.27 ± 0.34 MTs/min, mean \pm std (figure 2.42(a)). On average, fewer MTs grow in the arm compared to each end of the body. Furthermore, there is a slight negative correlation between cell size and MTs at the ends of the cell. Longer cells tend to have fewer MTs (figure 2.42(b)).

The mean number of MTs/min in the arm is correlated with the total growth of the arm ($R=0.65$, $p\text{-value}=10^{-22}$). A highly significant correlation is also seen between MTs/min in the arm and mean speed, as well as MTs/min in the arm and maximum speed ($R=0.60$, $p\text{-value}=10^{-18}$ and $R=0.53$, $p\text{-value}=10^{-22}$ respectively, figure 2.43). In

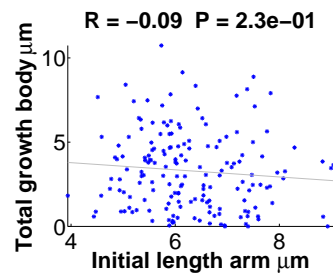


Figure 2.41: Arm-Body comparison in *bud6* Δ T-shaped cells.
Initial length of arm vs. total growth in body. n=170 cells.

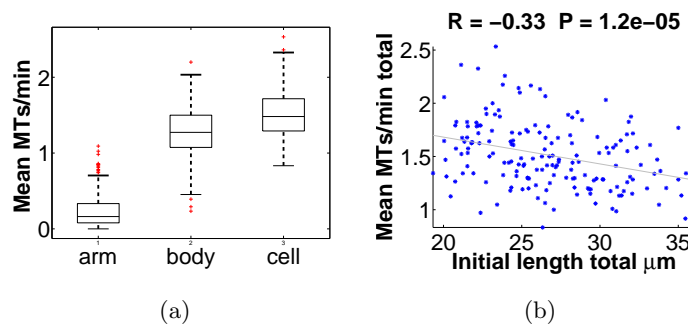


Figure 2.42: Microtubules in *bud6* Δ T-shaped cells in a region close to the tip.
(a) boxplot of mean MTs/min in the body. (b) scatterplot of total MTs (all MTs in all three ends) and initial total length (addition of the lengths of all cell parts). The gray line is the least-square line. n=170 cells.

the body, however, there is no correlation between MTs and growth, as measured by total growth, mean growth speed or maximum growth speed (figure 2.43, d-f). Similarly no correlation is found in the cell as a whole (figure 2.43, g-i).

Conclusion

We have accurately quantified the numbers of MTs plus ends that are in the proximity of the cell ends. From this analysis we conclude that MTs target preferentially the ends of the cell body. The quantification of the numbers of MTs plus ends that are in the proximity of the cell ends can be used for more in-depth analysis and comparison between MTs and growth in the different parts of the cell. In addition large cells receive fewer MTs contacts at their ends. The average number of MT plus ends that reach the ends of the cell correlates with parameters that measure growth (Total growth, mean and maximum speed of growth per cell), only in the arm and not in the body of the cells (either taken as a whole or between left and right ends individually). This finding

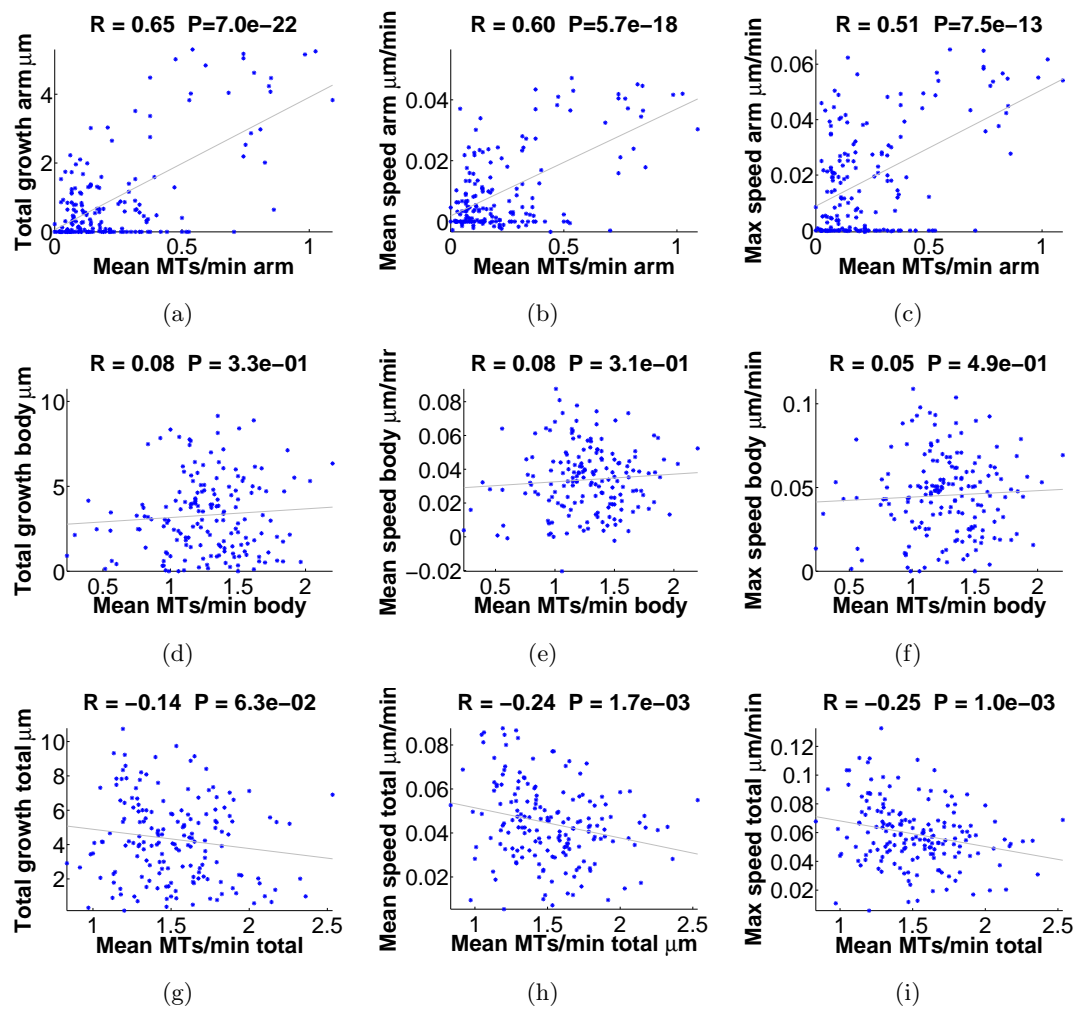


Figure 2.43: MTs vs. growth in *bud6* Δ T-shaped cells.

Mean MTs/min vs. growth, mean speed and maximum speed in arms (a-c), bodies (d-f) and whole cells (g-i). $n=170$ cells.

is reminiscent of the WT cells and it shows a fundamental difference in the nature of the growth zones in these parts of the cell.

2.6.5 Geometry vs MTs

Aim

Since MTs are correlated with growth and also geometry is correlated with growth, we wanted to investigate what the relationship is between geometry and microtubules. We compared both the lengths of body ends and the body asymmetry with growth and MT

organization. Body asymmetry is an inherent geometrical property of the T-shaped and we defined as the ratio of the longer body end to the shorter body end.

Results

There is slight positive correlation between initial arm length and MTs in arm ($R=0.36$, figure 2.44(a)). Quite surprisingly though, the situation is reverse in the body (figure 2.44(b)): there is slight negative correlation between initial length and MTs. There is also negative correlation between body asymmetry and MTs in arm (figure 2.44(c)).

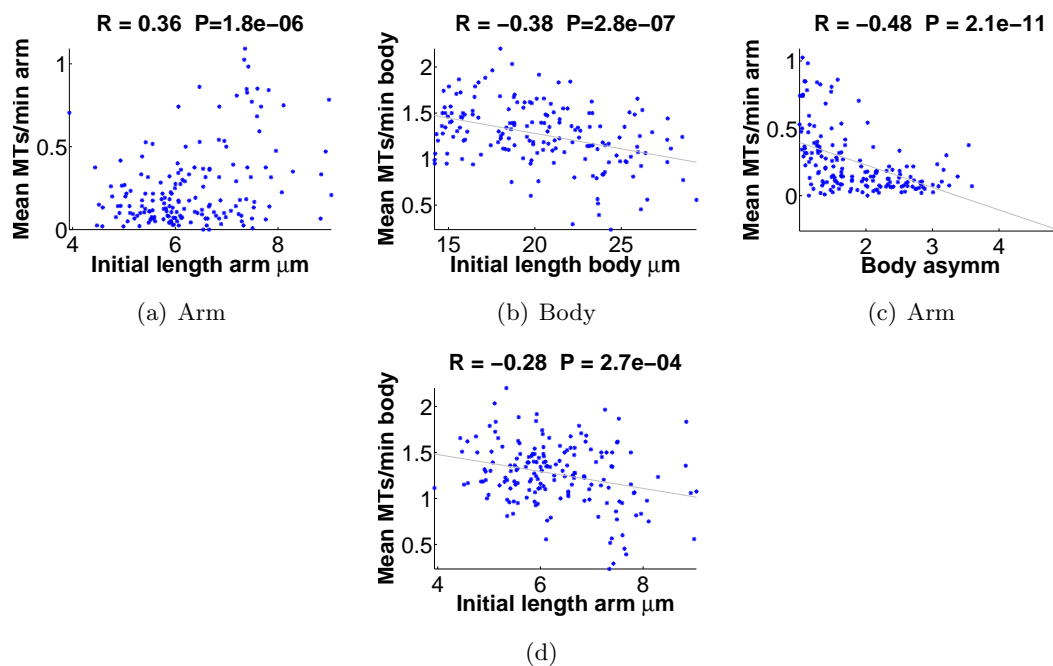


Figure 2.44: Geometry vs. MTs correlation in *bud6* Δ T-shaped cells.

Initial length vs. mean MTs/min in arms (a) and bodies (b) and body asymmetry (ratio of long to short body end) vs. mean MTs/min in the arm. $n=170$ cells.

2.6.6 Growth Maintenance - Growth Switch

As mentioned earlier, 76 out of 170 cells (44.7%), cease growing from the arm immediately upon MT repolymerization (figure 2.36, bars b., b.b). This is a very interesting observation since it shows a drastic effect of MT repolymerization 1) arms of the cell continue or cease growing, dependent on the number of MTs. 2) the growth speed of arms is dependent on the number of Mts in the arm.

Furthermore $\sim 12\%$ of cells display an interesting behavior. They continue growing from the arm after MT repolymerization, but cease afterwards (figure 2.36, bars a.b.b).

Simultaneously, one of the body ends that was not growing before starts growing. This behavior is exhibited only if MTs are present and therefore points out to the ability of MTs to establish a new growth zone in G2 phase of *bud6Δ* T-shaped fission yeast cells.

2.6.7 Conclusions

We set out to investigate the growth properties of T-shaped *bud6Δ* cells. We successfully perturbed the shape of WT cells and produced T-shaped cells. We acquired numbers on cell geometry, cell growth, nuclear position and MT organization and found interesting pairwise dependencies (table 2.5). Most importantly we found that the repolymerization of MTs after branching is necessary for repositioning growth from the arm to the body of the cell, pointing out that MTs are important both for polarity establishment and polarity maintenance. This growth switch has not been described before.

Comparison	arm	body	left	right
Initial length vs. growth	pos	no	pos	pos
MTs vs. growth	pos	no	no	no
Initial length vs. MTs	pos	neg	no	no

Table 2.5: Pairwise correlations in *bud6Δ* T-shaped cells.

Summary of the main comparisons. pos=positive correlation, neg=negative correlation, no=no correlation.

Chapter 3

Discussion

Here we summarize the main findings of the thesis. We discuss how this work fits into the current knowledge of the field and how our analysis was used to understand aspects of the system. Possible future experiments are also proposed.

3.1 Summary

In this thesis we addressed the problem of how MTs, direct polarized growth in inter-phase *S.pombe* cells. Though the main components of polarity establishment are known, the exact regulation of the process remains elusive. Many models have been proposed to explain morphogenesis in fission yeast, based on different pieces of experimental observations. More specifically:

- The Tea1p pathway couples MTs with polarization at the cell ends.
- The Mal3p-Bud6p pathway promotes polarization on the sides of bent cells.
- The nuclear pathway operates to promote polarization in the vicinity of the nucleus when the other two pathways are absent.

It is not clear though, how redundant these models are and to what extent they operate in parallel. The tight regulation of the cylindrical shape in fission yeast hinders further investigations, and various perturbations have been utilized to unravel hidden properties of the system.

We searched for an experimental method that could perturb the shape of the cells without applying external force. We used an adapted version of the method described by Sawin and Nurse (1998) and created cells with three ends. Our main findings are:

- MTs define the growth fates of T-shaped cells. This function of MTs is dependent on the proteins Tea1p and Tea4p, and to lesser degree on Mod5p. It is not dependent on Bud6p.

- MTs are important for the establishment and maintenance of growth zones in G2 T-shaped *S. pombe* cells. A cell end can cease growing in G2 and at the same time a previously non-growing end can initiate growth. These events are absent in the *tea1Δ* and *tea4Δ* T-shaped cells.
- The size of the arms at the time of MT repolymerization determines the growth speed of the arm. This effect is absent in *tea1Δ*, *tea4Δ* and *mod5Δ* cells.
- The number of MT plus ends that reach the end of the arm of a T-shaped cell determines the growth speed of that arm. This effect is absent in *tea1Δ* and *tea1Δ* cells.
- The nucleus assumes an organization that reflects the cell geometry, independent of the presence or absence of Tea1p, Tea4p, Mod5p, Bud6p. The nuclei are found to enter the arm area when the arm is growing and also to reside closer to the longer part of the body.

We suggest that growth zones that are formed in the absence of MTs exhibit instability. This instability remains as long as the MTs are kept depolymerized. When MTs are repolymerized, growth can cease from the arm and relocate to a previously non-growing end, dependent on the proteins Tea1p and Tea4p and Mod5p, but independent of Bud6p. In addition to the growth zone instability, we found that MTs are determining the growth speeds of ends in a Tea1p-Tea4p-Mod5 dependent manner.

3.2 Nuclear localization

We analyzed the positions of the nuclei in the analysis as complementary to the MT organization. The reason for that is recent work that has pointed out to the importance of MTs in offsetting growth to the ends of WT cells (Castagnetti et al., 2007). The nuclear pathway is one of the three polarity determining pathways, as suggested recently by (Minc et al., 2009). It is postulated that the determinants of polarity emanate from the vicinity of the nucleus and, if MTs are present, they are transported to the cell ends on the plus tips of MTs, and if MTs are absent, they diffuse from the nucleus and thus create a growth zone close to the nucleus.

In this work, the nucleus was not found to exert any influence on polarity. In the 5 strains we analyzed, the nuclear movements inside the cell are remarkably similar. Nuclei localize preferentially towards the longer part of the body and also towards growing arms, a behavior that is conserved among WT, *tea1Δ*, *tea4Δ*, *mod5Δ* and *bud6Δ* T-shaped cells. The nuclear position is not affected by the presence of Tea1p, Tea4p, Mod5p or Bud6p, but instead, is determined by the overall cell shape. The MTs explore the entire area of the cell and assume an organization that reflects the geometry of the cell. The nucleus is then actively positioned by MTs (Tran et al., 2001; Daga et al., 2006; Foethke et al., 2009).

3.3 Growth dependencies

In the arms of WT and *bud6* Δ cells, a strong positive correlation was observed between initial length of the arm (length at the time of TBZ wash - MT repolymerization) and total growth of the arm. Since we are comparing two parameters (initial length and growth) that are separated in time, we can also conclude on the causality. The initial length is a measurement that is taken in the beginning of the experiment, while growth occurs in the course of the experiment. Therefore, we can deduce that in the comparison between initial length and growth, the initial length is the cause and growth is the effect. That means that long arms, created and having grown in the absence of MTs, have the tendency to grow more, if MTs are repolymerized. One possibility is that longer arms have established a more mature growth zone, since they have already spent more time growing. This possibility is supported by the observation that 100% of arms $\leq 2 \mu\text{m}$ stop growing after MT repolymerization. According to this scenario, the growth zone that is formed in the absence of MTs, matures as it grows, losing progressively its instability.

Another possibility is that the arm does not have an inherent ‘measure’ of maturity, but that the number of MTs that reach the arm determine its probability to grow or not. Supporting this hypothesis, we observed a strong positive correlation between MTs reaching the end of the arm, and growth speed of the arm in WT, *tea4* Δ and *bud6* Δ T-shaped cells. From the correlation comparison alone it is impossible to determine causality. It is possible that more MTs in arms lead to higher growth, or that higher growth, leads to longer arms that in turn lead to higher MT numbers in the arm. If growth determined MTs, then MTs would organize passively in the cell, merely following the changes in cell dimensions. This means that we would find correlations between MTs and growth, in all strains, irrespective of mutations in polarity proteins. This correlation though, is absent in *tea1* Δ and *mod5* Δ T-shaped cells. More specifically, *tea1* Δ cells, that exhibit the greatest growth from the arm, have a very stable number of MTs in the arm irrespective of arm growth, a behavior that sharply contrasts that of WT cells (figure 3.1(b)). Therefore, MTs don’t merely enter the arm area in response to that arm’s growth, but rather actively determine how much this end of the cell will grow. This effect of MTs is absent in deletions of the proteins Tea1p and Mod5p. *tea4* Δ , despite having a phenotype very similar to that of *tea1* Δ cells at the unperturbed state, exhibit MT-dependent growth of arm, similar to the WT cells. It is not known to what extent *tea4* Δ could still utilize the Tea1p in the cell to determine growth, but it has been reported that *tea1* Δ bent cells create arms in the vicinity of the nucleus while *tea1* Δ *cdc25-22* cells create arms at the sites of MT contact in a Bud6p dependent manner (Minc et al., 2009). It is unclear whether Bud6p is the protein that enables the MTs of *tea4* Δ cells to determine the growth speed of arms, and if this is the case, why Bud6p is not localized cortically in *tea1* Δ cells.

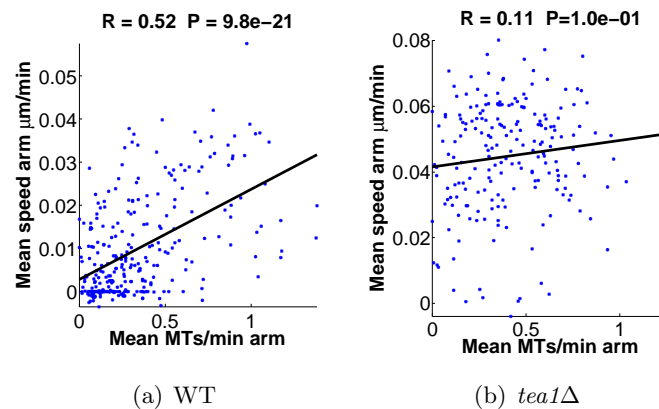


Figure 3.1: MTs vs. growth in WT and *tea1* Δ T-shaped cells.

Mean MTs/min in the arm vs. mean speed of growth in the arm of WT (a) and *tea1* Δ (b) T-shaped cells. The black line is the least-squares line. $n=285$ cells for WT, 205 cells for *tea1* Δ .

3.4 Growth switch

In WT and *bud6* Δ T-shaped cells MTs are responsible for the heterogeneity of growth from the different parts of the cell. A subset of these cells displays an interesting behavior, in that they cease growth from the arm, and initiate growth at another, previously non-growing end in the body. There are two important factors governing growth switch in G2:

- The cessation of growth from one end.
- The initiation of growth, at a previously non-growing site.

The cessation of growth by itself is not a surprising finding. Growing cells can sometimes be seen to stop growing from one end, especially if they are at the end of G2 phase and close to mitosis. The T-shaped cells generated with the current protocol are larger than WT, having been blocked in the cell cycle. In addition they have had the MTs depolymerized, therefore a certain amount of growth cessation is to be expected, especially after taking into account that some cells remain sick after MT repolymerization.

The initiation of body growth, in G2 phase of T-shaped cells, is a novel finding. This occurs after MT repolymerization and is dependent on the proteins Tea1p-Tea4p-Mod5p. This demonstrates that MTs can redirect growth in the G2 phase of the cell cycle in addition to their role prior to NETO

It is possible that in WT unperturbed cells as well, MTs have this capability, but this has not been observed because of the bipolar growth in G2 phase. Another possibility is that the transient depolymerization of actin during TBZ treatment can play a role. It has been shown that, upon TBZ treatment, the cortical actin cytoskeleton becomes

transiently depolarized (Sawin and Snaith, 2004). This transient actin depolarization might be responsible for influencing the role of MTs on polarity establishment. Lastly, it is possible that large T-shaped cells can have many growth zones, or more points in the cell cycle when they can activate growth. Normally, WT cells can switch to bipolar growth around the time of S-G2 transition at an event termed NETO. It is only then that the MTs have the ability to define a new growth site. It remains probable, that large T-shaped cells can initiate growth more than once.

The redistribution of growth propensity is the gradual decrease in growth speed of the arm, and the corresponding gradual increase in growth speed of the nascent growing site in the body (figure 3.2, decreasing green line, increasing red line). This observation is quite intriguing. It seems that the total growth propensity of the cell has a maximum limit. Indeed although the maximum growth speed of the arm and the body show substantial differences among the different strains (figures 3.3(a), 3.3(b)), the maximum growth of the cell in total (as measured by the addition of the lengths of all cell parts), remains remarkably similar (figure 3.3(c)).

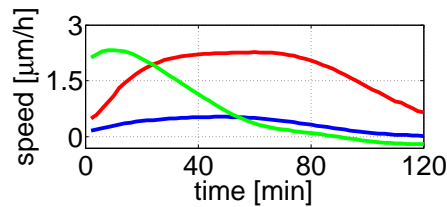


Figure 3.2: Growth propensity redistribution.

Growth speeds of the cells ends of a WT T-shaped cell exhibiting growth switch. Red=left body end, blue=right body end, green=arm).

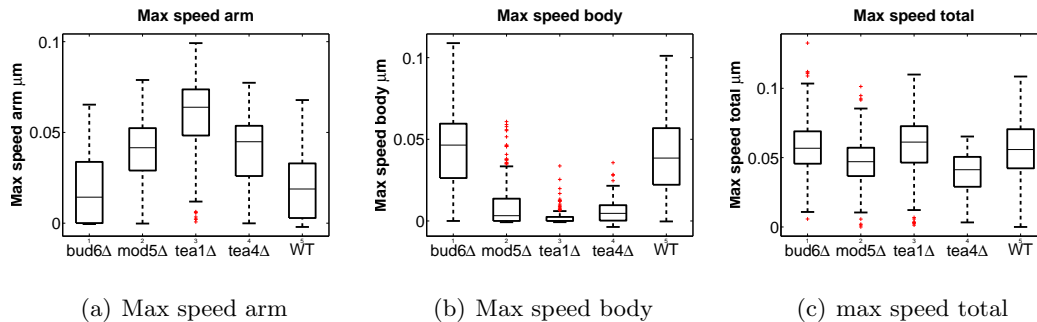


Figure 3.3: Maximum speed of growth.

Maximum growth speed of arms (a), bodies (b) and whole cells (c) in *bud6Δ*, *mod5Δ*, *tea1Δ*, *tea4Δ* and WT T-shaped cells.

Chapter 4

Methods

4.1 Overview

Here I describe yeast growing conditions, branching protocols, image acquisition and image processing techniques.

4.2 Cell Growing

Cells were grown in flat-bottom glass flasks at 25°C.

4.3 Branching protocols

The method I used to induce branches in fission yeast cells is the one described by Sawin and Nurse (1998) with some adaptations. Cells carrying a temperature sensitive version of *cdc10* (*cdc10-129*) are used. Cdc10p is required for S phase initiation, and therefore when incubated at the restrictive temperature (36°C) for ~4 hours, the cells are blocked at the end of G1 phase of the cell cycle. After the 4 hours, TBZ is added to the culture at a final concentration of 25µg/mL. After 1/2 hour the culture is put at 25°C, allowing the cell cycle to resume. Shortly afterwards the cells start creating branches and can be washed with EMM2 to allow MT repolymerization.

4.3.1 Heterogeneity of branching efficiency

For unknown reasons, different strains showed high heterogeneity in the branching efficiency as measured by the branching index, the percentage of cells in the population that have three ends. In wild-type cells (WT), *bud6pΔ*, *mod5pΔ*, *tea1pΔ* and *tea4pΔ* branched cells could be identified, whereas in *for3pΔ* and *tip1pΔ* the branching efficiency was zero.

4.4 Strain preparations

The strains that were used in this work are from the Brunner lab database and they were combined using standard fission yeast mating techniques.

4.5 Microscopy

4.5.1 Sample preparation

For imaging, glass bottom culture dishes were used (MatTek Corporation, 35mm petri dishes, 10mm Microwell, No. 1.5 coverglass [0.16-0.19mm], Part No.: P35G-1.5-10-C). The MatTek dishes were first treated with $1\mu\text{L}$ $2\mu\text{g}/\text{mL}$ lectin (SIGMA-L2380) to make their surface hydrophilic. Then, $200\mu\text{L}$ of cells were put on the microwell of the MatTek dishes, and left to sit for 10 minutes. After that, the dishes were gently washed with 3mL of the medium of preference for 2-3 times and they are ready for imaging.

4.5.2 Confocal Spinning Disk

The PerkinElmer Improvion Ultraview VoX Spinning disk confocal microscope was used. Movies were acquired with a Hamamatsu C9100-50 camera with pixel size of $8\mu\text{m}$.

4.5.3 Movie acquisition

T-shaped cells were identified and imaged for two hours. 16 fluorescent Z-slices were captured, with step size of $0.4\mu\text{m}$. This configuration results in a total width of $6.4\mu\text{m}$ which is significantly wider than the diameter of fission yeast cells that is approximately $4\mu\text{m}$.

4.6 Image processing

The time points after the time when a spindle was formed were excluded from the analysis. Therefore, some of the movies are shorter than 2 hours in total. Image processing was carried out by me using Matlab. The aim of image processing was to accurately quantify the outlines of the cells, to differentiate between the 3 cell ends, to locate the nucleus, and to measure properties of the MT cytoskeleton.

4.6.1 Cell Outlines

Cell outlines were detected from the maximum projections of the 16 fluorescent GFP-stacks. An average filter and afterwards a gaussian filtered was applied to the projections. The threshold was calculated using Huang's fuzzy entropy method [Huang and Wang (1995)], by using a code written in C and developed by M. Emre Celebi, Department of Computer Science, Louisiana State University in Shreveport, Shreveport, LA 71115, USA.

4.6.2 Cell Center - Cell Ends

The center of the cells was determined from the Euclidean Distance Transform (EDT). For each pixel $A(x_1, y_1)$ in a binary image, the distance transform assigns a number that is the distance between that pixel and the nearest nonzero pixel $B(x_2, y_2)$ of the binary image.

$$\sqrt{(x_1 - x_2)^2 + (y_1 - y_2)^2}$$

Thus, for all internal pixels of the cell the distance from that pixel to the cell boundary is assigned as the value of that pixel. Because of the geometry of the *S.pombe* branched cells, the maximum of the EDT is to be found in the body of the cell, at the base of the arm. I defined this point as the cell center throughout the analysis. The ends of the cells were identified as the maxima distance between the center of the cell and the cell outline.

4.6.3 Nucleus

The locations of the nucleus were determined manually for every timepoint of all the movies in the dataset.

4.6.4 Microtubules

The MTs plus ends were detected that were close to the cell tips. For each time point, the maximum projection image was thresholded, at a threshold where MTs plus ends are separated from each other. This is facilitated by the GFP-Mal3p localization preferentially at the cell tips. Subsequently, the MT plus ends were counted. We assigned a certain MT plus end to a particular cell end if that MT plus end was at a distance $\leq 1.6\mu\text{m}$ from the cell tip. The MTs that were farther away were excluded from the analysis.

4.7 Analysis

4.7.1 Box plots

For the box plots, the 'boxplot' function in Matlab was used. On each box, the central mark is the median, the edges of the box are the 25th and 75th percentiles, the whiskers extend to the most extreme data points not considered outliers, and outliers are plotted individually.

4.7.2 Scatterplots

For the scatterplots we calculated the correlation coefficient using the function `corrcoef` from Matlab. The matrix $R = \text{corrcoef}(X)$ is related to the covariance matrix $C = \text{cov}(X)$ by

$$R(i, j) = \frac{C(i, j)}{\sqrt{C(i, i)C(j, j)}}$$

Each p-value is the probability of getting a correlation as large as the observed value by random chance, when the true correlation is zero. If the p-value is small, less than 0.05, then the correlation R is significant.

Bibliography

- J. Adams, R. Kelso, and L. Cooley. The kelch repeat superfamily of proteins: propellers of cell function. *Trends Cell Biol.*, 10:17–24, Jan 2000.
- A. S. Alberts. Identification of a carboxyl-terminal diaphanous-related formin homology protein autoregulatory domain. *J. Biol. Chem.*, 276:2824–2830, Jan 2001.
- B. Alberts, A. Johnson, J. Lewis, M. Raff, K. Roberts, and P. Walter. *Molecular Biology of the Cell*, 2002.
- M. Arellano, T. Niccoli, and P. Nurse. Tea3p is a cell end marker activating polarized growth in *Schizosaccharomyces pombe*. *Curr. Biol.*, 12:751–756, Apr 2002.
- M. K. Balasubramanian, D. McCollum, L. Chang, K. C. Wong, N. I. Naqvi, X. He, S. Sazer, and K. L. Gould. Isolation and characterization of new fission yeast cytokinesis mutants. *Genetics*, 149:1265–1275, Jul 1998.
- R. Behrens and P. Nurse. Roles of fission yeast tea1p in the localization of polarity factors and in organizing the microtubular cytoskeleton. *J. Cell Biol.*, 157:783–793, May 2002.
- J. D. Beinhauer, I. M. Hagan, J. H. Hegemann, and U. Fleig. Mal3, the fission yeast homologue of the human APC-interacting protein EB-1 is required for microtubule integrity and the maintenance of cell form. *J. Cell Biol.*, 139:717–728, Nov 1997.
- P. Bieling, L. Laan, H. Schek, E. L. Munteanu, L. Sandblad, M. Dogterom, D. Brunner, and T. Surrey. Reconstitution of a microtubule plus-end tracking system in vitro. *Nature*, 450:1100–1105, Dec 2007.
- B. Bowerman and C. A. Shelton. Cell polarity in the early *Caenorhabditis elegans* embryo. *Curr. Opin. Genet. Dev.*, 9:390–395, Aug 1999.
- S. V. Bratman and F. Chang. Stabilization of overlapping microtubules by fission yeast CLASP. *Dev. Cell*, 13:812–827, Dec 2007.
- D. Bray, C. Thomas, and G. Shaw. Growth cone formation in cultures of sensory neurons. *Proc. Natl. Acad. Sci. U.S.A.*, 75:5226–5229, Oct 1978.
- H. Browning and D. D. Hackney. The EB1 homolog Mal3 stimulates the ATPase of the kinesin Tea2 by recruiting it to the microtubule. *J. Biol. Chem.*, 280:12299–12304, Apr 2005.
- H. Browning, J. Hayles, J. Mata, L. Aveline, P. Nurse, and J. R. McIntosh. Tea2p is a kinesin-like protein required to generate polarized growth in fission yeast. *J. Cell Biol.*, 151:15–28, Oct 2000.
- H. Browning, D. D. Hackney, and P. Nurse. Targeted movement of cell end factors in fission yeast. *Nat. Cell Biol.*, 5:812–818, Sep 2003.
- D. Brunner and P. Nurse. CLIP170-like tip1p spatially organizes microtubular dynamics in fission yeast. *Cell*, 102:695–704, Sep 2000.
- K. E. Busch and D. Brunner. The microtubule plus end-tracking proteins mal3p and tip1p cooperate for cell-end targeting of interphase microtubules. *Curr. Biol.*, 14:548–559, Apr 2004.

- K. E. Busch, J. Hayles, P. Nurse, and D. Brunner. Tea2p kinesin is involved in spatial microtubule organization by transporting tip1p on microtubules. *Dev. Cell*, 6:831–843, Jun 2004.
- P. Carvalho, J. S. Tirnauer, and D. Pellman. Surfing on microtubule ends. *Trends Cell Biol.*, 13:229–237, May 2003.
- L. Cassimeris and C. Spittle. Regulation of microtubule-associated proteins. *Int. Rev. Cytol.*, 210:163–226, 2001.
- S. Castagnetti, B. Novák, and P. Nurse. Microtubules offset growth site from the cell centre in fission yeast. *J. Cell. Sci.*, 120:2205–2213, Jul 2007.
- F. Chang and P. Nurse. How fission yeast fission in the middle. *Cell*, 84:191–194, Jan 1996.
- F. Chang and M. Peter. Yeasts make their mark. *Nat. Cell Biol.*, 5:294–299, Apr 2003.
- F. Chang, D. Drubin, and P. Nurse. cdc12p, a protein required for cytokinesis in fission yeast, is a component of the cell division ring and interacts with profilin. *J. Cell Biol.*, 137:169–182, Apr 1997.
- J. Chant. Cell polarity in yeast. *Annu. Rev. Cell Dev. Biol.*, 15:365–391, 1999.
- C. R. Chen, Y. C. Li, J. Chen, M. C. Hou, P. Papadaki, and E. C. Chang. Moe1, a conserved protein in *Schizosaccharomyces pombe*, interacts with a Ras effector, Scd1, to affect proper spindle formation. *Proc. Natl. Acad. Sci. U.S.A.*, 96:517–522, Jan 1999.
- C. R. Chen, J. Chen, and E. C. Chang. A conserved interaction between Moe1 and Mal3 is important for proper spindle formation in *Schizosaccharomyces pombe*. *Mol. Biol. Cell*, 11:4067–4077, Dec 2000.
- R. R. Daga, A. Yonetani, and F. Chang. Asymmetric microtubule pushing forces in nuclear centering. *Curr. Biol.*, 16:1544–1550, Aug 2006.
- D. G. Drubin and W. J. Nelson. Origins of cell polarity. *Cell*, 84:335–344, Feb 1996.
- D. R. Drummond and R. A. Cross. Dynamics of interphase microtubules in *Schizosaccharomyces pombe*. *Curr. Biol.*, 10:766–775, Jun 2000.
- M. Evangelista, D. Pruyne, D. C. Amberg, C. Boone, and A. Bretscher. Formins direct Arp2/3-independent actin filament assembly to polarize cell growth in yeast. *Nat. Cell Biol.*, 4:260–269, Mar 2002.
- B. Feierbach and F. Chang. Roles of the fission yeast formin for3p in cell polarity, actin cable formation and symmetric cell division. *Curr. Biol.*, 11:1656–1665, Oct 2001.
- B. Feierbach, F. Verde, and F. Chang. Regulation of a formin complex by the microtubule plus end protein tea1p. *J. Cell Biol.*, 165:697–707, Jun 2004.
- D. Foethke, T. Makushok, D. Brunner, and F. Nédélec. Force- and length-dependent catastrophe activities explain interphase microtubule organization in fission yeast. *Mol. Syst. Biol.*, 5:241, 2009.
- N. Fournier, L. Cerutti, N. Beltraminelli, E. Salimova, and V. Simanis. Bypass of the requirement for cdc16p GAP function in *Schizosaccharomyces pombe* by mutation of the septation initiation network genes. *Arch. Microbiol.*, 175:62–69, Jan 2001.
- S. Gasman, Y. Kalaidzidis, and M. Zerial. RhoD regulates endosome dynamics through Diaphanous-related Formin and Src tyrosine kinase. *Nat. Cell Biol.*, 5:195–204, Mar 2003.
- J. M. Glynn, R. J. Lustig, A. Berlin, and F. Chang. Role of bud6p and tea1p in the interaction between actin and microtubules for the establishment of cell polarity in fission yeast. *Curr. Biol.*, 11:836–845, Jun 2001.
- B. Goldstein and S. N. Hird. Specification of the anteroposterior axis in *Caenorhabditis elegans*. *Development*, 122:1467–1474, May 1996.

- S. Goldstone, C. Reyes, G. Gay, T. Courtheoux, M. Dubarry, S. Tournier, and Y. Gachet. Tip1/CLIP-170 protein is required for correct chromosome poleward movement in fission yeast. *PLoS ONE*, 5:e10634, 2010.
- B. L. Goode, D. G. Drubin, and G. Barnes. Functional cooperation between the microtubule and actin cytoskeletons. *Curr. Opin. Cell Biol.*, 12:63–71, Feb 2000.
- A. Grallert, C. Beuter, R. A. Craven, S. Bagley, D. Wilks, U. Fleig, and I. M. Hagan. S. pombe CLASP needs dynein, not EB1 or CLIP170, to induce microtubule instability and slows polymerization rates at cell tips in a dynein-dependent manner. *Genes Dev.*, 20:2421–2436, Sep 2006.
- I. M. Hagan. The fission yeast microtubule cytoskeleton. *J. Cell. Sci.*, 111 (Pt 12):1603–1612, Jun 1998.
- I. Hayashi and M. Ikura. Crystal structure of the amino-terminal microtubule-binding domain of end-binding protein 1 (EB1). *J. Biol. Chem.*, 278:36430–36434, Sep 2003.
- J. Hayles and P. Nurse. A journey into space. *Nat. Rev. Mol. Cell Biol.*, 2:647–656, Sep 2001.
- R. A. Heil-Chapdelaine, N. R. Adames, and J. A. Cooper. Formin’ the connection between microtubules and the cell cortex. *J. Cell Biol.*, 144:809–811, Mar 1999.
- J. L. Hoog, C. Schwartz, A. T. Noon, E. T. O’Toole, D. N. Mastronarde, J. R. McIntosh, and C. Antony. Organization of interphase microtubules in fission yeast analyzed by electron tomography. *Dev. Cell*, 12:349–361, Mar 2007.
- L.-K. Huang and M.-J.J. Wang. Image thresholding by minimizing the measures of fuzziness. *Pattern Recognition*, 28(1):41–51, 1995.
- H. Jin and D. C. Amberg. The secretory pathway mediates localization of the cell polarity regulator Aip3p/Bud6p. *Mol. Biol. Cell*, 11:647–661, Feb 2000.
- H. Jin and D. C. Amberg. Fission yeast Aip3p (spAip3p) is required for an alternative actin-directed polarity program. *Mol. Biol. Cell*, 12:1275–1291, May 2001.
- T. Kamasaki, R. Arai, M. Osumi, and I. Mabuchi. Directionality of F-actin cables changes during the fission yeast cell cycle. *Nat. Cell Biol.*, 7:916–917, Sep 2005.
- T. Kato, N. Watanabe, Y. Morishima, A. Fujita, T. Ishizaki, and S. Narumiya. Localization of a mammalian homolog of diaphanous, mDia1, to the mitotic spindle in HeLa cells. *J. Cell. Sci.*, 114:775–784, Feb 2001.
- A. Kobiela, H. A. Pasolli, and E. Fuchs. Mammalian formin-1 participates in adherens junctions and polymerization of linear actin cables. *Nat. Cell Biol.*, 6:21–30, Jan 2004.
- H. Kobori, N. Yamada, A. Taki, and M. Osumi. Actin is associated with the formation of the cell wall in reverting protoplasts of the fission yeast *Schizosaccharomyces pombe*. *J. Cell. Sci.*, 94 (Pt 4):635–646, Dec 1989.
- D. R. Kovar, J. R. Kuhn, A. L. Tichy, and T. D. Pollard. The fission yeast cytokinesis formin Cdc12p is a barbed end actin filament capping protein gated by profilin. *J. Cell Biol.*, 161:875–887, Jun 2003.
- D. R. Kovar, E. S. Harris, R. Mahaffy, H. N. Higgs, and T. D. Pollard. Control of the assembly of ATP- and ADP-actin by formins and profilin. *Cell*, 124:423–435, Jan 2006.
- N. B. Laferriere, T. H. MacRae, and D. L. Brown. Tubulin synthesis and assembly in differentiating neurons. *Biochem. Cell Biol.*, 75:103–117, 1997.
- S. Lall and N. H. Patel. Conservation and divergence in molecular mechanisms of axis formation. *Annu. Rev. Genet.*, 35:407–437, 2001.
- F. Li and H. N. Higgs. Dissecting requirements for auto-inhibition of actin nucleation by the formin, mDia1. *J. Biol. Chem.*, 280:6986–6992, Feb 2005.

- X. Li, D. Zhang, M. Hannink, and L. J. Beamer. Crystallization and initial crystallographic analysis of the Kelch domain from human Keap1. *Acta Crystallogr. D Biol. Crystallogr.*, 60:2346–2348, Dec 2004.
- G. Liao, T. Nagasaki, and G. G. Gundersen. Low concentrations of nocodazole interfere with fibroblast locomotion without significantly affecting microtubule level: implications for the role of dynamic microtubules in cell locomotion. *J. Cell. Sci.*, 108 (Pt 11): 3473–3483, Nov 1995.
- A. S. Maddox and K. Oegema. Deconstructing cytokinesis. *Nat. Cell Biol.*, 5:773–776, Sep 2003.
- J. Marks, I. M. Hagan, and J. S. Hyams. Growth polarity and cytokinesis in fission yeast: the role of the cytoskeleton. *J. Cell Sci. Suppl.*, 5:229–241, 1986.
- S. G. Martin and F. Chang. Cell polarity: a new mod(e) of anchoring. *Curr. Biol.*, 13: R711–713, Sep 2003.
- S. G. Martin and F. Chang. New end take off: regulating cell polarity during the fission yeast cell cycle. *Cell Cycle*, 4:1046–1049, Aug 2005.
- S. G. Martin and F. Chang. Dynamics of the formin for3p in actin cable assembly. *Curr. Biol.*, 16:1161–1170, Jun 2006.
- S. G. Martin, W. H. McDonald, J. R. Yates, and F. Chang. Tea4p links microtubule plus ends with the formin for3p in the establishment of cell polarity. *Dev. Cell*, 8:479–491, Apr 2005.
- S. G. Martin, S. A. Rincón, R. Basu, P. Pérez, and F. Chang. Regulation of the formin for3p by cdc42p and bud6p. *Mol. Biol. Cell*, 18: 4155–4167, Oct 2007.
- J. Mata and P. Nurse. Tea1 and the microtubular cytoskeleton are important for generating global spatial order within the fission yeast cell. *Cell*, 89:939–949, Jun 1997.
- J. Mata and P. Nurse. Discovering the poles in yeast. *Trends Cell Biol.*, 8:163–167, Apr 1998.
- N. Minc, S. V. Bratman, R. Basu, and F. Chang. Establishing new sites of polarization by microtubules. *Curr. Biol.*, 19:83–94, Jan 2009.
- J. M. Mitchison and P. Nurse. Growth in cell length in the fission yeast *Schizosaccharomyces pombe*. *J. Cell. Sci.*, 75:357–376, Apr 1985.
- T. Mitchison and M. Kirschner. Dynamic instability of microtubule growth. *Nature*, 312: 237–242, 1984.
- J. B. Moseley, I. Sagot, A. L. Manning, Y. Xu, M. J. Eck, D. Pellman, and B. L. Goode. A conserved mechanism for Bni1- and mDia1-induced actin assembly and dual regulation of Bni1 by Bud6 and profilin. *Mol. Biol. Cell*, 15:896–907, Feb 2004.
- F. Motegi, R. Arai, and I. Mabuchi. Identification of two type V myosins in fission yeast, one of which functions in polarized cell growth and moves rapidly in the cell. *Mol. Biol. Cell*, 12:1367–1380, May 2001.
- M. Nakamura, X. Z. Zhou, and K. P. Lu. Critical role for the EB1 and APC interaction in the regulation of microtubule polymerization. *Curr. Biol.*, 11:1062–1067, Jul 2001.
- K. Nakano, J. Imai, R. Arai, A. Toh-E, Y. Matsui, and I. Mabuchi. The small GTPase Rho3 and the diaphanous/formin For3 function in polarized cell growth in fission yeast. *J. Cell. Sci.*, 115:4629–4639, Dec 2002.
- W. J. Nelson. Adaptation of core mechanisms to generate cell polarity. *Nature*, 422:766–774, Apr 2003.
- T. Niccoli, M. Arellano, and P. Nurse. Role of Tea1p, Tea3p and Pom1p in the determination of cell ends in *Schizosaccharomyces pombe*. *Yeast*, 20:1349–1358, Dec 2003.

- O. Nielsen and J. Davey. Pheromone communication in the fission yeast *Schizosaccharomyces pombe*. *Semin. Cell Biol.*, 6:95–104, Apr 1995.
- P. Nurse. Fission yeast morphogenesis—posing the problems. *Mol. Biol. Cell*, 5:613–616, Jun 1994.
- P. Nurse, P. Thuriaux, and K. Nasmyth. Genetic control of the cell division cycle in the fission yeast *Schizosaccharomyces pombe*. *Mol. Gen. Genet.*, 146:167–178, Jul 1976.
- K. Ozaki-Kuroda, Y. Yamamoto, H. Nohara, M. Kinoshita, T. Fujiwara, K. Irie, and Y. Takai. Dynamic localization and function of Bni1p at the sites of directed growth in *Saccharomyces cerevisiae*. *Mol. Cell Biol.*, 21:827–839, Feb 2001.
- R. J. Pelham and F. Chang. Role of actin polymerization and actin cables in actin-patch movement in *Schizosaccharomyces pombe*. *Nat. Cell Biol.*, 3:235–244, Mar 2001.
- J. Petersen, D. Weilguny, R. Egel, and O. Nielsen. Characterization of fus1 of *Schizosaccharomyces pombe*: a developmentally controlled function needed for conjugation. *Mol. Cell Biol.*, 15:3697–3707, Jul 1995.
- J. Petersen, O. Nielsen, R. Egel, and I. M. Hagan. FH3, a domain found in formins, targets the fission yeast formin Fus1 to the projection tip during conjugation. *J. Cell Biol.*, 141:1217–1228, Jun 1998.
- S. Prag and J. C. Adams. Molecular phylogeny of the kelch-repeat superfamily reveals an expansion of BTB/kelch proteins in animals. *BMC Bioinformatics*, 4:42, Sep 2003.
- D. Pruyne and A. Bretscher. Polarization of cell growth in yeast. *J. Cell Sci.*, 113 (Pt 4):571–585, Feb 2000.
- D. Pruyne, M. Evangelista, C. Yang, E. Bi, S. Zigmund, A. Bretscher, and C. Boone. Role of formins in actin assembly: nucleation and barbed-end association. *Science*, 297:612–615, Jul 2002.
- D. Pruyne, L. Gao, E. Bi, and A. Bretscher. Stable and dynamic axes of polarity use distinct formin isoforms in budding yeast. *Mol. Biol. Cell*, 15:4971–4989, Nov 2004.
- J. E. Rickard and T. E. Kreis. CLIPs for organelle-microtubule interactions. *Trends Cell Biol.*, 6:178–183, May 1996.
- S. L. Rogers, G. C. Rogers, D. J. Sharp, and R. D. Vale. *Drosophila* EB1 is important for proper assembly, dynamics, and positioning of the mitotic spindle. *J. Cell Biol.*, 158:873–884, Sep 2002.
- S. Romero, C. Le Clainche, D. Didry, C. Egile, D. Pantaloni, and M. F. Carlier. Formin is a processive motor that requires profilin to accelerate actin assembly and associated ATP hydrolysis. *Cell*, 119:419–429, Oct 2004.
- A. Ruiz i Altaba and D. A. Melton. Axial patterning and the establishment of polarity in the frog embryo. *Trends Genet.*, 6:57–64, Feb 1990.
- I. Rupes, Z. Jia, and P. G. Young. Ssp1 promotes actin depolymerization and is involved in stress response and new end take-off control in fission yeast. *Mol. Biol. Cell*, 10:1495–1510, May 1999.
- I. Sagot, A. A. Rodal, J. Moseley, B. L. Goode, and D. Pellman. An actin nucleation mechanism mediated by Bni1 and profilin. *Nat. Cell Biol.*, 4:626–631, Aug 2002.
- L. Sandblad, K. E. Busch, P. Tittmann, H. Gross, D. Brunner, and A. Hoenger. The *Schizosaccharomyces pombe* EB1 homolog Mal3p binds and stabilizes the microtubule lattice seam. *Cell*, 127:1415–1424, Dec 2006.
- K. E. Sawin and P. Nurse. Regulation of cell polarity by microtubules in fission yeast. *J. Cell Biol.*, 142:457–471, Jul 1998.
- K. E. Sawin and H. A. Snaith. Role of microtubules and tea1p in establishment and

- maintenance of fission yeast cell polarity. *J. Cell. Sci.*, 117:689–700, Feb 2004.
- K. E. Sawin, P. C. Lourenco, and H. A. Snaith. Microtubule nucleation at non-spindle pole body microtubule-organizing centers requires fission yeast centrosome-related protein mod20p. *Curr. Biol.*, 14:763–775, May 2004.
- T. A. Schroer. Microtubules don and doff their caps: dynamic attachments at plus and minus ends. *Curr. Opin. Cell Biol.*, 13:92–96, Feb 2001.
- S. C. Schuyler and D. Pellman. Microtubule "plus-end-tracking proteins": The end is just the beginning. *Cell*, 105:421–424, May 2001.
- J. E. Segall. Polarization of yeast cells in spatial gradients of alpha mating factor. *Proc. Natl. Acad. Sci. U.S.A.*, 90:8332–8336, Sep 1993.
- S. E. Siegrist and C. Q. Doe. Microtubule-induced cortical cell polarity. *Genes Dev.*, 21:483–496, Mar 2007.
- J. V. Small and I. Kaverina. Microtubules meet substrate adhesions to arrange cell polarity. *Curr. Opin. Cell Biol.*, 15:40–47, Feb 2003.
- H. A. Snaith and K. E. Sawin. Fission yeast mod5p regulates polarized growth through anchoring of tea1p at cell tips. *Nature*, 423:647–651, Jun 2003.
- H. A. Snaith, I. Samejima, and K. E. Sawin. Multistep and multimode cortical anchoring of tea1p at cell tips in fission yeast. *EMBO J.*, 24:3690–3699, Nov 2005.
- V. Snell and P. Nurse. Genetic analysis of cell morphogenesis in fission yeast—a role for casein kinase II in the establishment of polarized growth. *EMBO J.*, 13:2066–2074, May 1994.
- G. Steinberg and J. R. McIntosh. Effects of the myosin inhibitor 2,3-butanedione monoxime on the physiology of fission yeast. *Eur. J. Cell Biol.*, 77:284–293, Dec 1998.
- L. K. Su, M. Burrell, D. E. Hill, J. Gyuris, R. Brent, R. Wiltshire, J. Trent, B. Vogelstein, and K. W. Kinzler. APC binds to the novel protein EB1. *Cancer Res.*, 55:2972–2977, Jul 1995.
- E. Tanaka and J. Sabry. Making the connection: cytoskeletal rearrangements during growth cone guidance. *Cell*, 83:171–176, Oct 1995.
- E. Tanaka, T. Ho, and M. W. Kirschner. The role of microtubule dynamics in growth cone motility and axonal growth. *J. Cell Biol.*, 128:139–155, Jan 1995.
- H. Tatebe, K. Shimada, S. Uzawa, S. Morigasaki, and K. Shiozaki. Wsh3/Tea4 is a novel cell-end factor essential for bipolar distribution of Tea1 and protects cell polarity under environmental stress in *S. pombe*. *Curr. Biol.*, 15:1006–1015, Jun 2005.
- C. R. Terenna, T. Makushok, G. Velasco-Casquillas, D. Baigl, Y. Chen, M. Bornens, A. Paoletti, M. Piel, and P. T. Tran. Physical mechanisms redirecting cell polarity and cell shape in fission yeast. *Curr. Biol.*, 18:1748–1753, Nov 2008.
- J. S. Tirnauer, E. O'Toole, L. Berrueta, B. E. Bierer, and D. Pellman. Yeast Bim1p promotes the G1-specific dynamics of microtubules. *J. Cell Biol.*, 145:993–1007, May 1999.
- J. S. Tirnauer, J. C. Canman, E. D. Salmon, and T. J. Mitchison. EB1 targets to kinetochores with attached, polymerizing microtubules. *Mol. Biol. Cell*, 13:4308–4316, Dec 2002a.
- J. S. Tirnauer, S. Grego, E. D. Salmon, and T. J. Mitchison. EB1-microtubule interactions in *Xenopus* egg extracts: role of EB1 in microtubule stabilization and mechanisms of targeting to microtubules. *Mol. Biol. Cell*, 13:3614–3626, Oct 2002b.
- T. Toda, K. Umesono, A. Hirata, and M. Yanagida. Cold-sensitive nuclear division

- arrest mutants of the fission yeast *Schizosaccharomyces pombe*. *J. Mol. Biol.*, 168:251–270, Aug 1983.
- P. T. Tran, V. Doye, F. Chang, and S. Inoué. Microtubule-dependent nuclear positioning and nuclear-dependent septum positioning in the fission yeast *Schizosaccharomyces pombe*. *Biol. Bull.*, 199:205–206, Oct 2000.
- P. T. Tran, L. Marsh, V. Doye, S. Inoué, and F. Chang. A mechanism for nuclear positioning in fission yeast based on microtubule pushing. *J. Cell Biol.*, 153:397–411, Apr 2001.
- K. Umesono, T. Toda, S. Hayashi, and M. Yanagida. Cell division cycle genes *nda2* and *nda3* of the fission yeast *Schizosaccharomyces pombe* control microtubular organization and sensitivity to anti-mitotic benzimidazole compounds. *J. Mol. Biol.*, 168:271–284, Aug 1983.
- F. Verde. On growth and form: control of cell morphogenesis in fission yeast. *Curr. Opin. Microbiol.*, 1:712–718, Dec 1998.
- F. Verde. Cell polarity: a tale of two Ts. *Curr. Biol.*, 11:R600–602, Aug 2001.
- F. Verde, J. Mata, and P. Nurse. Fission yeast cell morphogenesis: identification of new genes and analysis of their role during the cell cycle. *J. Cell Biol.*, 131:1529–1538, Dec 1995.
- B. J. Wallar and A. S. Alberts. The formins: active scaffolds that remodel the cytoskeleton. *Trends Cell Biol.*, 13:435–446, Aug 2003.
- F. Wang, R. K. Hansen, D. Radisky, T. Yoneda, M. H. Barcellos-Hoff, O. W. Petersen, E. A. Turley, and M. J. Bissell. Phenotypic reversion or death of cancer cells by altering signaling pathways in three-dimensional contexts. *J. Natl. Cancer Inst.*, 94:1494–1503, Oct 2002.
- S. Wasserman. FH proteins as cytoskeletal organizers. *Trends Cell Biol.*, 8:111–115, Mar 1998.
- C. M. Waterman-Storer and E. Salmon. Positive feedback interactions between microtubule and actin dynamics during cell motility. *Curr. Opin. Cell Biol.*, 11:61–67, Feb 1999.
- C. M. Waterman-Storer, R. A. Worthyake, B. P. Liu, K. Burridge, and E. D. Salmon. Microtubule growth activates Rac1 to promote lamellipodial protrusion in fibroblasts. *Nat. Cell Biol.*, 1:45–50, May 1999.
- V. M. Weaver, S. Lelievre, J. N. Lakins, M. A. Chrenek, J. C. Jones, F. Giancotti, Z. Werb, and M. J. Bissell. beta4 integrin-dependent formation of polarized three-dimensional architecture confers resistance to apoptosis in normal and malignant mammary epithelium. *Cancer Cell*, 2:205–216, Sep 2002.
- A. Yamamoto, R. R. West, J. R. McIntosh, and Y. Hiraoka. A cytoplasmic dynein heavy chain is required for oscillatory nuclear movement of meiotic prophase and efficient meiotic recombination in fission yeast. *J. Cell Biol.*, 145(6):1233–49, Jun 1999.
- F. Yarm, I. Sagot, and D. Pellman. The social life of actin and microtubules: interaction versus cooperation. *Curr. Opin. Microbiol.*, 4:696–702, Dec 2001.
- S. H. Zigmond, M. Evangelista, C. Boone, C. Yang, A. C. Dar, F. Sicheri, J. Forkey, and M. Pring. Formin leaky cap allows elongation in the presence of tight capping proteins. *Curr. Biol.*, 13:1820–1823, Oct 2003.

List of Figures

1.1	A DIC-picture of fission yeast.	5
1.2	Interphasic microtubule cytoskeleton in fission yeast.	7
1.3	Model of interphasic microtubule cytoskeleton in fission yeast.	9
1.4	Localization of Mal3p in interphase	11
1.5	Localization of Tip1p in interphase	12
1.6	Localization of Tea2p in logarithmic phase cells	13
1.7	Localization of Tea1p-GFP in vivo.	14
1.8	Interactions between Tea1p-Tea3p-Mod5p.	16
1.9	Percentage of cells forming branches in in WT, <i>mod5Δ</i> and <i>tea1Δ</i>	16
1.10	Localization of Mod5p in interphase.	17
1.11	Localization of Tea3p in interphase	19
1.12	Growth patterns in WT, <i>tea1Δ</i> and <i>pom1Δ</i> cells	19
1.13	Growth patterns in <i>tea1Δ</i> , <i>tea3Δ</i> , <i>pom1Δ</i> cells and double mutants.	19
1.14	Localization of Tea4p in interphase.	20
1.15	Localization of Bud6p in interphase and mitosis	22
1.16	Growth pattern of <i>bud6Δ</i> , <i>tea1Δ</i> and <i>bud6Δ tea1Δ</i> double mutants.	23
1.17	Growth patterns of WT and <i>for3Δ</i> cells	24
2.1	Terminology of the different parts of T-shaped cells.	32
2.2	Microtubule organization in a T-shaped cell.	32
2.3	Heterogeneity of growth fates in the presence of MTs.	33
2.4	Growth plots WT T-shaped cells switching growth.	34
2.5	Polarity of WT T-shaped cells.	35
2.6	Boxplots of geometry, growth, mean and maximum speed of WT T-shaped cells.	37
2.7	Nuclei and cell ends in growing and non-growing arms of WT T-shaped cells.	38
2.8	Initial length vs. growth in WT T-shaped cells.	39
2.9	Arm-Body comparison in WT T-shaped cells.	40
2.10	Microtubules in WT T-shaped cells in a region close to the tip.	41
2.11	MTs vs. growth in WT T-shaped cells.	42
2.12	Geometry vs. MTs correlation in WT T-shaped cells.	43
2.13	Conditional inference tree for arm total growth in WT T-shaped cells.	44
2.14	Polarity of <i>tea1Δ</i> T-shaped cells.	47
2.15	Boxplots of geometry, growth, mean and maximum speed of <i>tea1Δ</i> T-shaped cells.	48
2.16	Nuclei and cell ends in <i>tea1Δ</i> T-shaped cells.	49
2.17	Initial length vs. growth in <i>tea1Δ</i> T-shaped cells.	50
2.18	Microtubules in <i>tea1Δ</i> T-shaped cells in a region close to the tip.	51
2.19	MTs vs. growth in <i>tea1Δ</i> T-shaped cells.	51

2.20	Geometry vs. MTs correlation in <i>tea1</i> Δ T-shaped cells.	52
2.21	Polarity of <i>tea4</i> Δ T-shaped cells.	55
2.22	Boxplots of geometry, growth, mean and maximum speed of <i>tea4</i> Δ T-shaped cells.	56
2.23	Nuclei and cell ends in <i>tea4</i> Δ T-shaped cells.	56
2.24	Initial length vs. growth in <i>tea4</i> Δ T-shaped cells.	57
2.25	Microtubules in <i>tea4</i> Δ T-shaped cells in a region close to the tip.	59
2.26	MTs vs. growth in <i>tea4</i> Δ T-shaped cells.	59
2.27	Geometry vs. MTs correlation in <i>tea4</i> Δ T-shaped cells.	61
2.28	Growth plot of growing <i>mod5</i> Δ T-shaped cells.	63
2.29	Polarity of <i>mod5</i> Δ T-shaped cells.	64
2.30	Boxplots of geometry, growth, mean and maximum speed of <i>mod5</i> Δ T-shaped cells.	65
2.31	Nuclei and cell ends in <i>mod5</i> Δ T-shaped cells.	65
2.32	Initial length vs. growth in <i>mod5</i> Δ T-shaped cells.	66
2.33	Microtubules in <i>mod5</i> Δ T-shaped cells in a region close to the tip.	67
2.34	MTs vs. growth in <i>mod5</i> Δ T-shaped cells.	68
2.35	Geometry vs. MTs correlation in <i>mod5</i> Δ T-shaped cells.	69
2.36	Polarity of <i>bud6</i> Δ T-shaped cells.	72
2.37	Growth plot of growing <i>bud6</i> Δ T-shaped cells.	72
2.38	Boxplots of geometry, growth, mean and maximum speed of <i>bud6</i> Δ T-shaped cells.	73
2.39	Nuclei and cell ends in growing and non-growing arms of <i>bud6</i> Δ T-shaped cells.	74
2.40	Initial length vs. growth in <i>bud6</i> Δ T-shaped cells.	76
2.41	Arm-Body comparison in <i>bud6</i> Δ T-shaped cells.	77
2.42	Microtubules in <i>bud6</i> Δ T-shaped cells in a region close to the tip.	77
2.43	MTs vs. growth in <i>bud6</i> Δ T-shaped cells.	78
2.44	Geometry vs. MTs correlation in <i>bud6</i> Δ T-shaped cells.	79
3.1	MTs vs. growth in WT and <i>tea1</i> Δ T-shaped cells.	84
3.2	Growth propensity redistribution.	85
3.3	Maximum speed of growth.	85
C.1	Polarity of T-shaped cells.	109
C.2	Total growth of different cell parts in all strains.	110
C.3	Mean MTs/min of different cell parts in the different strains.	110

List of Tables

2.1	Pairwise correlations in WT T-shaped cells.	45
2.2	Pairwise correlations in <i>tea1</i> Δ T-shaped cells.	53
2.3	Pairwise correlations in <i>tea4</i> Δ T-shaped cells.	61
2.4	Pairwise correlations in <i>mod5</i> Δ T-shaped cells.	70
2.5	Pairwise correlations in <i>bud6</i> Δ T-shaped cells.	80
A.1	The strains used in this study.	105
B.1	Measurements of growth in T-shaped cells - all strains.	107

Acknowledgements

I would like to thank François Nédélec for giving me freedom in the project and the opportunity to carry out my PhD at EMBL. Thanks goes to Damian Brunner for providing scientific insights into *S. pombe* biology.

I thank Lindsay Murrells and Paulo Alves for help regarding experimental techniques, Tatyana Makushok for advice on image processing techniques and Yury Belyaev for microscopy techniques.

Special thanks goes to Jonathan Ward for invaluable discussions and input.

Finally I would like to thank Laure Plantard, Jonathan Ward, Michael Mitchel, Beat Rupp and Antonio Politi for useful comments on the manuscript and all present and past members of the Nédélec and Brunner lab for an enjoyable atmosphere.

Appendix A

List of strains

Genotype	Database number	mating type
nmt1-GFP-mal3::kanr cdc10-129	FN 0096	h-
nmt1-GFP-mal3::kanr cdc10-129 cut11-GFP:ura4+	FN 0184	h -
nmt1-GFP-mal3::kanr cdc10-129 cut11-GFP:ura4+ tea1 Δ ::ura4+	FN 0193	h?
nmt1-GFP-mal3::kanr cdc10-129 cut11-GFP:ura4+ tea4::kanMX	FN 0206	h?
nmt1-GFP-mal3::kanr cdc10-129 cut11-GFP:ura4+ bud6::kanr	FN 0223	h?
nmt1-GFP-mal3::kanr cdc10-129 cut11-GFP:ura4+ mod5 Δ ::kanMX	FN 0230	h?

Table A.1: The strains used in this study.

Appendix B

Quantifications

Measurement	WT	<i>tea1</i> Δ	<i>tea4</i> Δ	<i>mod5</i> Δ	<i>bud6</i> Δ
Arm growth	1.01 \pm 1.11	4.05 \pm 2.00	2.56 \pm 1.63	2.31 \pm 1.47	1.02 \pm 1.40
Body growth	2.73 \pm 1.97	0.08 \pm 0.22	0.22 \pm 0.25	0.59 \pm 1.09	3.30 \pm 2.30
Total growth	3.74 \pm 1.79	4.13 \pm 2.01	2.79 \pm 1.57	2.90 \pm 1.69	4.32 \pm 2.43
Arm mean speed	0.010 \pm 0.012	0.045 \pm 0.017	0.025 \pm 0.014	0.029 \pm 0.015	0.011 \pm 0.014
Body mean speed	0.026 \pm 0.018	-0.002 \pm 0.004	-0.001 \pm 0.005	0.004 \pm 0.011	0.034 \pm 0.020
Total mean speed	0.037 \pm 0.017	0.043 \pm 0.017	0.024 \pm 0.012	0.033 \pm 0.015	0.044 \pm 0.018
Arm max speed	0.020 \pm 0.018	0.060 \pm 0.020	0.040 \pm 0.019	0.040 \pm 0.017	0.019 \pm 0.019
Body max speed	0.040 \pm 0.024	0.002 \pm 0.004	0.006 \pm 0.007	0.010 \pm 0.014	0.045 \pm 0.024
Total max speed	0.057 \pm 0.020	0.058 \pm 0.020	0.039 \pm 0.015	0.046 \pm 0.018	0.059 \pm 0.022

Table B.1: Measurements of growth in T-shaped cells - all strains.

values are in μm for growth, and in $\mu\text{m}/\text{min}$ for speed, mean \pm std

Appendix C

Summarizing graphs

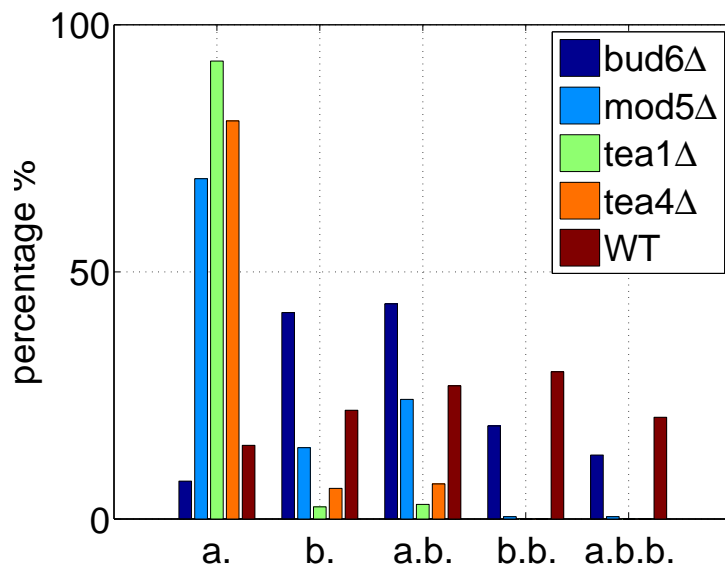


Figure C.1: Polarity of T-shaped cells.

Growth from 1,2 or all 3 ends of the t-cells. For each cell in the population the total growth of each end was measured, and if this growth was more than $0.5 \mu\text{m}$ this end was treated as having grown (n=985 cells, a.=growth only from arm, b. growth only from 1 body end, a.b. growth from arm and 1 body end, b.b. growth from 2 body ends, a.b.b. growth from all 3 cell ends).

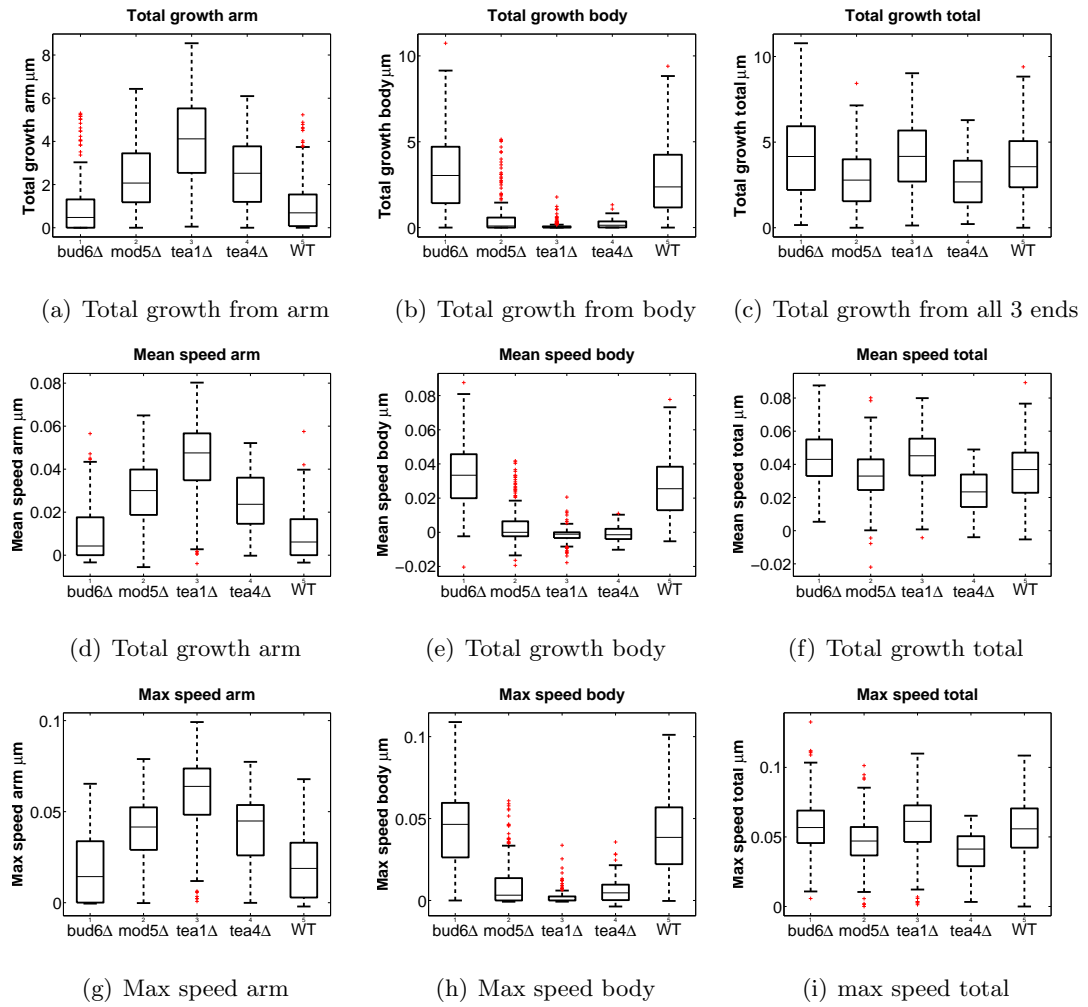


Figure C.2: Total growth of different cell parts in all strains

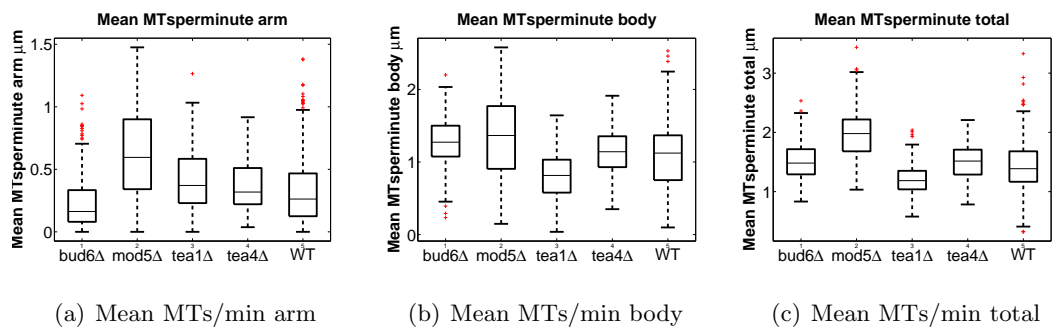


Figure C.3: Mean MTs/min of different cell parts in the different strains.